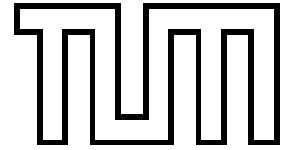


Technische Universität München  
Physik Department  
Institut für Theoretische Physik T30d  
Univ.-Prof. Dr. M. Lindner



## Lepton Masses and Dimensional Deconstruction

Dipl.-Phys. Univ. Gerhart Seidl

Vollständiger Abdruck der von der Fakultät für Physik der Technischen Universität München zur Erlangung des akademischen Grades eines

*Doktors der Naturwissenschaften (Dr. rer. nat.)*

genehmigten Dissertation.

Vorsitzender: Univ.-Prof. Dr. L. Oberauer

Prüfer der Dissertation:

1. Univ.-Prof. Dr. M. Lindner
2. Univ.-Prof. Dr. A. J. Buras

Die Dissertation wurde am 23.6.2003 bei der Technischen Universität München eingereicht und durch die Fakultät für Physik am 14.7.2003 angenommen.



# Contents

<b>1</b>	<b>Introduction</b>	<b>1</b>
1.1	Motivation . . . . .	1
1.2	Outline . . . . .	5
<b>2</b>	<b>Bilarge Leptonic Mixing</b>	<b>7</b>
2.1	Bilarge mixing patterns . . . . .	7
2.1.1	Large mixings from neutrinos . . . . .	7
2.1.2	Large mixings from charged leptons . . . . .	9
2.2	Particle content of the model . . . . .	10
2.3	The multi-scalar potential . . . . .	13
2.3.1	Yukawa interactions of the scalar $\mathcal{G}$ -singlets . . . . .	13
2.3.2	Yukawa interactions of the scalar $\mathcal{G}$ -doublets . . . . .	15
2.4	Yukawa interactions of the charged leptons . . . . .	24
2.4.1	The first row and column of the charged lepton mass matrix . . . . .	25
2.4.2	The 2-3-submatrix of the charged lepton mass matrix . . . . .	26
2.4.3	The charged lepton mass matrix . . . . .	27
2.5	Yukawa interactions of the neutrinos . . . . .	28
2.5.1	Effective Yukawa interactions of the neutrinos . . . . .	28
2.5.2	The neutrino mass matrix . . . . .	29
2.6	Lepton masses and mixing angles . . . . .	31
2.7	The leptonic mixing angles . . . . .	33
<b>3</b>	<b>Hierarchies from Mooses</b>	<b>36</b>
3.1	Deconstruction . . . . .	36
3.1.1	The periodic model . . . . .	36
3.1.2	The aliphatic model for fermions . . . . .	40
3.2	Enlarged gauge symmetries . . . . .	41
3.3	Discrete horizontal symmetries . . . . .	43
3.3.1	Abelian charges . . . . .	43

---

3.3.2	Non-Abelian charges . . . . .	44
3.3.3	Normal structure . . . . .	47
3.4	Construction of the scalar potential . . . . .	53
3.5	The vacuum alignment mechanism . . . . .	55
3.6	The charged lepton mass matrix . . . . .	57
3.7	The neutrino mass matrix . . . . .	62
3.7.1	Aliphatic model for neutrinos . . . . .	62
3.7.2	The one-generation-case . . . . .	62
3.7.3	Adding the 2nd and 3rd generation . . . . .	64
3.7.4	Neutrino masses and mixing angles . . . . .	64
<b>4</b>	<b>Latticized Geometries</b>	<b>67</b>
4.1	The two-site model . . . . .	67
4.1.1	Charge assignment . . . . .	67
4.1.2	General properties of the two-site model . . . . .	69
4.2	Four-site model . . . . .	71
4.2.1	Non-renormalizable Yukawa interactions . . . . .	71
4.2.2	Neutrino masses and mixing angles . . . . .	74
4.3	Three-site models . . . . .	76
4.3.1	A $SU(3)^3$ model . . . . .	76
4.3.2	A $U(1)^3$ model . . . . .	78
4.4	Deconstructed large extra dimensions . . . . .	80
<b>5</b>	<b>Summary and Conclusions</b>	<b>85</b>
<b>A</b>	<b>The Wilson-Dirac Action</b>	<b>88</b>
A.1	Four-dimensional lattice . . . . .	88
A.2	Transverse lattice description of a 5D fermion . . . . .	91
<b>B</b>	<b>The Dihedral Group <math>\mathcal{D}_4</math></b>	<b>94</b>
<b>C</b>	<b>Minimization of the Tree-Level Potential</b>	<b>97</b>
	<b>Acknowledgments</b>	<b>103</b>
	<b>Bibliography</b>	<b>104</b>

# Chapter 1

## Introduction

### 1.1 Motivation

Gauge theories in higher dimensions provide intriguing possibilities to understand the origin of the Standard Model (SM). One important virtue of higher-dimensional theories is, for example, that they offer a geometric notion of gauge symmetry breaking via Kaluza-Klein (KK) compactification [1] of the extra spatial dimensions on singular manifolds [2]. In particular, orbifold compactification allows to generate four-dimensional (4D) chiral theories by projecting out unwanted states through boundary conditions. Moreover, higher-dimensional gauge theories give new solutions to the hierarchy problem by parameterizing the electroweak scale in terms of the compactification radius [3]. In extra-dimensional theories, gauge and Yukawa couplings may be “unified” [4] and are therefore expected to be of the same order. Thus, after dimensional reduction, the hierarchical SM Yukawa coupling matrices should be highly predictable from symmetries and quantum numbers [5]. Actually, most of the free parameters of the SM are described by Yukawa couplings which then translate into the 22 fermion mass and mixing parameters<sup>1</sup> of the low-energy theory. In an effective field theory approach, it is therefore attractive to predict the 4D fermion mass matrices from horizontal (or flavor) symmetries which are sequentially broken.

In most attempts to obtain the hierarchical pattern of charged fermion masses from a non-Abelian horizontal symmetry, the first and the second generations have been treated as practically massless, resulting in small CKM mixing angles [8]. While this works well for the quarks, lepton-quark symmetry would then most naturally suggest the mixing angles in the lepton sector to be small too. However, with the advent of solar [9, 10] and atmospheric [11] neutrino data it has become clear that lepton-quark symmetry is badly broken by large mixing angles in the lepton sector. In fact, the KamLAND reactor neutrino experiment [12] has recently confirmed the Mikheyev-Smirnov-Wolfenstein (MSW) [13] large mixing angle (LMA) solution of

---

<sup>1</sup>These are: 6 quark masses, 6 lepton masses, 3 CKM mixing angles [6], 3 MNS mixing angles [7], 2 Dirac  $\mathcal{CP}$  violation phases, and 2 Majorana phases.

the solar neutrino problem at a significant level [14]. In the basis where the charged lepton mass matrix is diagonal, the  $3 \times 3$  neutrino mixing matrix is now determined to be to a good first approximation given by

$$\begin{pmatrix} \nu_e \\ \nu_\mu \\ \nu_\tau \end{pmatrix} = \begin{pmatrix} \cos \theta_{12} & -\sin \theta_{12} & 0 \\ \sin \theta_{12}/\sqrt{2} & \cos \theta_{12}/\sqrt{2} & -1/\sqrt{2} \\ \sin \theta_{12}/\sqrt{2} & \cos \theta_{12}/\sqrt{2} & 1/\sqrt{2} \end{pmatrix} \begin{pmatrix} \nu_1 \\ \nu_2 \\ \nu_3 \end{pmatrix}, \quad (1.1)$$

where  $\nu_\alpha$  ( $\alpha = e, \mu, \tau$ ) are the neutrino flavor states,  $\nu_i$  ( $i = 1, 2, 3$ ) are the Majorana neutrino mass eigenstates, and  $\theta_{12}$  is the solar mixing angle. In Eq. (1.1), we have already assumed the atmospheric mixing angle  $\theta_{23}$  to be maximal, *i.e.*,  $\theta_{23} = \pi/4$  and set the reactor angle  $\theta_{13}$  equal to zero.

Roughly speaking, the MSW LMA solution tells us that the leptons exhibit a *bilarge* mixing in which the solar mixing angle  $\theta_{12}$  is large, but not close to maximal, the atmospheric mixing angle  $\theta_{23}$  is close to maximal, and the reactor mixing angle  $\theta_{13}$  is small. More exactly, we actually have at 90% C.L. for the atmospheric angle  $\sin^2 2\theta_{23} \gtrsim 0.92$  and a best-fit value  $\sin^2 2\theta_{23} \simeq 1$ , *i.e.*,  $|\theta_{23}| \simeq 1$  [11]. The reactor angle  $\theta_{13}$  obeys  $\sin^2 \theta_{13} \lesssim 0.10$ , implying that  $|\theta_{13}| \lesssim 9.2^\circ$  [15]. Denoting the mass of the neutrino mass eigenstate  $\nu_i$  by  $m_i$ , solar neutrino data [9, 10] require that  $m_2^2 > m_1^2$ , where  $\theta_{12} < \pi/4$ . The combined solar and KamLAND neutrino data allows at 99.73% C.L. for the solar mixing angle the region  $0.29 \lesssim \tan^2 \theta_{12} \lesssim 0.86$  and for the solar mass squared difference  $\Delta m_\odot^2 \equiv m_2^2 - m_1^2$  the two regions  $5.1 \times 10^{-5} \text{ eV}^2 \lesssim \Delta m_\odot^2 \lesssim 9.7 \times 10^{-5} \text{ eV}^2$  (LMA-I) and  $1.2 \times 10^{-4} \text{ eV}^2 \lesssim \Delta m_\odot^2 \lesssim 1.9 \times 10^{-4} \text{ eV}^2$  (LMA-II) [14]. Atmospheric neutrino data [11] yield for the atmospheric mass squared difference  $\Delta m_{\text{atm}}^2 \equiv m_3^2 - m_2^2$  the absolute value  $|\Delta m_{\text{atm}}^2| = |m_3^2 - m_2^2| \simeq 2.5 \cdot 10^{-3} \text{ eV}^2$ , where  $m_3^2 > m_{1,2}^2$  or  $m_3^2 < m_{1,2}^2$  is possible. The combined data of the Wilkinson Microwave Anisotropy Probe (WMAP) [16] and the 2dF Galaxy Redshift Survey (2dFGRS) [17] sets an upper bound  $m_i \lesssim 0.23 \text{ eV}$  on the neutrino masses [18]. Hence, the neutrino mass spectrum can be either of the normal hierarchical (*i.e.*,  $m_1 \ll m_2 \ll m_3$ ), inverse hierarchical (*i.e.*,  $m_1 \simeq m_2 \gg m_3$ ), or the degenerate (*i.e.*,  $m_1 \simeq m_2 \simeq m_3$ ) type.

The relevance of the properties of neutrino masses for our understanding of the fundamental particle interactions can be seen as follows. In the SM, the baryon number  $B$  and the three lepton numbers  $L_e, L_\mu$ , and  $L_\tau$ , together with the total lepton number  $L = L_e + L_\mu + L_\tau$ , are exactly conserved by all renormalizable interactions. As a result, neutrinos are massless<sup>2</sup> in the SM. In Grand Unified Theories (GUTs), however, the baryon and lepton numbers are typically violated, which is a result of putting quarks and leptons into the same gauge multiplets.

In the minimal  $SU(5)$  model, for example, each generation of the SM is combined

---

<sup>2</sup>Since a left-handed neutrino  $\nu_\alpha$  carries a conserved charge  $L_\alpha$ , it cannot be combined with the right-handed anti-neutrino into a massive Majorana fermion.

into the  $\mathbf{10}$  and  $\bar{\mathbf{5}}$  multiplets, reading in component form, *e.g.*, for the first generation

$$\begin{pmatrix} 0 & u^c & u^c & u & d \\ & 0 & u^c & u & d \\ & & 0 & u & d \\ & & & 0 & e^c \\ & & & & 0 \end{pmatrix}_L \oplus \begin{pmatrix} d^c \\ d^c \\ d^c \\ e \\ \nu \end{pmatrix}_L, \quad (1.2)$$

where we have dropped the color indices. Clearly, transitions inside  $\mathbf{10}$  and  $\bar{\mathbf{5}}$  violate baryon and lepton numbers and only the linear combination  $B - L$  of the four global symmetries is conserved. Although  $B - L$  conservation is still sufficient to forbid neutrino masses, the  $B - L$  symmetry is usually broken in the embedding groups such as  $SO(10)$  or  $E_6$  and also in string theories [19]. In this context, the lowest dimensional lepton number violating operator in the SM is the dimension-five neutrino mass operator  $\sim HH\ell\ell/\Lambda$ , where  $H$  is the Higgs doublet,  $\ell$  denotes some arbitrary lepton doublet, and  $\Lambda$  is the cutoff scale at which the SM is embedded into some GUT. Choosing  $10^{15} \text{ GeV} \lesssim \Lambda \lesssim 10^{19} \text{ GeV}$ , we obtain an absolute neutrino mass scale  $m_\nu$  in the range  $10^{-5} \text{ eV} \lesssim m_\nu \lesssim 10^{-1} \text{ eV}$ , which is just right to solve the solar and atmospheric neutrino anomalies in terms of neutrino oscillations. An elegant way to generate the dimension-five operator  $\sim HH\ell\ell/\Lambda$  is given by the seesaw mechanism [20–22] which can be naturally included in GUTs. It is therefore seen, that mechanisms for neutrino mass generation can shed light on the physics at the GUT scale and, consequently, it is highly relevant to reproduce in neutrino mass models the observed neutrino mass and mixing parameters.

A large, but not necessarily maximal, atmospheric mixing angle  $\theta_{23}$  can be obtained by assuming Abelian horizontal  $U(1)$  [23] or  $Z_n$  [24] symmetries. However, the closer the lower experimental bound on  $|\theta_{23}|$  comes to  $\pi/4$ , the more pressing it is to give a rationale for maximal atmospheric mixing. In fact, a naturally maximal  $\nu_\mu$ - $\nu_\tau$ -mixing can be viewed as a strong hint for some non-Abelian flavor symmetry acting on the 2nd and 3rd generations [25–27]. Models for neutrino masses predicting large or maximal solar and atmospheric mixing angles by assigning the 2nd and 3rd generations discrete charges of the symmetric groups  $S_2$  [28] or  $S_3$  [29] are, in general, plagued with a fine-tuning problem in the charged lepton sector. The reason is, that by putting different neutrinos into the same multiplet of a horizontal symmetry, the corresponding charged lepton masses are generally expected to be of the same order, which is in conflict with the observed strict hierarchy of charged fermion masses. One possibility to resolve this problem may be provided in a supersymmetric framework by the non-Abelian group  $A_4$ , the symmetry group of the tetrahedron [30]. In this model, on the other hand, parameters must be tuned to give the solar angle  $\theta_{12}$  of the MSW LMA solution and, moreover, the neutrino masses are practically degenerate. In GUTs, however, a normal hierarchical neutrino mass spectrum is more plausible than an inverted or degenerate one [31]. In general, a survey of existing neutrino mass schemes shows that the MSW LMA solution is somewhat difficult to be obtained in

models [32] and, in particular, the imposition of non-Abelian horizontal symmetries to arrive at exact predictions is only partially successful, since additional fine-tuning in other sectors seems to be required.

As we have seen, the idea of unification in more than four dimensions can motivate horizontal symmetries in an effective 4D framework. However, gauge theories in  $4 + \delta$  dimensions have gauge couplings with negative dimension of mass  $g = [m]^{-\delta/2}$  and are usually non-renormalizable. As a result, they require a truncation on the number of KK modes near some cutoff scale  $M_f$  at which the perturbative regime of the higher-dimensional gauge theory breaks down. These theories can therefore be considered as an effective low-energy description of some more fundamental theory with sensible ultraviolet (UV) behavior. Here, one may imagine a class of possible UV completions which are similar in the infrared but differ radically above the cutoff  $M_f$ . Actually, some UV completions of higher-dimensional gauge theories have been found in the context of string theory [33] but these types of constructions suffer from various other problems, *e.g.*, they cannot be formulated in more than six dimensions. Recently, however, a new class of 4D gauge-invariant field theories for deconstructed or latticized extra dimensions has been proposed, which generate the physics of extra dimensions in their infrared limit [34, 35]. In deconstruction, extra-dimensional physics is regularized by an enlarged gauge symmetry in four dimensions. Since these theories are manifestly gauge-invariant and renormalizable, they can be viewed as viable UV completions [36–40] of some fundamental non-perturbative field theory. As a result, one obtains new calculational tools for studying higher-dimensional theories by reduction to a 4D setup. One possibility is, for example, to analyze the power-law running of gauge couplings in five dimensions [41] in terms of conventional field theory [35]. At a more general level, deconstruction can be considered as a model building tool which offers the benefits of extra dimensions even when there is no exact extra-dimensional correspondence [42]. In this context, one has found new mechanisms for electroweak symmetry breaking [36, 37] and supersymmetry breaking [43]. Another important aspect of deconstruction is, that it provides a novel technique to understand small physical parameters [44] like the hierarchical pattern of Yukawa couplings and fermion masses [45]. This suggests to include also (discrete) non-Abelian horizontal charges in models of dimensional deconstruction, which are generally characterized by a large collection of symmetries. In fact, inspired by deconstruction, several solutions to the doublet triplet splitting problem in product GUT groups like  $SU(5) \times SU(5)$  have been formulated, which essentially rely on discrete symmetries [38, 46]. In the lepton sector, one may think of similar approaches which solve the fine-tuning problem of charged lepton masses when a maximal atmospheric mixing angle is to be predicted from a non-Abelian horizontal symmetry. Moreover, it is appealing to associate the inverse lattice spacing of latticized extra dimensions with the GUT scale, thereby relating the usual dimension-five neutrino mass operator to properties of finite geometries. In this way, one could study topological aspects of fermion mass generation in an approach, which is complementary to the conventional treatment of extra dimensions.



## 1.2 Outline

In this thesis, we will be mainly interested in models of lepton mass generation which naturally give the MSW LMA solution from underlying symmetry principles. In order to establish contact with the present status of neutrino mass schemes which are promising in this respect, we will in Chapter 2 first briefly review the main attempts that have been undertaken to understand the MSW LMA solution (Sec. 2.1). Next, we will present in detail a specific model for bilarge leptonic mixing which predicts a maximal atmospheric mixing angle  $\theta_{23}$  and the hierarchical lepton mass spectrum from horizontal symmetries of the Abelian and non-Abelian type. The horizontal symmetries and the particle content of the model are introduced in Section 2.2. The problem of naturally obtaining a maximal  $\nu_\mu$ - $\nu_\tau$ -mixing as well as the mass-splitting  $m_\mu \ll m_\tau$  is solved by employing a vacuum alignment mechanism for a set of extra SM singlet scalar fields which generate the effective Yukawa couplings of the leptons. The vacuum structure emerging from the vacuum alignment mechanism is determined in Section 2.3 by minimizing the potential of these scalars. Next, we demonstrate in Section 2.4, how the vacuum structure translates into a set of effective Yukawa tensor operators of the charged leptons which produce the hierarchy  $m_\mu \ll m_\tau$  via an exact cancellation of specific components of these tensors. In addition, we obtain a small, but significant mixing of the first two generations of charged leptons, which will finally contribute to the leptonic mixing angles. In Section 2.5, it is shown that the horizontal symmetries in conjunction with the vacuum alignment mechanism predict bimaximal neutrino mixing for an inverted hierarchy form of the neutrino mass matrix. The hierarchical charged lepton mass spectrum, the inverse hierarchical neutrino masses and the mixing angles of the charged leptons and neutrinos are calculated in Section 2.6. In the total leptonic mixing angles, which are determined in Section 2.7, the contributions from the charged lepton sector lead to a significant deviation from maximal solar mixing, while the atmospheric mixing angle stays practically maximal due to the non-Abelian horizontal symmetry, *i.e.*, we have  $|\theta_{23} - \frac{\pi}{4}| \ll 1$ . Specifically, the model leads to the relation  $\theta_{12} \simeq \frac{\pi}{4} - \theta_{13}$  between the solar and the reactor mixing angle which typically take the values  $\theta_{12} \simeq 41^\circ$  and  $\theta_{13} \simeq 4^\circ$ . Hence, the model is in agreement with the MSW LMA solution but the solar mixing angle is necessarily bounded from below by  $37^\circ \lesssim \theta_{12}$  and cannot get close to the best-fit value  $\theta_{12} \simeq 32^\circ$  [14].

A lepton mass model which yields more comfortably the MSW LMA solution for normal hierarchical neutrino mass spectra is presented in Chapter 3. This model makes use of a similar vacuum alignment mechanism like the inverted hierarchy model but employs deconstruction as a technically elegant organizing principle for the enlarged scalar sector and the collection of horizontal symmetries. Therefore, the deconstruction setup is briefly reviewed in Section 3.1 for two important cases, before the replicated gauge symmetries and the particle content of the model are introduced in Section 3.2. The deconstructed extra-dimensional gauge symmetries are related to a realistic phenomenology of lepton masses and mixing angles by discrete Abelian

charges (Sec. 3.3.1) and by a discrete non-Abelian horizontal symmetry  $\mathcal{G}$  which acts on the 2nd and 3rd generation, as well as on the link fields of the latticized extra dimensions (Sec. 3.3.2). In Section 3.3.3, we identify the group  $\mathcal{G}$  as an extension of the Klein group  $Z_2 \times Z_2$  based on the dihedral group  $\mathcal{D}_4$ . The analysis of  $\mathcal{G}$  includes also the discussion of the coset graphs of relevant subgroups of  $\mathcal{G}$  and their relation to incidence geometry. Using the decomposition rules of the dihedral group  $\mathcal{D}_4$ , we construct in Section 3.4 the potential for the scalar representations of  $\mathcal{G}$  and determine the vacuum structure by minimizing the scalar potential in Section 3.5. Next, we describe in Section 3.6, how a linear combination of Wilson-line type effective operators, corresponding to a five-dimensional (5D) gauge theory compactified on  $\mathcal{S}^1$ , predicts the charged lepton mass spectrum from the vacuum alignment mechanism. The neutrino masses, on the other hand, are generated through the mixing with a right-handed Dirac-neutrino propagating in a latticized  $\mathcal{S}^1/Z_2$  orbifold extra dimension (Sec. 3.7). The resulting neutrino mass and mixing parameters are calculated in Section 3.7.4, where we also relate the types of latticizations of the orbifold to the presently allowed ranges for the solar mass squared difference  $\Delta m_{\odot}^2$  as implied by recent KamLAND results. Consequently, the model gives the MSW LMA solution at the 90% C.L. without any tuning of parameters.

A different and more minimalistic approach to neutrino masses is presented in Chapter 4. For a basic two-site model, it is shown that deconstruction can provide a dynamical origin of the seesaw mechanism when the inverse lattice spacing of specific latticized geometries is identified with the seesaw scale and the generations are put on different lattice sites (Sec. 4.1). Realistic applications to four-site and three-site models are given in Sections 4.2 and 4.3, where we show that bimaximal mixing can be obtained when the link fields break the lepton numbers down to the diagonal subgroup  $\bar{L} = L_e - L_\mu - L_\tau$  in the right-handed Majorana sector. The bimaximal mixing is then translated into the bilarge mixing of the MSW LMA solution by non-renormalizable operators. Since deconstruction serves as a 4D description of a 5D gauge theory, one would generally expect the inverse lattice spacings to be of order TeV or larger. Hence, to remodel large extra dimensions, one would usually need a large number of lattice sites. However, in Section 4.4, we present a novel mechanism which generates an inverse lattice spacing in the sub-eV range. This makes it possible to study deconstructed sub-mm extra dimensions with a number of lattice sites which can be as small as  $\lesssim 10$ .

Finally, in Section 5, we present a summary as well as our conclusions. In addition, in Appendix A, we determine the Wilson-Dirac action for the transverse lattice description of a 5D fermion. Moreover, Appendix B gives a brief review of the dihedral group  $\mathcal{D}_4$  and in Appendix C, the minimization of the scalar potentials is explicitly carried out.

## Chapter 2

# Bilarge Leptonic Mixing

In this chapter, we will present a model for lepton mass generation which yields bilarge leptonic mixing for an inverse neutrino mass hierarchy. The model predicts an exactly maximal atmospheric mixing angle from a non-Abelian horizontal symmetry. In addition, strictly hierarchical charged lepton masses arise from a vacuum-alignment mechanism. Before discussing the model in detail, we will first look at the main attempts which have been made in order to understand the bilarge leptonic mixing pattern observed in neutrino oscillations.

### 2.1 Bilarge mixing patterns

The MSW LMA solution of the solar neutrino problem has now been well established by the KamLAND reactor neutrino experiment. From the theoretical point of view, the MSW LMA solution is interesting, since it is somewhat difficult to obtain naturally the associated bilarge mixing and neutrino mass spectrum in models [32]. We shall therefore briefly review the main types of existing neutrino mass model schemes, which show a natural preference for the MSW LMA solution. Broadly, one can divide them into scenarios where the leptonic mixing predominantly stems either from the neutrino sector or from the charged lepton sector.

#### 2.1.1 Large mixings from neutrinos

As has already been mentioned in the introduction, the present experimental situation concerning the possible types of neutrino mass hierarchies is still ambiguous, since the neutrinos could exhibit either a hierarchical, inverse hierarchical, or degenerate mass spectrum. In inverted hierarchy models, the effective neutrino mass matrix is of the form

$$M_\nu = \begin{pmatrix} m_{11} & cM & sM \\ cM & m_{22} & m_{23} \\ sM & m_{32} & m_{33} \end{pmatrix}, \quad (2.1)$$

where  $c \equiv \cos \theta_{23}^\nu$ ,  $s \equiv \sin \theta_{23}^\nu$ , for  $\theta_{23}^\nu \sim 1$ , and  $m_{ij} \ll M$ . Application of a rotation in the 2-3-plane through an angle  $\theta_{23}^\nu$  brings  $M_\nu$  to the form

$$M'_\nu = \begin{pmatrix} m_{11} & M & 0 \\ M & m'_{22} & m'_{23} \\ 0 & m'_{32} & m'_{33} \end{pmatrix}, \quad (2.2)$$

which clearly gives an inverse neutrino mass hierarchy  $m_1 \simeq m_2 \simeq M \gg m_3$ . Moreover, it is  $\Delta m_{\text{atm}}^2 \simeq M^2$  and  $\Delta m_\odot^2 \simeq 2(m_{11} + m'_{22})M$ . In absence of some cancellations coming from the charged lepton sector, we have  $\theta_{23} \sim \theta_{23}^\nu \sim 1$ , *i.e.*, the atmospheric mixing angle can be large. The 1-2-block in Eq. (2.2) is approximately diagonalized by a rotation through an angle  $\theta_{12}^\nu \simeq \pi/4 - (m'_{22} - m_{11})/(4M)$ . Now, for the LMA-II solution [14] we have the ratio  $\Delta m_\odot^2/\Delta m_{\text{atm}}^2 \simeq 2(m'_{22} + m_{11})/M \simeq 6 \cdot 10^{-2}$ , implying that  $\theta_{12}^\nu \simeq \pi/4 + \mathcal{O}(10^{-3})$ . If the left-handed charged leptons are practically unmixed, this would imply that the solar mixing angle  $\theta_{12}$  is too close to maximal to be at the 99.73% C.L. in agreement with solar data [14]. However, it is expected that  $\theta_{12}$  gets also a contribution  $\theta_{12}^\ell$  from the charged lepton sector, which is of the order  $\theta_{12}^\ell \sim \sqrt{m_e/m_\mu} \simeq 0.07$ , where  $m_e$  and  $m_\mu$  denote the mass of the electron and the muon respectively [32]. As a result, for an appropriate sign of  $\theta_{12}^\ell$ , the inverted hierarchy models can give  $\tan^2 \theta_{12} \simeq 0.75$ , which is in better agreement with the global analyses. A simple way to obtain an inverse neutrino mass hierarchy is provided by models with approximately conserved  $\bar{L} = L_e - L_\mu - L_\tau$  lepton number. If the  $\bar{L}$  symmetry is softly broken in the effective neutrino mass matrix  $M_\nu$ , the form as in Eq. (2.1) can arise [47]. A recent realistic inverted hierarchy model based on a horizontal  $SU(2)$  symmetry has been given in Ref. [48].

For degenerate neutrino masses, one attractive possibility to predict a maximal atmospheric mixing angle  $\theta_{23}$  is offered by models based on the non-Abelian flavor symmetry  $A_4$ , the symmetry group of the tetrahedron [30]. Here, the neutrino mass matrix texture is approximately on the form

$$M_\nu \simeq m_\nu \begin{pmatrix} 1 + \epsilon & \epsilon & \epsilon \\ \epsilon & \epsilon & 1 \\ \epsilon & 1 & \epsilon \end{pmatrix}, \quad (2.3)$$

where  $m_\nu$  is the absolute neutrino mass scale, and  $\epsilon \ll 1$  parameterizes the radiative corrections to the leading form. In a supersymmetric version, the holomorphy and renormalizability of the superpotential allows the  $A_4$  symmetry to be spontaneously broken such that hierarchical quark and lepton masses can naturally arise. Although this type of model predicts a maximal atmospheric mixing angle  $\theta_{23} = \pi/4$ , the solar mixing angle  $\theta_{12}$  is essentially arbitrary and depends crucially on the order-unity coefficients associated with the radiative corrections. As a result, these coefficients must be tuned to be consistent with the presently preferred value of the solar mixing angle.

The MSW LMA solution is comfortably obtained in normal hierarchical models, in which the effective neutrino mass matrix is on the approximate form

$$M_\nu \simeq \begin{pmatrix} m_{11} & m_{12} & m_{13} \\ m_{12} & s^2 M & scM \\ m_{13} & scM & c^2 M \end{pmatrix}, \quad (2.4)$$

where, again,  $c \equiv \cos \theta_{23}^\nu$ ,  $s \equiv \sin \theta_{23}^\nu$ , for  $\theta_{23}^\nu \sim 1$ , and  $m_{ij} \ll M$ . Note that, to leading order, the 2-3-subblock has a vanishing sub-determinant. As a consequence, we get  $\Delta m_{\odot}^2 \simeq \mathcal{O}(m_{ij}^2)$  and  $\Delta m_{\text{atm}}^2 \simeq M^2$ , and choosing the appropriate ratios  $m_{ij}/M$  reproduces the preferred hierarchy between  $\Delta m_{\odot}^2$  and  $\Delta m_{\text{atm}}^2$ . Like it is the case for the inverted hierarchy models, one observes that the atmospheric mixing angle  $\theta_{23}$  can be large or even maximal. In contrast to the inverted hierarchy models, however, the solar mixing angle  $\theta_{12}$  can be large with no preference for close to maximal mixing. The normal hierarchical form in Eq. (2.4) can emerge from non-Abelian flavor symmetries [25–27, 29] or, more simply, in scenarios of single right-handed neutrino dominance [49]. If the charged lepton mass matrix is diagonal, maximal atmospheric mixing requires  $\theta_{23}^\nu = \pi/4$  in Eq. (2.4). This has been achieved by putting the 2nd and 3rd generations of leptons into the regular representation of the symmetric group  $S_2$  in conjunction with a soft breaking of lepton numbers in the right-handed Majorana sector [28]. In this approach, however, fine-tuning is required to obtain the hierarchy  $m_\mu \ll m_\tau$  of charged lepton masses. Generally speaking, it is interesting to note, that in GUTs a normal neutrino mass hierarchy seems to be more plausible than an inverted or degenerate one [31].

### 2.1.2 Large mixings from charged leptons

A prominent scheme to accommodate the MSW LMA solution, where large leptonic mixing angles come (also) from the charged lepton sector, has been realized in so-called “lopsided” GUT models [50]. In the case of an  $SU(5)$  GUT, for example, one makes use of the fact that the left-handed charged leptons are in the same multiplet  $\bar{\mathbf{5}}$  as the right-handed down quarks (see Eq. (1.2)). As a result, large mixings of the left-handed leptons would generally be related by  $SU(5)$  to an irrelevant large mixing of the right-handed quarks. Additionally,  $SU(5)$  relates the small CKM angles of the left-handed up and down quarks in the  $\mathbf{10}$  representation to small mixings of the right-handed leptons, which cannot be observed in neutrino oscillations. The lopsided  $SU(5)$  model of Ref. [32] applies the Froggatt-Nielsen mechanism [51] for an approximately conserved  $U(1)$  flavor symmetry under which the quark and lepton multiplets are charged as  $\mathbf{10}_1(2)$ ,  $\mathbf{10}_2(1)$ ,  $\mathbf{10}_3(0)$ ,  $\bar{\mathbf{5}}_1(1)$ ,  $\bar{\mathbf{5}}_2(0)$ , and  $\bar{\mathbf{5}}_2(0)$ . If we parameterize the breaking of the flavor symmetry by the small number  $\epsilon \ll 1$ , the resulting mass matrix patterns  $M_u$  and  $M_d$  of the up and down quarks are given by

$$M_u \simeq m_u \begin{pmatrix} \epsilon^4 & \epsilon^3 & \epsilon^2 \\ \epsilon^3 & \epsilon^2 & \epsilon \\ \epsilon^2 & \epsilon & 1 \end{pmatrix} \quad \text{and} \quad M_d \simeq m_d \begin{pmatrix} \epsilon^3 & \epsilon^2 & \epsilon^2 \\ \epsilon^2 & \epsilon & \epsilon \\ \epsilon & 1 & 1 \end{pmatrix}, \quad (2.5)$$

where  $m_u$  and  $m_d$  denote the absolute up and down quark mass scales and only the orders of magnitude of the matrix elements has been indicated. Correspondingly, the mass matrices  $M_\nu$  and  $M_\ell$  of the neutrinos and the charged leptons are found to be

$$M_\nu \simeq m_\nu \begin{pmatrix} \epsilon^2 & \epsilon & \epsilon \\ \epsilon & 1 & 1 \\ \epsilon & 1 & 1 \end{pmatrix} \quad \text{and} \quad M_\ell \simeq m_d \begin{pmatrix} \epsilon^3 & \epsilon^2 & \epsilon \\ \epsilon^2 & \epsilon & 1 \\ \epsilon^2 & \epsilon & 1 \end{pmatrix}, \quad (2.6)$$

where  $m_\nu \simeq m_d^2/\Lambda$  denotes the absolute neutrino mass scale. Note in Eqs. (2.5) and (2.6) the lopsided forms of  $M_d$  and  $M_\ell$ . From Eq. (2.6), it is obvious that both the matrices  $M_\ell$  and  $M_\nu$  contribute to the atmospheric mixing angle  $\theta_{23}$ , which will generally be large, but not necessarily maximal. Unfortunately, the 2-3-subblock of  $M_\nu$  must be tuned to give a ratio of the order  $\Delta m_\odot^2/\Delta m_{\text{atm}}^2 = \mathcal{O}(10^{-2})$ . With this choice, however, the solar mixing angle is for  $\epsilon \simeq 1/20$  predicted to be close to the best-fit value  $\tan^2\theta_{12} \simeq 0.4$  of the MSW LMA solution.

To put it in a nutshell, the main types of schemes claiming to provide an understanding of the MSW LMA solution are actually not fully satisfactory with respect to their predictivity, since they typically involve some fine-tuning. The parameters in models based on non-Abelian horizontal symmetries must either be adjusted to give the charged lepton mass hierarchy or depend crucially on fine-tuned radiative corrections which are supposed to generate the presently preferred solar mixing angle. Models using only Abelian symmetries, on the other hand, can at best give an order-of-magnitude-understanding of the lepton mass and mixing parameters [23,24]. In the remainder of this chapter, we will consider a specific model for inverse hierarchical neutrino masses, which avoids these problems by employing a vacuum alignment mechanism. This model predicts a naturally maximal  $\nu_\mu$ - $\nu_\tau$ -mixing from a non-Abelian symmetry as well as the strict hierarchy  $m_e \ll m_\mu \ll m_\tau$  of charged lepton masses. Moreover, a substantial deviation from maximal solar mixing is achieved by contributions coming from the charged lepton sector.

## 2.2 Particle content of the model

Let us now consider an extension of the SM, which yields bilarge leptonic mixing and the hierarchical mass pattern of the leptons from both Abelian and non-Abelian horizontal symmetries. In particular, we suppose that a discrete non-Abelian horizontal symmetry  $\mathcal{G}$  ensures (nearly) maximal  $\nu_\mu$ - $\nu_\tau$ -mixing and the hierarchical Yukawa couplings are generated by higher-dimensional operators [52] through the Froggatt-Nielsen mechanism [51]. (A classification of effective neutrino mass operators has been given in Ref. [53].) For simplicity, we omit the quark sector in our further discussion<sup>1</sup>. We will denote the lepton doublets as  $\ell_\alpha = (\nu_{\alpha L} \ e_{\alpha L})$  and the right-handed charged leptons as  $E_\alpha = e_{\alpha R}$ , where  $\alpha = e, \mu, \tau$ . The electroweak Higgs sector is assumed to

<sup>1</sup>A related study including also the quark sector can be found in Ref. [54].

consist only of the SM Higgs doublet  $H$ , but the standard two-Higgs-doublet model is also possible. In the charged lepton sector, the masses arise through the mixing with additional heavy right-handed (*i.e.*,  $SU(2)_L$  singlet) charged fermions, which all have masses of the order of some characteristic mass scale  $M_1$ . Apart from some general prescriptions of their transformations under the flavor symmetries, which will be introduced below, it is not necessary to explicitly present the fundamental theory of these additional charged fermions. This is in contrast with the neutrino sector, which we will extend by five additional heavy SM singlet Dirac neutrinos  $N_e$ ,  $N_\mu$ ,  $N_\tau$ ,  $F_1$ , and  $F_2$ . We suppose that  $F_1$  and  $F_2$  have masses of the same order  $M_1$  as the charged intermediate Froggatt-Nielsen states, whereas  $N_e$ ,  $N_\mu$ , and  $N_\tau$  all have masses of the order of some relevant high (unification) mass scale  $M_2$ . While  $M_2$  takes the rôle of some seesaw scale [20–22] (and it is therefore responsible for the smallness of the neutrino masses),  $M_1$  can be as low as several TeV [55].

The horizontal symmetry  $\mathcal{G}$ , which will be presented further below in terms of its generators, is supposed to act on the 2nd and 3rd generation of leptons in terms of a two-dimensional irreducible representation (irrep). Hence, we combine the  $SU(2)_L$ -doublet fields  $\ell_\mu$  and  $\ell_\tau$ , the right-handed charged leptons  $E_\mu$  and  $E_\tau$  as well as the right-handed Dirac neutrinos  $N_\mu$  and  $N_\tau$  into the doublet representations  $\mathbf{2}_\ell \equiv (\ell_\mu \ \ell_\tau)^T$ ,  $\mathbf{2}_E \equiv (E_\mu \ E_\tau)^T$ , and  $\mathbf{2}_N \equiv (N_\mu \ N_\tau)^T$  of  $\mathcal{G}$ . Now,  $\mathcal{G}$  relates in the  $\mu$ - $\tau$ -subsector the Yukawa couplings of the muon and tau, which makes it difficult to understand why  $m_\mu \ll m_\tau$ . This problem seems to correspond somewhat to the well known problem of splitting the SM Higgs doublets and their color triplet partners in 4D GUTs. However, the doublet-triplet splitting problem has a straightforward solution in higher dimensions and one has also recently given purely 4D solutions in terms of dimensional deconstruction [38,46]. In these theories, a number of additional replicated scalar non-linear sigma model fields is introduced, which are themselves subject to an enlarged collection of symmetries. With respect to the problem of naturally obtaining the hierarchy  $m_\mu \ll m_\tau$  in the presence of the symmetry  $\mathcal{G}$ , these ideas motivate to extend the SM by a number of “copies” of SM singlet scalar fields which transform as replicated doublets under  $\mathcal{G}$ :

$$\begin{aligned} \Phi_1 &= (\phi_1, \phi_2)^T, & \Phi_2 &= (\phi_3, \phi_4)^T, & \Phi_3 &= (\phi_5, \phi_6)^T, & \Phi_4 &= (\phi_7, \phi_8)^T, \\ \Phi'_1 &= (\phi'_1, \phi'_2)^T, & \Phi'_2 &= (\phi'_3, \phi'_4)^T, & \Phi'_3 &= (\phi'_5, \phi'_6)^T. \end{aligned} \quad (2.7)$$

Furthermore, we introduce three scalar fields  $\phi_9$ ,  $\phi_{10}$ , and  $\theta$ , which are trivial representations of  $\mathcal{G}$ . Moreover, we impose additional replicated  $U(1)$  gauge symmetries with charges  $Q_1$ ,  $Q_2$ , and  $Q_3$ . The corresponding  $U(1)$  charge assignment is shown in Table 2.1. In what follows, it will always be understood that the Higgs doublet  $H$  is a total singlet under transformations other than the SM gauge transformations. Note that the charges  $Q_1$  and  $Q_2$  are anomalous. However, it is known that anomalous  $U(1)$  charges may arise in effective field theories from strings. Then, the cancellation of the anomalies must be accomplished by the Green-Schwarz mechanism [56].

	$(Q_1, Q_2, Q_3)$
$\ell_e, E_e$	$(1, 0, 0)$
$\mathbf{2}_\ell, \mathbf{2}_E$	$(0, 1, 0)$
$N_e$	$(1, 0, 0)$
$\mathbf{2}_N$	$(0, 1, 0)$
$F_1$	$(1, 0, 0)$
$F_2$	$(-1, 0, 1)$
$\Phi_1$	$(1, -1, 2)$
$\Phi_4$	$(-1, -1, 0)$
$\phi_9$	$(-2, 0, 1)$
$\theta$	$(0, 0, -1)$

Table 2.1: Assignment of the  $U(1)$  charges  $Q_1, Q_2$ , and  $Q_3$  to the fermionic and scalar fields. The fields not shown here carry zero  $U(1)$  charges.

The first generation of the charged leptons is distinguished from the second and third generations if we require for  $P \equiv e^{2\pi i/n}$ , where the integer  $n$  obeys  $n \geq 5$ , invariance of the Lagrangian under transformation of the following  $Z_n$  symmetry:

$$\mathcal{D}_1 : \quad E_e \rightarrow P^{-4}E_e, \quad \mathbf{2}_E \rightarrow P^{-1}\mathbf{2}_E, \quad \Phi_i \rightarrow P \Phi_i \quad (i = 1, 2, 3), \quad (2.8)$$

where we assume that the fundamental states in the heavy neutrino sector  $N_e, \mathbf{2}_N, F_1$ , and  $F_2$  are  $\mathcal{D}_1$ -singlets. Hence, the symmetry  $\mathcal{D}_1$  forbids the fields  $\Phi_1, \Phi_2$ , and  $\Phi_3$  to participate in the leading-order mass terms for the neutrinos. With the  $\mathcal{G}$ -doublet representation content given above, we can now define  $\mathcal{G}$  as the group which is generated by the following set of discrete symmetry transformations

$$\mathcal{D}_2 : \quad \begin{cases} \mathbf{2}_\ell \rightarrow D(C_b) \mathbf{2}_\ell, & \mathbf{2}_E \rightarrow D(C_b) \mathbf{2}_E, & \mathbf{2}_N \rightarrow D(C_b) \mathbf{2}_N, \\ \Phi_1 \rightarrow D(C_{b'}) \Phi_1, & \Phi'_1 \rightarrow D(C_{b'}) \Phi'_1, & \Phi_4 \rightarrow D(C_b) \Phi_4, \end{cases} \quad (2.9a)$$

$$\mathcal{D}_3 : \quad \begin{cases} \mathbf{2}_\ell \rightarrow D(C_b) \mathbf{2}_\ell, & \mathbf{2}_N \rightarrow D(C_b) \mathbf{2}_N, \\ \Phi_i \rightarrow D(C_{b'}) \Phi_i, & \Phi'_i \rightarrow D(C_{b'}) \Phi'_i \quad (i = 2, 3), \\ \Phi_4 \rightarrow D(C_b) \Phi_4, \end{cases} \quad (2.9b)$$

$$\mathcal{D}_4 : \quad \begin{cases} \mathbf{2}_\ell \rightarrow D(C_{b'}) \mathbf{2}_\ell, & \mathbf{2}_E \rightarrow D(C_{b'}) \mathbf{2}_E, & \mathbf{2}_N \rightarrow D(C_{b'}) \mathbf{2}_N, \\ \Phi_i \rightarrow D(C_a) \Phi_i \quad (i = 1, 2, 3), \\ \Phi_4 \rightarrow D(C_{b'}) \Phi_4, \end{cases} \quad (2.9c)$$

$$\mathcal{D}_5 : \quad \Phi_i \rightarrow D(C_b) \Phi_i, \quad \Phi'_i \rightarrow D(C_b) \Phi'_i \quad (i = 1, 2, 3), \quad (2.9d)$$

where  $D(C_a), D(C_b)$ , and  $D(C_{b'})$  denote generators of the two-dimensional vector representation of the non-Abelian dihedral group  $\mathcal{D}_4$  (see App. B) and can be explicitly



written as follows

$$D(C_a) = \begin{pmatrix} 1 & 0 \\ 0 & -1 \end{pmatrix}, \quad D(C_b) = \begin{pmatrix} -1 & 0 \\ 0 & 1 \end{pmatrix}, \quad D(C_{b'}) = \begin{pmatrix} 0 & 1 \\ 1 & 0 \end{pmatrix}. \quad (2.10)$$

Inspection of the discrete symmetry transformations shows that  $\mathcal{G}$  can be considered as an  $n$ -valued representation of  $\mathcal{D}_4$ , where  $n = 8$ . Note that  $\mathcal{G}$  is a subgroup of the  $n$ -fold replicated dihedral group  $(\mathcal{D}_4)^n \equiv \mathcal{D}_4 \times \dots \times \mathcal{D}_4$ . The permutation-reflection symmetries  $\mathcal{D}_2$ ,  $\mathcal{D}_3$ , and  $\mathcal{D}_4$  are responsible for generating a naturally maximal atmospheric mixing angle, since they establish exact degeneracies of the Yukawa couplings in the leptonic 2-3-subsector. These permutation symmetries also play a crucial rôle in the scalar sector, in which they restrict some of the couplings in the multi-scalar potential to be exactly degenerate (at tree-level), which means that degenerate vacuum expectation values (VEVs) can emerge after spontaneous symmetry breaking (SSB). This so-called vacuum alignment mechanism can work if we assume the cyclic symmetry

$$\mathcal{D}_6 : \begin{cases} E_e \rightarrow P^{-(4l+1)} E_e, & N_e \rightarrow P N_e, \\ \Phi_1 \rightarrow P^k \Phi_1, & \Phi_2 \rightarrow P^l \Phi_2, & \Phi_3 \rightarrow P^m \Phi_3, \\ \Phi'_1 \rightarrow P^{-k} \Phi'_1, & \Phi'_2 \rightarrow P^{-l} \Phi'_2, & \Phi'_3 \rightarrow P^{-m} \Phi'_3, \\ \phi_9 \rightarrow P^{-1} \phi_9, & \phi_{10} \rightarrow P \phi_{10}, \end{cases} \quad (2.11)$$

where  $k$ ,  $l$ , and  $m$  are some integers. For the symmetry  $\mathcal{D}_6$  we additionally require that the heavy states in the charged lepton sector can only be multiplied by factors  $P^n$ , where  $n$  is an integer multiple of  $k$ ,  $l$ , or  $m$ , and that the differences  $|k-l|$ ,  $|k-m|$ , and  $|l-m|$  are sufficiently large. These symmetries impose constraints on the higher-dimensional lepton mass operators as well as on the allowed renormalizable terms in the multi-scalar potential. With this, one can forbid possibly dangerous terms, which could otherwise spoil the vacuum alignment mechanism.

## 2.3 The multi-scalar potential

In this section, we will analyze the tree-level vacuum structure which spontaneously breaks the discrete symmetry  $\mathcal{G}$  when the SM singlet scalar fields acquire their VEVs. For non-fine-tuned couplings, we will find a minimum of the multi-scalar potential in which the  $\mathcal{G}$ -doublet fields are aligned either in parallel or orthogonal directions. In the low-energy lepton mass matrices, the orientation of these VEVs will then translate into an exact prediction for the  $\mu$ - $\tau$ -mixing while providing an order-of-magnitude-understanding of the lepton mass hierarchies.

### 2.3.1 Yukawa interactions of the scalar $\mathcal{G}$ -singlets

#### The electroweak Higgs potential

Since the electroweak Higgs-sector consists only of the  $SU(2)$  Higgs doublet  $H$ , we conclude that  $H$  appears only to the second or fourth power in the multi-scalar

potential. Hence, in any renormalizable terms of the multi-scalar potential which mix  $H$  with the SM singlet scalar fields, the Higgs doublet is only allowed to appear in terms of its absolute square  $|H|^2$ . Next, since the Higgs doublet carries zero  $Q_1, Q_2$ , and  $Q_3$  charges and is a  $\mathcal{D}_i$ -singlet, where  $i = 1, 2, \dots, 6$ , there exists a range of parameters in the multi-scalar potential for which the standard electroweak symmetry breaking is possible. Furthermore, this implies that we can, without loss of generality, separate the SM singlet scalar part from the Higgs-doublet part in the multi-scalar potential by formally absorbing the absolute square of the VEV  $|\langle H \rangle|^2$  into the coupling constants of the mixed terms. Then, since the vacuum alignment mechanism of the SM singlet fields is independent from the details of the electroweak Higgs physics, we can in what follows leave aside the effects of  $H$  and focus on the properties of the SM singlet scalar fields.

### Interactions of the fields $\phi_9$ and $\phi_{10}$

The  $\mathcal{D}_6$  and  $U(1)$  charge assignments require the fields  $\phi_9$  and  $\phi_{10}$  to enter the renormalizable interactions of the scalar fields only in terms of the operators

$$|\phi_9|^2, \quad |\phi_{10}|^2, \quad |\phi_9^\dagger \phi_{10}|^2.$$

Since the fields  $\phi_9$  and  $\phi_{10}$  are singlets under transformations of all the permutation-reflection symmetries  $\mathcal{D}_2, \mathcal{D}_3$ , and  $\mathcal{D}_4$ , they will have no effect on the relative alignment of the rest of the scalar fields, when both of the fields  $\phi_9$  and  $\phi_{10}$  finally develop non-vanishing VEVs. Following the example of the Higgs doublet  $H$ , we can therefore discard the terms in the scalar potential which involve the fields  $\phi_9$  and  $\phi_{10}$  in our considerations concerning the vacuum alignment.

### Interactions of the field $\theta$

From the  $\mathcal{D}_6$  and  $U(1)$  charge assignments it follows that any renormalizable term in the scalar potential which involves  $\theta$  or the component fields of  $\Phi_1, \Phi_3$ , or  $\Phi_4$ , can only be allowed if these fields appear in one of the following combinations:

$$\Phi_1^\dagger M \Phi_1, \quad \Phi_3^\dagger M \Phi_3, \quad \Phi_3^T M \theta, \quad \Phi_4^\dagger M \Phi_4, \quad |\theta|^2, \quad (2.12)$$

or their complex conjugates, where in each of the above terms  $M$  denotes some arbitrary complex  $2 \times 2$  matrix which summarizes symmetry-related geometric factors. Among the products in Eq. (2.12), only  $\Phi_3^T M \theta$  transforms non-trivially under the symmetry  $\mathcal{D}_1$ . Moreover, since  $\Phi_1', \Phi_2'$ , and  $\Phi_3'$  are  $\mathcal{D}_1$ -singlets, we see that the component fields  $\phi_3$  and  $\phi_4$ , which are  $\mathcal{D}_1$ -singlets, can only appear either in the combination  $\Phi_2^\dagger M \Phi_2$  or  $\Phi_2^\dagger M \Phi_3 \theta$ , where  $M$  again denotes some complex  $2 \times 2$  matrix. Under the symmetry  $\mathcal{D}_6$ , however, the term  $\Phi_2^\dagger M \Phi_3 \theta$  transforms non-trivially and it is therefore forbidden. Except for the product  $\Phi_3^T M \theta$  in Eq. (2.12), all scalar interactions involve an equal number (0, 1, or 2) of the fields  $\theta$  and its adjoint  $\theta^\dagger$ , which can

then be combined into the absolute square  $|\theta|^2$ . Now, the interaction  $\Phi_3^T M \theta |\theta|^2$  is forbidden by the symmetries  $\mathcal{D}_1$  and  $\mathcal{D}_6$ . Also,  $\theta$  is a total singlet under the discrete symmetry transformations. Thus, all terms which involve the absolute square  $|\theta|^2$  will have no influence on the relative alignment of the  $\mathcal{G}$ -doublets when  $\theta$  acquires a non-vanishing VEV. For this reason, we can in the discussion of the  $\mathcal{G}$ -doublet potential omit all terms which involve  $|\theta|^2$ .

### 2.3.2 Yukawa interactions of the scalar $\mathcal{G}$ -doublets

#### Parameterization of the $\mathcal{G}$ -doublets

In order to determine the vacuum structure in  $\mathcal{G}$ -space, it is instructive to examine the accidental global symmetries of the Lagrangian, which are broken by tree-level operators representing specific Yukawa interactions of the scalar  $\mathcal{G}$ -doublets. For any such operator, we shall denote by  $\Phi$  and  $\Omega$  a general pair of  $\mathcal{G}$ -doublet scalars which participate in the interaction, *i.e.*, we will most generally have  $\Phi, \Omega \in \{\Phi_i, \Phi'_i, \Phi_4\}$ , where  $i = 1, 2, 3$ . Next, it is suitable to parameterize the VEVs of the  $\mathcal{G}$ -doublets  $\Phi$  and  $\Omega$  as

$$\langle \Phi \rangle = \begin{pmatrix} \langle \phi_a \rangle \\ \langle \phi_b \rangle \end{pmatrix} = v_1 \begin{pmatrix} e^{i\varphi_1} \cos \alpha \\ e^{i\varphi'_1} \sin \alpha \end{pmatrix} \equiv v_1 \begin{pmatrix} e^{i\varphi_1} c_\alpha \\ e^{i\varphi'_1} s_\alpha \end{pmatrix}, \quad (2.13a)$$

$$\langle \Omega \rangle = \begin{pmatrix} \langle \omega_a \rangle \\ \langle \omega_b \rangle \end{pmatrix} = v_2 \begin{pmatrix} e^{i\varphi_2} \cos \beta \\ e^{i\varphi'_2} \sin \beta \end{pmatrix} \equiv v_2 \begin{pmatrix} e^{i\varphi_2} c_\beta \\ e^{i\varphi'_2} s_\beta \end{pmatrix}, \quad (2.13b)$$

where  $v_1, v_2$  are positive numbers and  $\varphi_1, \varphi'_1, \varphi_2, \varphi'_2$  denote the phases of the VEVs. Actually, we will mostly work with the relative phases  $\varphi \equiv \varphi'_1 - \varphi_1$  and  $\psi \equiv \varphi'_2 - \varphi_2$ . In fact, since an arbitrary element  $u \in SU(2)$  can be represented by the matrix

$$u = \begin{pmatrix} e^{i\varphi_a} \cos \alpha & -e^{-i\varphi_b} \sin \alpha \\ e^{i\varphi_b} \sin \alpha & e^{-i\varphi_a} \cos \alpha \end{pmatrix}, \quad (2.14)$$

it is seen from Eqs. (2.13), that in the non-linear sigma model approximation each of the VEVs  $\langle \Phi \rangle$  and  $\langle \Omega \rangle$  can be associated with the breakdown of an accidental  $SU(2)_{\text{acc}}$  symmetry. Let us denote by  $V_\Delta(\Phi, \Omega)$  the most general renormalizable  $SU(2)_{\text{acc}}$  symmetry breaking operator in the potential involving the fields  $\Phi$  and  $\Omega$ . As it will prove later,  $V_\Delta(\Phi, \Omega)$  splits into two potentials via  $V_\Delta(\Phi, \Omega) = V_A(\Phi, \Omega) + V_B(\Phi, \Omega)$  which can be explicitly written as

$$\begin{aligned} V_A(\Phi, \Omega) &\equiv d_1 |\phi_a^\dagger \phi_b|^2 + d_2 |\omega_a^\dagger \omega_b|^2 + d_3 (|\phi_a|^2 - |\phi_b|^2)(|\omega_a|^2 - |\omega_b|^2), \\ V_B(\Phi, \Omega) &\equiv d_4 \left[ (\phi_a^\dagger \phi_b)^2 + (\phi_b^\dagger \phi_a)^2 \right] + d_5 \left[ (\omega_a^\dagger \omega_b)^2 + (\omega_b^\dagger \omega_a)^2 \right] \\ &\quad + d_6 (\phi_a^\dagger \phi_b + \phi_b^\dagger \phi_a)(\omega_a^\dagger \omega_b + \omega_b^\dagger \omega_a) \\ &\quad + d_7 (\phi_a^\dagger \phi_b - \phi_b^\dagger \phi_a)(\omega_a^\dagger \omega_b - \omega_b^\dagger \omega_a), \end{aligned} \quad (2.15)$$

where the coefficients  $d_1, \dots, d_7$  are some real-valued numbers. Note that the potential  $V_A(\Phi, \Omega)$  depends only on the angles  $\alpha$  and  $\beta$  whereas  $V_B(\Phi, \Omega)$  is, in addition, also a function of  $\varphi$  and  $\psi$ . More generally, one can view the parameters  $\alpha, \beta, \varphi$ , and  $\psi$  as the VEVs of scalar fields. The scalar field  $\alpha(x)$ , *e.g.*, is then the coordinate of the manifold of cosets  $SU(2)_{\text{acc}}/U(1)_\alpha$  at each point of space-time, where  $U(1)_\alpha$  is the accidental  $U(1)$  symmetry associated with  $\alpha$ . An alignment of  $\langle \Phi \rangle$  and  $\langle \Omega \rangle$  with respect to  $\alpha$  happens, when in the lowest energy state  $\alpha(x)$  provides only a non-linear realization of the group  $SU(2)_{\text{acc}}$  (corresponding statements apply to the fields  $\beta(x), \varphi(x)$ , and  $\psi(x)$ ).

### Interactions of the field $\Phi_4$

From the  $U(1)$  charge assignment in Table 2.1 it is seen that only an even number of the component fields  $\phi_7$  and  $\phi_8$  of  $\Phi_4$  (or their complex conjugates) can participate in the scalar interactions. Consider first the product  $\phi_7^\dagger \phi_8$  (or equivalently its complex conjugate). The operator  $\phi_7^\dagger \phi_8$  is odd under application of each of the symmetries  $\mathcal{D}_2$  and  $\mathcal{D}_3$ . As a consequence, the transformation  $\mathcal{D}_2$  requires  $\phi_7^\dagger \phi_8$  to couple to  $\phi_7$  or to one of the component fields of  $\Phi_1$  or  $\Phi'_1$ . Additionally, the transformation  $\mathcal{D}_3$  requires  $\phi_7^\dagger \phi_8$  to couple only to  $\phi_7$  or to one of the component fields from  $\Phi_2, \Phi_3, \Phi'_2$ , or  $\Phi'_3$ . This can only be satisfied if  $\phi_7^\dagger \phi_8$  couples to  $\phi_7$  or  $\phi_7^\dagger$ , but not to the operator products  $(\phi_7)^2, (\phi_7^\dagger)^2$ , or  $|\phi_7|^2$ . As for  $\phi_7^\dagger \phi_8$  is a  $U(1)$  singlet, the operator  $\phi_7^\dagger \phi_8$  can only couple to some linear combination of  $\phi_7 \phi_8^\dagger$  and  $\phi_8 \phi_7^\dagger$ . Hence, if a product of the type  $\Phi_4^\dagger M \Phi_4$  enters an interaction with scalars which are different from the component fields  $\phi_7$  and  $\phi_8$ , then this operator  $\Phi_4^\dagger M \Phi_4$  is a linear combination of the absolute squares  $|\phi_7|^2$  and  $|\phi_8|^2$ .

We will now denote by  $\phi_i$  and  $\phi_j$  two component fields of  $\Phi_i$  or  $\Phi'_i$ , where  $i = 1, 2, 3$ . Taking Eq. (2.12) and the product  $\Phi_2^\dagger M \Phi_2$  into account, it follows that the operator  $\phi_i \phi_j$  can enter the interactions with the component fields of  $\Phi_4$  only in terms of one of the following combinations:

$$\Phi_1^\dagger M \Phi_1, \quad \Phi_2^\dagger M \Phi_2, \quad \Phi_3^\dagger M \Phi_3, \quad \Phi_1'^\dagger M \Phi_1', \quad \Phi_2'^\dagger M \Phi_2', \quad \Phi_3'^\dagger M \Phi_3', \quad (2.16)$$

where the last three products are found by applying the symmetry  $\mathcal{D}_6$ . Actually, for all terms in Eq. (2.16) the symmetry  $\mathcal{D}_5$  requires  $M \propto \text{diag}(1, 1)$ . Using the result of the previous paragraph, application of the symmetry  $\mathcal{D}_4$ , which permutes  $\phi_7 \leftrightarrow \phi_8$ , gives for the most general interactions of  $\Phi_4$  with the other scalar fields the terms

$$(|\phi_7|^2 + |\phi_8|^2) \sum_{\varphi_i \notin \Phi_4} c_i |\varphi_i|^2, \quad (2.17)$$

where  $\varphi_i$  can be any of the scalar fields, which are not identical with the component fields  $\phi_7$  or  $\phi_8$  of  $\Phi_4$  and  $c_i$  are some real-valued coupling constants. (Dimension-three terms like  $|\phi_7|^2 \varphi_i$  or  $|\phi_8|^2 \varphi_i$ , where  $\varphi_i \neq \phi_7, \phi_8$ , are forbidden by the  $\mathcal{D}_6$  and  $U(1)$  charge assignment.) Taking everything into account, the  $U(1)$  symmetries and

invariance under  $\mathcal{D}_4$  restrict the most general terms in the scalar potential, involving the component fields of  $\Phi_4$ , to be

$$\begin{aligned}
V(\Phi_4) &= \mu^2(|\phi_7|^2 + |\phi_8|^2) + \kappa(|\phi_7|^2 + |\phi_8|^2)^2 + (|\phi_7|^2 + |\phi_8|^2) \sum_{\varphi_i \notin \Phi_4} c_i |\varphi_i|^2 \\
&+ a|\phi_7|^2|\phi_8|^2 + b \left[ (\phi_7^\dagger \phi_8)^2 + (\phi_8^\dagger \phi_7)^2 \right] \\
&= \mu^2 \Phi_4^\dagger \Phi_4 + \kappa \left( \Phi_4^\dagger \Phi_4 \right)^2 + \Phi_4^\dagger \Phi_4 \sum_{\varphi_i \notin \Phi_4} c_i |\varphi_i|^2 + V_\Delta(\Phi_4, \Phi_4), \tag{2.18}
\end{aligned}$$

where  $\mu^2$ ,  $\kappa$ ,  $a$ , and  $b$  are real-valued constants and the  $SU(2)_{\text{acc}}$  symmetry breaking parts  $V_\Delta(\Phi_4, \Phi_4) = V_A(\Phi_4, \Phi_4) + V_B(\Phi_4, \Phi_4)$  for  $\Phi_4$  read

$$V_A(\Phi_4, \Phi_4) = a|\phi_7|^2|\phi_8|^2, \quad V_B(\Phi_4, \Phi_4) = b \left[ (\phi_7^\dagger \phi_8)^2 + (\phi_8^\dagger \phi_7)^2 \right]. \tag{2.19}$$

In Eq. (2.18), we will choose  $\kappa > 0$  and assume the rest of the coupling constants to be negative. Then, we find from App. C that the VEV of  $\Phi_4$  is given by

$$\langle \Phi_4 \rangle = \begin{pmatrix} \langle \phi_7 \rangle \\ \langle \phi_8 \rangle \end{pmatrix} = \frac{|\Phi_4|}{\sqrt{2}} e^{i\alpha} \begin{pmatrix} 1 \\ \pm 1 \end{pmatrix}, \tag{2.20}$$

*i.e.*, in this basis, the VEVs of the component fields are relatively real and degenerate up to a sign. When considering the Yukawa interactions of the neutrinos, it will turn out that the orientation of  $\langle \Phi_4 \rangle$  in Eq. (2.20) is responsible for a nearly maximal atmospheric mixing angle. Thus, we can from now on restrict our discussion of the scalar potential to the fields  $\Phi_i$  and  $\Phi'_i$  ( $i = 1, 2, 3$ ).

### The potential of the fields $\Phi_1, \Phi_2$ , and $\Phi_3$

In all two-fold and four-fold products involving only the component fields  $\phi_i$  ( $i = 1, \dots, 6$ ) of  $\Phi_1, \Phi_2$ , and  $\Phi_3$ , the transformation  $\mathcal{D}_5$  requires the number of the fields carrying an even (or odd) index  $i$ , to be even. In the scalar potential, linear and tri-linear terms of these component fields are forbidden by  $\mathcal{D}_6$ -invariance. Taking the operators in Eq. (2.12) and  $\Phi_2^\dagger M \Phi_2$  into account, the allowed two-fold products of the fields  $\phi_i$  are unmixed and must be absolute squares  $\sim |\phi_i|^2$ . In the same way, it follows that all four-fold products of the fields  $\phi_i$  must be of the following forms

$$\begin{aligned}
&(\phi_1^\dagger \phi_2)^2, \quad \phi_1^\dagger \phi_2 \phi_3^\dagger \phi_4, \quad \phi_1^\dagger \phi_2 \phi_4^\dagger \phi_3, \quad \phi_1^\dagger \phi_2 \phi_5^\dagger \phi_6, \quad \phi_1^\dagger \phi_2 \phi_6^\dagger \phi_5, \\
&(\phi_3^\dagger \phi_4)^2, \quad \phi_3^\dagger \phi_4 \phi_5^\dagger \phi_6, \quad \phi_3^\dagger \phi_4 \phi_6^\dagger \phi_5, \quad (\phi_5^\dagger \phi_6)^2, \quad |\phi_i|^2 |\phi_j|^2, \quad |\phi_i|^4, \tag{2.21}
\end{aligned}$$

and their complex conjugates, where  $i, j = 1, 2, \dots, 6$ . In order to determine also the relative phases which will be taken by the component fields  $\phi_i$  in the lowest energy

state, let us rewrite a general four-fold product of the type given in Eq. (2.21) as

$$\begin{aligned}
& (a\phi_i^\dagger\phi_j + b\phi_j^\dagger\phi_i)\phi_k^\dagger\phi_l + (c\phi_i^\dagger\phi_j + d\phi_j^\dagger\phi_i)\phi_l^\dagger\phi_k + \text{h.c.} \\
&= \left[ (a + d^*)\phi_i^\dagger\phi_j + (b + c^*)\phi_j^\dagger\phi_i \right] \phi_k^\dagger\phi_l \\
&+ \left[ (c + b^*)\phi_i^\dagger\phi_j + (d + a^*)\phi_j^\dagger\phi_i \right] \phi_l^\dagger\phi_k, \tag{2.22}
\end{aligned}$$

where  $a, b, c$ , and  $d$  are complex-valued constants. Assume that  $i \neq j$ . Then, from Eq. (2.21) we observe that  $k \neq l$  and we can, without loss of generality, assume that the index-pairs  $(i, j)$  and  $(k, l)$ , respectively, combine the fields which are interchanged by the discrete symmetry  $\mathcal{D}_2$  or  $\mathcal{D}_3$ . (If  $i = j$ , then it follows from Eq. (2.21) that  $k = l$ , which will be discussed below.) Let, in addition,  $\{i, j\} \neq \{k, l\}$ . Then, application of the symmetries  $\mathcal{D}_2$  and  $\mathcal{D}_3$  yields  $a + d^* = d + a^*$  and  $b + c^* = c + b^*$ . We can therefore rename the constants as  $a + d^* \rightarrow a$  and  $b + c^* \rightarrow b$ , where now  $a$  and  $b$  are real constants, and write the term in Eq. (2.22) as

$$\begin{aligned}
& (a\phi_i^\dagger\phi_j + b\phi_j^\dagger\phi_i)\phi_k^\dagger\phi_l + (b\phi_i^\dagger\phi_j + a\phi_j^\dagger\phi_i)\phi_l^\dagger\phi_k \\
&= \frac{a+b}{2}(\phi_i^\dagger\phi_j + \phi_j^\dagger\phi_i)(\phi_k^\dagger\phi_l + \phi_l^\dagger\phi_k) + \frac{a-b}{2}(\phi_i^\dagger\phi_j - \phi_j^\dagger\phi_i)(\phi_k^\dagger\phi_l - \phi_l^\dagger\phi_k) \\
&= \frac{a+b}{2} \Re(\phi_i^\dagger\phi_j) \Re(\phi_k^\dagger\phi_l) - \frac{a-b}{2} \Im(\phi_i^\dagger\phi_j) \Im(\phi_k^\dagger\phi_l). \tag{2.23}
\end{aligned}$$

Since the fields  $\phi_3, \phi_4, \phi_5$ , and  $\phi_6$  are singlets under transformation of the discrete symmetry  $\mathcal{D}_2$ , we can have  $a \neq b$  in the case that  $(\phi_i, \phi_j)^T = \Phi_2$  and  $(\phi_k, \phi_l)^T = \Phi_3$ . However, if  $(i, j) = (1, 2)$ , then application of the discrete symmetry  $\mathcal{D}_2$  further constrains the constants in the above general form to fulfill  $a = b$ , and therefore, the last term in Eq. (2.23) vanishes. As a cause of the symmetries  $\mathcal{D}_2$  and  $\mathcal{D}_3$ , the products  $(\phi_i\phi_j^\dagger)^2$  in Eq. (2.21), where  $(\phi_i, \phi_j)^T \in \{\Phi_1, \Phi_2, \Phi_3\}$ , appear in the potential always as

$$a \left[ (\phi_i\phi_j^\dagger)^2 + (\phi_j^\dagger\phi_i)^2 \right] = 2a\Re \left[ (\phi_i\phi_j^\dagger)^2 \right], \tag{2.24}$$

where  $a$  is some real-valued constant.

Let us now turn the discussion to the terms  $|\phi_i|^2|\phi_k|^2$  in Eq. (2.21), where  $i \neq k$ . Assume that the fields  $\phi_i$  and  $\phi_k$  cannot be combined into one of the doublets  $\Phi_1, \Phi_2$ , or  $\Phi_3$ . Then, a general term of this type is on the form

$$(a|\phi_i|^2 + b|\phi_j|^2)|\phi_k|^2 + (c|\phi_i|^2 + d|\phi_j|^2)|\phi_l|^2, \tag{2.25}$$

where  $a, b, c$ , and  $d$  are real-valued constants and  $(\phi_i, \phi_j)^T, (\phi_k, \phi_l)^T \in \{\Phi_1, \Phi_2, \Phi_3\}$ . Application of the symmetries  $\mathcal{D}_2$  and  $\mathcal{D}_3$  yields the conditions  $a = d$  and  $b = c$ , and thus, we can rewrite the above part of the potential as

$$\frac{a+b}{2}(|\phi_i|^2 + |\phi_j|^2)(|\phi_k|^2 + |\phi_l|^2) + \frac{a-b}{2}(|\phi_i|^2 - |\phi_j|^2)(|\phi_k|^2 - |\phi_l|^2). \tag{2.26}$$

If  $(\phi_i, \phi_j)^T = \Phi_2$  and  $(\phi_k, \phi_l)^T = \Phi_3$ , then in general  $a \neq b$ , since  $\Phi_2$  and  $\Phi_3$  are  $\mathcal{D}_2$ -singlets. However, if  $(\phi_i, \phi_j)^T = \Phi_1$ , then  $a = b$  and the part in Eq. (2.26) which is proportional to  $(a - b)/2$  vanishes. If for the term  $|\phi_i|^2|\phi_j|^2$  in Eq. (2.21) we have  $(\phi_i, \phi_j)^T \in \{\Phi_1, \Phi_2, \Phi_3\}$ , then  $|\phi_i|^2|\phi_j|^2$  is a total singlet (on its own) and can be written directly into the scalar potential as  $a|\phi_i|^2|\phi_j|^2$ , where  $a$  is some real-valued constant. Moreover, the symmetries  $\mathcal{D}_2$  and  $\mathcal{D}_3$  enforce the products  $|\phi_i|^2$  and  $|\phi_i|^4$  [in Eq. (2.21)] to appear in the scalar potential only as

$$\begin{aligned} & \mu_1^2 (|\phi_1|^2 + |\phi_2|^2) + \mu_2^2 (|\phi_3|^2 + |\phi_4|^2) + \mu_3^2 (|\phi_5|^2 + |\phi_6|^2) \\ & + \kappa_1 (|\phi_1|^4 + |\phi_2|^4) + \kappa_2 (|\phi_3|^4 + |\phi_4|^4) + \kappa_3 (|\phi_5|^4 + |\phi_6|^4), \end{aligned} \quad (2.27)$$

where  $\mu_1^2, \mu_2^2, \mu_3^2, \kappa_1, \kappa_2,$  and  $\kappa_3$  are real-valued constants. In total, the most general scalar potential involving only the component fields of  $\Phi_1, \Phi_2,$  and  $\Phi_3$  is given by

$$\begin{aligned} V(\Phi_i) = & \mu_1^2 (|\phi_1|^2 + |\phi_2|^2) + \mu_2^2 (|\phi_3|^2 + |\phi_4|^2) + \mu_3^2 (|\phi_5|^2 + |\phi_6|^2) \\ & + \kappa_1 (|\phi_1|^2 + |\phi_2|^2)^2 + \kappa_2 (|\phi_3|^2 + |\phi_4|^2)^2 + \kappa_3 (|\phi_5|^2 + |\phi_6|^2)^2 \\ & + a_1 (|\phi_1|^2 + |\phi_2|^2) (|\phi_3|^2 + |\phi_4|^2) + a_2 (|\phi_1|^2 + |\phi_2|^2) (|\phi_5|^2 + |\phi_6|^2) \\ & + a_3 (|\phi_3|^2 + |\phi_4|^2) (|\phi_5|^2 + |\phi_6|^2) + a_4 (|\phi_3|^2 - |\phi_4|^2) (|\phi_5|^2 - |\phi_6|^2) \\ & + a_5 |\phi_1^\dagger \phi_2|^2 + a_6 |\phi_3^\dagger \phi_4|^2 + a_7 |\phi_5^\dagger \phi_6|^2 + a_8 [(\phi_1^\dagger \phi_2)^2 + (\phi_2^\dagger \phi_1)^2] \\ & + a_9 [(\phi_3^\dagger \phi_4)^2 + (\phi_4^\dagger \phi_3)^2] + a_{10} [(\phi_5^\dagger \phi_6)^2 + (\phi_6^\dagger \phi_5)^2] \\ & + a_{11} (\phi_1^\dagger \phi_2 + \phi_2^\dagger \phi_1) (\phi_3^\dagger \phi_4 + \phi_4^\dagger \phi_3) \\ & + a_{12} (\phi_1^\dagger \phi_2 + \phi_2^\dagger \phi_1) (\phi_5^\dagger \phi_6 + \phi_6^\dagger \phi_5) \\ & + a_{13} (\phi_3^\dagger \phi_4 + \phi_4^\dagger \phi_3) (\phi_5^\dagger \phi_6 + \phi_6^\dagger \phi_5) \\ & + a_{14} (\phi_3^\dagger \phi_4 - \phi_4^\dagger \phi_3) (\phi_5^\dagger \phi_6 - \phi_6^\dagger \phi_5), \end{aligned} \quad (2.28)$$

where  $a_1, a_2, \dots, a_{14}$  are real-valued constants. Note in Eq. (2.28), that the couplings to the operators  $\Phi_4, \phi_9,$  and  $\phi_{10}$  or  $|\theta|^2$  have been dropped, since these are irrelevant for the vacuum alignment of the fields  $\Phi_1, \Phi_2,$  and  $\Phi_3$  in  $\mathcal{G}$ -space. The  $SU(2)_{\text{acc}}$  symmetry properties of the potential  $V(\Phi_i)$  become more transparent when it is rewritten as

$$\begin{aligned} V(\Phi_i) = & \mu_1^2 \Phi_1^\dagger \Phi_1 + \mu_2^2 \Phi_2^\dagger \Phi_2 + \mu_3^2 \Phi_3^\dagger \Phi_3 + \kappa_1 (\Phi_1^\dagger \Phi_1)^2 + \kappa_2 (\Phi_2^\dagger \Phi_2)^2 \\ & + \kappa_3 (\Phi_3^\dagger \Phi_3)^2 + a_1 (\Phi_1^\dagger \Phi_1) (\Phi_2^\dagger \Phi_2) + a_2 (\Phi_1^\dagger \Phi_1) (\Phi_3^\dagger \Phi_3) \\ & + a_3 (\Phi_2^\dagger \Phi_2) (\Phi_3^\dagger \Phi_3) + V_\Delta(\Phi_1, \Phi_2) + V_\Delta(\Phi_1, \Phi_3) + V_\Delta(\Phi_2, \Phi_3), \end{aligned} \quad (2.29)$$

where the  $SU(2)_{\text{acc}}$  symmetry breaking parts can be symmetrically organized as

$$\begin{aligned}
V_{\Delta}(\Phi_1, \Phi_2) &= \frac{1}{2}a_5|\phi_1^\dagger\phi_2|^2 + \frac{1}{2}a_6|\phi_3^\dagger\phi_4|^2 \\
&+ \frac{1}{2}a_8\left[(\phi_1^\dagger\phi_2)^2 + (\phi_2^\dagger\phi_1)^2\right] + \frac{1}{2}a_9\left[(\phi_3^\dagger\phi_4)^2 + (\phi_4^\dagger\phi_3)^2\right] \\
&+ a_{11}\left(\phi_1^\dagger\phi_2 + \phi_2^\dagger\phi_1\right)\left(\phi_3^\dagger\phi_4 + \phi_4^\dagger\phi_3\right), \\
V_{\Delta}(\Phi_1, \Phi_3) &= \frac{1}{2}a_5|\phi_1^\dagger\phi_2|^2 + \frac{1}{2}a_7|\phi_5^\dagger\phi_6|^2 \\
&+ \frac{1}{2}a_8\left[(\phi_1^\dagger\phi_2)^2 + (\phi_2^\dagger\phi_1)^2\right] + \frac{1}{2}a_{10}\left[(\phi_5^\dagger\phi_6)^2 + (\phi_6^\dagger\phi_5)^2\right] \\
&+ a_{12}\left(\phi_1^\dagger\phi_2 + \phi_2^\dagger\phi_1\right)\left(\phi_5^\dagger\phi_6 + \phi_6^\dagger\phi_5\right), \\
V_{\Delta}(\Phi_2, \Phi_3) &= \frac{1}{2}a_6|\phi_3^\dagger\phi_4|^2 + \frac{1}{2}a_7|\phi_5^\dagger\phi_6|^2 + a_4\left(|\phi_3|^2 - |\phi_4|^2\right)\left(|\phi_5|^2 - |\phi_6|^2\right) \\
&+ \frac{1}{2}a_9\left[(\phi_3^\dagger\phi_4)^2 + (\phi_4^\dagger\phi_3)^2\right] + \frac{1}{2}a_{10}\left[(\phi_5^\dagger\phi_6)^2 + (\phi_6^\dagger\phi_5)^2\right] \\
&+ a_{13}\left(\phi_3^\dagger\phi_4 + \phi_4^\dagger\phi_3\right)\left(\phi_5^\dagger\phi_6 + \phi_6^\dagger\phi_5\right) \\
&+ a_{14}\left(\phi_3^\dagger\phi_4 - \phi_4^\dagger\phi_3\right)\left(\phi_5^\dagger\phi_6 - \phi_6^\dagger\phi_5\right). \tag{2.30}
\end{aligned}$$

In Eq. (2.28), we will assume  $\kappa_1, \kappa_2, \kappa_3 > 0$  and  $a_{11}, a_{13} > 0$  and we will choose all other coupling constants to be negative. We shall briefly outline the impact which the operators in Eq. (2.30) have on the vacuum structure. First, we note that the term with the coefficient  $a_4$  tends (for large values of  $|a_4|$ ) to induce a splitting between  $|\langle\phi_3\rangle|$  and  $|\langle\phi_4\rangle|$  as well as between  $|\langle\phi_5\rangle|$  and  $|\langle\phi_6\rangle|$ . Second, we observe that the term with the coefficient  $a_{14}$  prefers (for large values of  $|a_{14}|$ ) arbitrary relative phases (which are different from 0 and  $\pi$ ) between  $\langle\phi_3\rangle$  and  $\langle\phi_4\rangle$  as well as between  $\langle\phi_5\rangle$  and  $\langle\phi_6\rangle$ . However, using App. C, we see that for the parameter range

$$a_6a_7 > (8a_4)^2 \quad \text{and} \quad a_9a_{10} > a_{14}^2, \tag{2.31}$$

the potential  $V(\Phi_i)$  is minimized by the VEVs of the component fields which are pairwise degenerate in their magnitudes, *i.e.*, they satisfy

$$|\langle\phi_1\rangle| = |\langle\phi_2\rangle|, \quad |\langle\phi_3\rangle| = |\langle\phi_4\rangle|, \quad |\langle\phi_5\rangle| = |\langle\phi_6\rangle| \tag{2.32a}$$

and are also pairwise relatively real, *i.e.*,

$$\frac{\langle\phi_1\rangle}{\langle\phi_2\rangle}, \frac{\langle\phi_3\rangle}{\langle\phi_4\rangle}, \frac{\langle\phi_5\rangle}{\langle\phi_6\rangle} \in \{-1, 1\}, \tag{2.32b}$$

where, in addition, the choice  $a_{12} < 0$  and  $a_{11}, a_{13} > 0$  implies a correlation between the different pairs of VEVs in terms of

$$\frac{\langle\phi_1\rangle}{\langle\phi_2\rangle} \frac{\langle\phi_5\rangle}{\langle\phi_6\rangle} = 1 \quad \text{and} \quad \frac{\langle\phi_1\rangle}{\langle\phi_2\rangle} \frac{\langle\phi_3\rangle}{\langle\phi_4\rangle} = -1, \tag{2.32c}$$



*i.e.*, the relative sign between  $\langle\phi_1\rangle$  and  $\langle\phi_2\rangle$  is equal to the relative sign between  $\langle\phi_5\rangle$  and  $\langle\phi_6\rangle$  and opposite to the relative sign between  $\langle\phi_3\rangle$  and  $\langle\phi_4\rangle$ . In  $\mathcal{G}$ -space, the VEVs of  $\Phi_1, \Phi_2$ , and  $\Phi_3$  can therefore be written as

$$\langle\Phi_i\rangle = \frac{|\Phi_i|}{\sqrt{2}} e^{i\alpha_i} \begin{pmatrix} 1 \\ \pm 1 \end{pmatrix} \quad (i = 1, 3) \quad \text{and} \quad \langle\Phi_2\rangle = \frac{|\Phi_2|}{\sqrt{2}} e^{i\alpha_2} \begin{pmatrix} 1 \\ \mp 1 \end{pmatrix}, \quad (2.32d)$$

where  $\alpha_1, \alpha_2$ , and  $\alpha_3$  are arbitrary phases. Thus, we see that  $\langle\Phi_1\rangle$  is parallel to  $\langle\Phi_3\rangle$  whereas  $\langle\Phi_2\rangle$  is orthogonal to  $\langle\Phi_1\rangle$  and  $\langle\Phi_3\rangle$ .

### The potential of the fields $\Phi'_1, \Phi'_2$ , and $\Phi'_3$

In analogy with the potential  $V(\Phi_i)$ , we will denote by  $V(\Phi'_i)$  the most general renormalizable scalar potential involving only the primed fields  $\Phi'_1, \Phi'_2$ , and  $\Phi'_3$ . Among the symmetries  $\mathcal{D}_2, \mathcal{D}_3, \mathcal{D}_4$ , and  $\mathcal{D}_5$  which generate the discrete group  $\mathcal{G}$ , the group operations  $\mathcal{D}_2, \mathcal{D}_3$ , and  $\mathcal{D}_5$  act diagonally on the fields  $\Phi_i$  and  $\Phi'_i$ , for  $i = 1, 2, 3$ . Now, the action  $\mathcal{D}_4 : \Phi_i \rightarrow D(C_a)\Phi_i$  ( $i = 1, 2, 3$ ) (under which  $\Phi'_1, \Phi'_2$ , and  $\Phi'_3$  are singlets) is for the fields  $\Phi_i$  identical with the subsequent application of the transformations  $\mathcal{D}_3, \mathcal{D}_5$ , and  $\mathcal{D}_3$  (in this order). However, since  $\mathcal{D}_3$  and  $\mathcal{D}_5$  act diagonally on  $\Phi_i$  and  $\Phi'_i$ , the discrete group  $\mathcal{G}$  imposes identical constraints on the potentials  $V(\Phi_i)$  and  $V(\Phi'_i)$ . Next, taking into account that the fields  $\Phi_i$  and  $\Phi'_i$  carry opposite  $\mathcal{D}_6$  charges, it is seen that  $V(\Phi_i)$  and  $V(\Phi'_i)$  have similar structures. As a result, the minimization of  $V(\Phi'_i)$  goes along the same lines as the minimization of  $V(\Phi_i)$ . We can therefore define  $V(\Phi'_i)$  as the potential which is obtained from the general form of  $V(\Phi_i)$  in Eq. (2.28) by making the identifications

$$\Phi_i \rightarrow \Phi'_i, \quad \mu_i \rightarrow \mu'_i, \quad \kappa_i \rightarrow \kappa'_i, \quad a_k \rightarrow a'_k, \quad (2.33)$$

where  $i = 1, 2, 3$  and  $k = 1, 2, \dots, 14$ . Note that in Eq. (2.33) all coupling constants  $\mu'_i, \kappa'_i$ , and  $a'_k$  are real-valued. In  $V(\Phi'_i)$ , we assume that  $\kappa'_1, \kappa'_2, \kappa'_3 > 0$  and we will choose all other coupling constants to be negative. If we, in analogy with the potential  $V(\Phi_i)$ , require that

$$a'_6 a'_7 > (8a'_4)^2 \quad \text{and} \quad a'_9 a'_{10} > (a'_{14})^2, \quad (2.34)$$

the potential  $V(\Phi'_i)$  is minimized by the VEVs of the primed fields, which are pairwise degenerate in their magnitudes, *i.e.*, they satisfy

$$|\langle\phi'_1\rangle| = |\langle\phi'_2\rangle|, \quad |\langle\phi'_3\rangle| = |\langle\phi'_4\rangle|, \quad |\langle\phi'_5\rangle| = |\langle\phi'_6\rangle|, \quad (2.35a)$$

and are also pairwise relatively real, obeying

$$\frac{\langle\phi'_1\rangle}{\langle\phi'_2\rangle} = \frac{\langle\phi'_3\rangle}{\langle\phi'_4\rangle} = \frac{\langle\phi'_5\rangle}{\langle\phi'_6\rangle} = \pm 1. \quad (2.35b)$$

In  $\mathcal{G}$ -space, the VEVs are therefore given by

$$\langle\Phi'_i\rangle = \frac{|\langle\Phi'_i\rangle|}{\sqrt{2}} e^{i\alpha'_i} \begin{pmatrix} 1 \\ \pm 1 \end{pmatrix} \quad (i = 1, 2, 3), \quad (2.35c)$$

where  $\alpha'_1, \alpha'_2$ , and  $\alpha'_3$  are arbitrary phases. Note that the VEVs  $\langle\Phi'_i\rangle$  ( $i = 1, 2, 3$ ) are parallel.

### Mixing among the fields $\Phi_1, \Phi_2, \Phi_3$ and $\Phi'_1, \Phi'_2, \Phi'_3$

In the scalar potential, the transformation  $\mathcal{D}_6$  requires all renormalizable terms mixing the unprimed component fields  $\phi_i$  ( $i = 1, \dots, 6$ ) of  $\Phi_1, \Phi_2$ , and  $\Phi_3$  with the primed component fields  $\phi'_j$  ( $j = 1, 2, \dots, 6$ ) of  $\Phi'_1, \Phi'_2$ , and  $\Phi'_3$ , to be actually either a two- or a four-fold product of these fields. Taking the combinations in Eq. (2.12) and the product  $\Phi_2^\dagger M \Phi_2$  into account (which are singlets under  $\mathcal{D}_6$ ), it is seen that the  $\mathcal{D}_1$ -invariant operator products, which mix the fields  $\phi_i$  and  $\phi'_j$ , are of the types

$$(\phi'_i{}^\dagger \phi'_j) \Phi_1^\dagger M \Phi_1, \quad (\phi'_i{}^\dagger \phi'_j) \Phi_2^\dagger M \Phi_2, \quad (\phi'_i{}^\dagger \phi'_j) \Phi_3^\dagger M \Phi_3, \quad (2.36)$$

where  $i, j = 1, \dots, 6$ . The transformation  $\mathcal{D}_4$ , which acts only on the fields  $\Phi_1, \Phi_2$ , and  $\Phi_3$ , requires the matrices  $M$  in Eq. (2.36) to be on diagonal form, *i.e.*, the products in Eq. (2.36) decompose into the terms  $\sim \phi'_i{}^\dagger \phi'_j |\phi_k|^2$ , where  $k = 1, \dots, 6$ . Moreover, the symmetries  $\mathcal{D}_5$  and  $\mathcal{D}_6$  imply that the operators in Eq. (2.36) are all in fact  $\sim |\phi'_i|^2 |\phi_j|^2$ . As a result, the most general renormalizable interactions of the fields  $\Phi_1, \Phi_2, \Phi_3$  with the fields  $\Phi'_1, \Phi'_2, \Phi'_3$  are

$$\begin{aligned} V_{\text{mix}} &= (|\phi'_1|^2 + |\phi'_2|^2) \\ &\times [b_1 (|\phi_1|^2 + |\phi_2|^2) + b_2 (|\phi_3|^2 + |\phi_4|^2) + b_3 (|\phi_5|^2 + |\phi_6|^2)] \\ &+ b_4 (|\phi'_1|^2 - |\phi'_2|^2) (|\phi_1|^2 - |\phi_2|^2) \\ &+ (|\phi'_3|^2 + |\phi'_4|^2) \\ &\times [b_5 (|\phi_1|^2 + |\phi_2|^2) + b_6 (|\phi_3|^2 + |\phi_4|^2) + b_7 (|\phi_5|^2 + |\phi_6|^2)] \\ &+ (|\phi'_3|^2 - |\phi'_4|^2) [b_8 (|\phi_3|^2 - |\phi_4|^2) + b_9 (|\phi_5|^2 - |\phi_6|^2)] \\ &+ (|\phi'_5|^2 + |\phi'_6|^2) \\ &\times [b_{10} (|\phi_1|^2 + |\phi_2|^2) + b_{11} (|\phi_3|^2 + |\phi_4|^2) + b_{12} (|\phi_5|^2 + |\phi_6|^2)] \\ &+ (|\phi'_5|^2 - |\phi'_6|^2) [b_{13} (|\phi_3|^2 - |\phi_4|^2) + b_{14} (|\phi_5|^2 - |\phi_6|^2)], \end{aligned} \quad (2.37)$$

where  $b_1, b_2, \dots, b_{14}$  are real-valued constants. In Eq. (2.37), we will assume all coupling constants to be positive. The relation to the  $SU(2)_{\text{acc}}$  symmetries becomes more evident, when  $V_{\text{mix}}$  is rewritten as

$$\begin{aligned} V_{\text{mix}} &= \Phi_1'^\dagger \Phi_1' [b_1 \Phi_1^\dagger \Phi_1 + b_2 \Phi_2^\dagger \Phi_2 + b_3 \Phi_3^\dagger \Phi_3] \\ &+ \Phi_2'^\dagger \Phi_2' [b_5 \Phi_1^\dagger \Phi_1 + b_6 \Phi_2^\dagger \Phi_2 + b_7 \Phi_3^\dagger \Phi_3] \\ &+ \Phi_3'^\dagger \Phi_3' [b_{10} \Phi_1^\dagger \Phi_1 + b_{11} \Phi_2^\dagger \Phi_2 + b_{12} \Phi_3^\dagger \Phi_3] \\ &+ \sum_{i=1}^3 V_\Delta(\Phi_i, \Phi'_i) + V_\Delta(\Phi_2, \Phi'_3) + V_\Delta(\Phi_3, \Phi'_2), \end{aligned} \quad (2.38)$$

where the  $SU(2)_{\text{acc}}$  symmetry breaking parts are given by

$$\begin{aligned}
V_{\Delta}(\Phi_1, \Phi'_1) &= b_4 (|\phi_1|^2 - |\phi_2|^2) (|\phi'_1|^2 - |\phi'_2|^2), \\
V_{\Delta}(\Phi_2, \Phi'_2) &= b_8 (|\phi_3|^2 - |\phi_4|^2) (|\phi'_3|^2 - |\phi'_4|^2), \\
V_{\Delta}(\Phi_3, \Phi'_3) &= b_{14} (|\phi_5|^2 - |\phi_6|^2) (|\phi'_5|^2 - |\phi'_6|^2), \\
V_{\Delta}(\Phi_2, \Phi'_3) &= b_{13} (|\phi_3|^2 - |\phi_4|^2) (|\phi'_5|^2 - |\phi'_6|^2), \\
V_{\Delta}(\Phi_3, \Phi'_2) &= b_9 (|\phi_5|^2 - |\phi_6|^2) (|\phi'_3|^2 - |\phi'_4|^2).
\end{aligned} \tag{2.39}$$

In order to recover the (same) vacuum alignment mechanism that is operative for the potentials  $V(\Phi_i)$ ,  $V(\Phi'_i)$ , and  $V(\Phi_4)$  also for the full SM singlet scalar potential  $V \equiv V(\Phi_i) + V(\Phi'_i) + V(\Phi_4) + V_{\text{mix}}$ , we will have to ensure that the mixed terms in the potential  $V_{\text{mix}}$  do not induce a splitting between the pairwise degenerate magnitudes of the VEVs. For this purpose, let us redefine the potentials  $V(\Phi_i)$ ,  $V(\Phi'_i)$ , and  $V_{\text{mix}}$  as follows:

$$\begin{aligned}
V(\Phi_i) &\rightarrow V(\Phi_i) - \frac{1}{3}a_5|\phi_1^\dagger\phi_2|^2 - \frac{1}{2}a_6|\phi_3^\dagger\phi_4|^2 - \frac{1}{2}a_7|\phi_5^\dagger\phi_6|^2, \\
V(\Phi'_i) &\rightarrow V(\Phi'_i) - \frac{1}{3}a'_5|\phi_1'^\dagger\phi_2'|^2 - \frac{1}{2}a'_6|\phi_3'^\dagger\phi_4'|^2 - \frac{1}{2}a'_7|\phi_5'^\dagger\phi_6'|^2, \\
V_{\Delta}(\Phi_1, \Phi'_1) &\rightarrow V_{\Delta}(\Phi_1, \Phi'_1) + \frac{1}{3}a_5|\phi_1^\dagger\phi_2|^2 + \frac{1}{3}a'_5|\phi_1'^\dagger\phi_2'|^2, \\
V_{\Delta}(\Phi_2, \Phi'_2) &\rightarrow V_{\Delta}(\Phi_2, \Phi'_2) + \frac{1}{4}a_6|\phi_3^\dagger\phi_4|^2 + \frac{1}{4}a'_6|\phi_3'^\dagger\phi_4'|^2, \\
V_{\Delta}(\Phi_3, \Phi'_3) &\rightarrow V_{\Delta}(\Phi_3, \Phi'_3) + \frac{1}{4}a_7|\phi_5^\dagger\phi_6|^2 + \frac{1}{4}a'_7|\phi_5'^\dagger\phi_6'|^2, \\
V_{\Delta}(\Phi_2, \Phi'_3) &\rightarrow V_{\Delta}(\Phi_2, \Phi'_3) + \frac{1}{4}a_6|\phi_3^\dagger\phi_4|^2 + \frac{1}{4}a'_7|\phi_5'^\dagger\phi_6'|^2, \\
V_{\Delta}(\Phi_3, \Phi'_2) &\rightarrow V_{\Delta}(\Phi_3, \Phi'_2) + \frac{1}{4}a_7|\phi_5^\dagger\phi_6|^2 + \frac{1}{4}a'_6|\phi_3'^\dagger\phi_4'|^2,
\end{aligned} \tag{2.40}$$

which leaves the total potential  $V = V(\Phi_i) + V(\Phi'_i) + V(\Phi_4) + V_{\text{mix}}$  invariant. Now, if the coupling constants in  $V(\Phi_i)$ ,  $V(\Phi'_i)$ , and  $V_{\text{mix}}$  satisfy

$$\begin{aligned}
a_5a'_5 &> (6b_4)^2, & a_6a'_6 &> (8b_8)^2, & a_7a'_7 &> (8b_{14})^2, \\
a_6a'_7 &> (8b_{13})^2, & a_7a'_6 &> (8b_9)^2,
\end{aligned} \tag{2.41}$$

it is seen with App. C, that the total multi-scalar potential  $V$  is indeed minimized by the VEVs of Eqs. (2.20), (2.32), and (2.35). Since the  $U(1)$  and discrete symmetries are only approximately conserved in the lepton sector, the vacuum structure as specified in Eqs. (2.20), (2.32), and (2.35) has important impact on the generation of the lepton mass matrices via non-renormalizable Yukawa interactions. As it will turn out in the following sections, the orientation of the VEVs in  $\mathcal{G}$ -space will lead to maximal  $\nu_\mu$ - $\nu_\tau$ -mixing and the strict hierarchy of charged lepton masses.

## 2.4 Yukawa interactions of the charged leptons

One way to understand the hierarchical pattern of fermion masses is to assume horizontal symmetries which are sequentially broken. In our model, we assume that the SM singlet scalar fields break the horizontal symmetries by acquiring their VEVs at a high mass scale (somewhat below the fundamental scale  $M_1$ ), thereby giving rise to a small expansion parameter

$$\epsilon \simeq \frac{\langle \Phi_i \rangle}{M_1} \simeq \frac{\langle \Phi'_j \rangle}{M_1} \simeq \frac{\langle \phi_9 \rangle}{M_1} \simeq \frac{\langle \phi_{10} \rangle}{M_1} \simeq \frac{\langle \theta \rangle}{M_1} \simeq 10^{-1}, \quad (2.42)$$

where  $i = 1, 2, 3, 4$  and  $j = 1, 2, 3$ . Such small hierarchies can emerge from large hierarchies in supersymmetric theories when the scalar fields acquire their VEVs along a D-flat direction [57]. Moreover, we suppose that the effective Yukawa coupling operators  $\mathcal{O}_{\alpha\beta}^\ell$  which generate the entries in the charged lepton mass matrix via the mass terms

$$\mathcal{L}_Y^\ell = \bar{\ell}_\alpha H \mathcal{O}_{\alpha\beta}^\ell E_\beta + \text{h.c.}, \quad (2.43)$$

where  $\alpha, \beta = e, \mu, \tau$ , arise from the Froggatt-Nielsen mechanism [51] (see Fig. 2.1). Consequently, the structure of the operators  $\mathcal{O}_{\alpha\beta}^\ell$  is (almost) completely determined

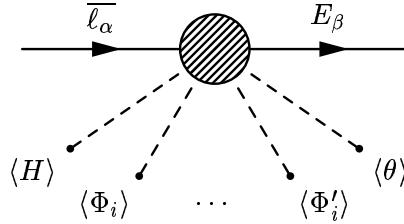


Figure 2.1: Non-renormalizable terms generating the effective Yukawa couplings in the matrix  $(\mathcal{O}_{\alpha\beta}^\ell)$ .

by the horizontal charges of  $\ell_\alpha$ ,  $E_\beta$ , and the SM singlet scalars, *i.e.*, it is not necessary to consider in detail the fundamental theory of the Froggatt-Nielsen states which are integrated out.

We will denote the total number of times that the component fields  $\phi_1, \phi_2, \dots, \phi_6$  appear in the operator  $\mathcal{O}_{\alpha\beta}^\ell$  by  $n_1$  and the total number of times that their complex conjugates  $\phi_1^\dagger, \phi_2^\dagger, \dots, \phi_6^\dagger$  appear in the operator  $\mathcal{O}_{\alpha\beta}^\ell$  by  $n_2$ . Now, invariance under  $\mathcal{D}_1$  implies that for the first column of the Yukawa interaction matrix  $(\mathcal{O}_{\alpha\beta}^\ell)$ , *i.e.*, for  $\beta = e$ , it must hold that  $n_1 - n_2 = 4$ . For the second and third column of the Yukawa interaction matrix, *i.e.*, for  $\beta = \mu, \tau$ , the discrete symmetry  $\mathcal{D}_1$  instead requires that  $n_1 - n_2 = 1$ . In addition, we conclude from the transformation properties of the fundamental Froggatt-Nielsen states under  $\mathcal{D}_6$ , that the operators  $\mathcal{O}_{\alpha\mu}^\ell$  and  $\mathcal{O}_{\alpha\tau}^\ell$ , where  $\alpha = e, \mu, \tau$ , can neither involve the field  $\phi_9$  nor the field  $\phi_{10}$ . This is, however, not true for the operators  $\mathcal{O}_{\alpha e}^\ell$  ( $\alpha = e, \mu, \tau$ ) in the first column of the effective Yukawa coupling matrix.

### 2.4.1 The first row and column of the charged lepton mass matrix

Invariance under transformations of the  $U(1)$  symmetries requires the  $U(1)$  charges of the entries  $\mathcal{O}_{e\mu}^\ell$  and  $\mathcal{O}_{e\tau}^\ell$  in the first row of the effective Yukawa coupling matrix ( $\mathcal{O}_{\alpha\beta}^\ell$ ) to be  $(1, -1, 0)$ . Since the fields  $\phi_9$  and  $\phi_{10}$  cannot be involved in the generation of the  $e$ - $\mu$ - and  $e$ - $\tau$ -elements of the charged lepton mass matrix, the  $U(1)$  charge assignment immediately implies that any mass operator giving rise to these  $e$ - $\mu$ - and  $e$ - $\tau$ -elements must involve the term  $\sim \Phi_1^T M \theta^2 / (M_1)^3$ , where  $M$  denotes again an arbitrary complex  $2 \times 2$  matrix. Next, the symmetries  $\mathcal{D}_5$  and  $\mathcal{D}_6$  yield to leading order for the operators  $\mathcal{O}_{e\mu}^\ell$  and  $\mathcal{O}_{e\tau}^\ell$  the two possible terms  $\sim \phi_1 \phi_1' \theta^2 / (M_1)^4$  and  $\sim \phi_2 \phi_2' \theta^2 / (M_1)^4$ . In conjunction with the requirement  $n_1 - n_2 = 1$ , the symmetry  $\mathcal{D}_6$  implies that any further operators contributing to  $\mathcal{O}_{e\mu}^\ell$  or  $\mathcal{O}_{e\tau}^\ell$  must have at least two powers of mass dimension more than the terms  $\phi_1 \phi_1' \theta^2 / (M_1)^4$  and  $\phi_2 \phi_2' \theta^2 / (M_1)^4$ . We will therefore neglect these additional operators.

From the transformation properties of the right-handed electron  $E_e$  and the fundamental Froggatt-Nielsen states under  $\mathcal{D}_1$  and  $\mathcal{D}_6$ , we conclude that  $\mathcal{O}_{ee}^\ell$ ,  $\mathcal{O}_{\mu e}^\ell$ , and  $\mathcal{O}_{\tau e}^\ell$  in the first column of the effective Yukawa coupling matrix must involve at least a four-fold product of component fields taken from  $\Phi_1$ ,  $\Phi_2$ , or  $\Phi_3$ , times a field taken from the set  $\{\phi_9, \phi_{10}\}$ . Possible lowest-dimensional contributions to  $\mathcal{O}_{ee}^\ell$ , which are consistent with the symmetries of our model, are, *e.g.*, given by  $\sim \phi_{10} [(\phi_3)^4 + (\phi_4)^4] / (M_1)^5$  and  $\sim \phi_{10} (\phi_3)^2 (\phi_4)^2 / (M_1)^5$ . For brevity, we will take the operator

$$\mathcal{O}_{ee}^\ell = \frac{\phi_{10}}{(M_1)^5} [(\phi_3)^4 + (\phi_4)^4] \quad (2.44)$$

as a representative of these contributions. The remaining operators  $\mathcal{O}_{\mu e}^\ell$  and  $\mathcal{O}_{\tau e}^\ell$  have a mass dimension that is greater than or equal to the mass dimension of the terms in Eq. (2.44). However, the effects of these terms on the leptonic mixing angles will turn out to be negligible in comparison with the contributions coming from other entries of the charged lepton mass matrix.

In total, the first row of the effective Yukawa coupling matrix of the charged leptons, which is consistent with all of the discrete symmetries, is to leading order

$$(\mathcal{O}_{e\alpha}^\ell) = (A_1 [(\phi_3)^4 + (\phi_4)^4] \quad B_1 [\phi_1 \phi_1' - \phi_2 \phi_2'] \quad B_1 [\phi_1 \phi_1' + \phi_2 \phi_2']). \quad (2.45a)$$

Here, the dimensionful coefficients  $A_1$  and  $B_1$  are given by

$$A_1 = Y_a^\ell \frac{\phi_{10}}{(M_1)^5}, \quad B_1 = Y_b^\ell \frac{\theta^2}{(M_1)^4}, \quad (2.45b)$$

where the quantities  $Y_a^\ell$  and  $Y_b^\ell$  are arbitrary order unity coefficients and  $M_1$  is the high mass scale of the intermediate Froggatt-Nielsen states. Note that at the level of the fundamental theory, the permutation symmetry  $\mathcal{D}_4$ , which interchanges the

second and third generations of the leptons, is also propagated to the heavy Froggatt-Nielsen states. This establishes a degeneracy of the associated Yukawa couplings and the explicit masses of these states, which is then translated into a degeneracy of the corresponding effective Yukawa couplings of the low-energy theory.

## 2.4.2 The 2-3-submatrix of the charged lepton mass matrix

In the 2-3-submatrix of the charged lepton mass matrix, the U(1) charges of the operators  $\mathcal{O}_{\alpha\beta}^\ell$  ( $\alpha, \beta = \mu, \tau$ ) must be (0, 0, 0). The lowest dimensional operators which fulfill this condition as well as the constraint  $n_1 - n_2 = 1$  are proportional to  $\Phi_2^T M/M_1$  or  $\Phi_3^T M\theta/(M_1)^2$ . Furthermore, invariance under transformation of the discrete symmetries  $\mathcal{D}_5$  and  $\mathcal{D}_6$  implies that the lowest dimensional operators  $\mathcal{O}_{\alpha\beta}^\ell$  in the 2-3-submatrix with  $n_1 - n_2 = 1$  are of the types

$$\frac{\phi'_3\phi_3}{(M_1)^2}, \quad \frac{\phi'_4\phi_4}{(M_1)^2}, \quad \frac{\phi'_5\phi_5\theta}{(M_1)^3}, \quad \frac{\phi'_6\phi_6\theta}{(M_1)^3}. \quad (2.46)$$

Thus, the most general 2-3-submatrix of the matrix ( $\mathcal{O}_{\alpha\beta}^\ell$ ), which involves only these combinations and is invariant under the remaining discrete symmetries, is found to be

$$\begin{pmatrix} C(\phi'_3\phi_3 - \phi'_4\phi_4) + D(\phi'_5\phi_5 - \phi'_6\phi_6) & 0 \\ 0 & C(\phi'_3\phi_3 + \phi'_4\phi_4) + D(\phi'_5\phi_5 + \phi'_6\phi_6) \end{pmatrix}. \quad (2.47a)$$

Here, the dimensionful coefficients  $C$  and  $D$  are given by

$$C = Y_c^\ell \frac{1}{(M_1)^2}, \quad D = Y_d^\ell \frac{\theta}{(M_1)^3}, \quad (2.47b)$$

where the quantities  $Y_c^\ell$  and  $Y_d^\ell$  are arbitrary order unity coefficients. Actually, contributions to the next-leading operators  $\mathcal{O}_{\mu\tau}^\ell$  and  $\mathcal{O}_{\tau\mu}^\ell$  are, *e.g.*, given by

$$\mu\text{-}\tau : \quad \frac{1}{(M_1)^4} (a_1\phi_7\phi_8^\dagger + a_2\phi_8\phi_7^\dagger)(\phi_3 + \phi_4)\phi'_3, \quad (2.48a)$$

$$\tau\text{-}\mu : \quad \frac{1}{(M_1)^4} (a_2\phi_7\phi_8^\dagger + a_1\phi_8\phi_7^\dagger)(\phi_3 - \phi_4)\phi'_3, \quad (2.48b)$$

where  $a_1$  and  $a_2$  are some complex-valued constants. Note that the terms in Eqs. (2.48) carry only one unit of mass dimension more than, *e.g.*, the term  $\phi'_5\phi_5\theta/(M_1)^3$  in Eq. (2.47a). When diagonalizing the mass matrix, however, it will turn out that the associated corrections to the leptonic mixing parameters and the lepton masses are in fact negligible.

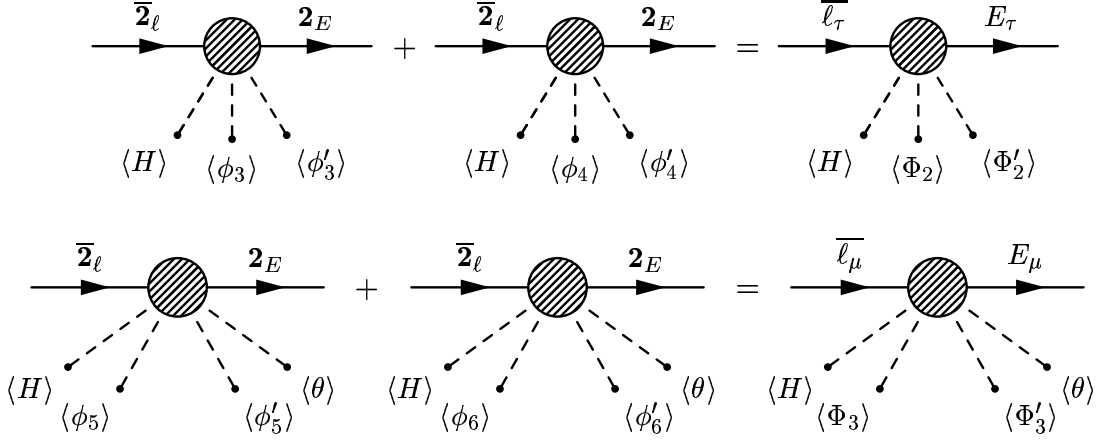


Figure 2.2: Froggatt-Nielsen type diagrams which generate the hierarchy  $m_\mu \ll m_\tau$  in the 2-3 subsector of the charged leptons. The dimension-six operators add up to  $\sim m_\tau \bar{\ell}_\tau E_\tau$  (top panel). The dimension-seven operators add up to  $\sim m_\mu \bar{\ell}_\mu E_\mu$  (bottom panel).

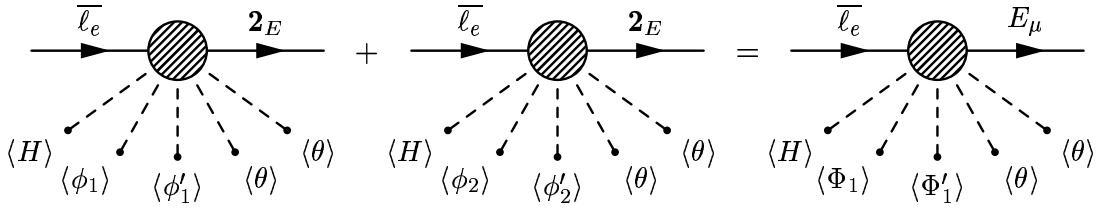


Figure 2.3: Effective Yukawa couplings  $\sim \bar{\ell}_e 2_E$  in the first row of the charged lepton mass matrix. The dimension-eight terms add up to  $\sim m_{e\mu} \bar{\ell}_e E_\mu$ , thereby generating a nonzero  $e$ - $\mu$ -mixing in the charged lepton sector.

### 2.4.3 The charged lepton mass matrix

Combining the results of Secs. 2.4.1 and 2.4.2, the leading order effective Yukawa coupling matrix of the charged leptons is

$$(\mathcal{O}_{\alpha\beta}^\ell) = \begin{pmatrix} A_1 [(\phi_3)^4 + (\phi_4)^4] & B_1 [\phi_1 \phi'_1 - \phi_2 \phi'_2] & B_1 [\phi_1 \phi'_1 + \phi_2 \phi'_2] \\ 0 & C(\phi'_3 \phi_3 - \phi'_4 \phi_4) + D(\phi'_5 \phi_5 - \phi'_6 \phi_6) & 0 \\ 0 & 0 & C(\phi'_3 \phi_3 + \phi'_4 \phi_4) + D(\phi'_5 \phi_5 + \phi'_6 \phi_6) \end{pmatrix}, \quad (2.49)$$

where the dimensionful couplings  $A_1$ ,  $B_1$ ,  $C$ , and  $D$  are given in Eqs. (2.45b) and (2.47b), respectively. Inserting the VEVs in Eqs. (2.35) and (2.32) into the corresponding operators of the matrix  $(\mathcal{O}_{\alpha\beta}^\ell)$ , we observe that, due to the vacuum alignment mechanism of the SM singlet scalar fields, in some of the entries of the matrix  $((M_\ell)_{\alpha\beta})$ , the spontaneously generated effective mass terms of a given order exactly cancel, whereas in other entries they do not (see Figs. 2.2 and 2.3). Furthermore, the vacuum alignment mechanism correlates these cancellations in the different entries

of the matrix  $((M_\ell)_{\alpha\beta})$  in such a way that after SSB the charged lepton mass matrix  $M_\ell$  can be of the two possible asymmetric forms

$$M_\ell \simeq m_\ell \begin{pmatrix} \epsilon^3 & \epsilon^2 & \epsilon^4 \\ \epsilon^3 & \epsilon & \epsilon^2 \\ \epsilon^3 & \epsilon^2 & 1 \end{pmatrix} \quad \text{and} \quad M_\ell \simeq m_\ell \begin{pmatrix} \epsilon^3 & \epsilon^4 & \epsilon^2 \\ \epsilon^3 & 1 & \epsilon^2 \\ \epsilon^3 & \epsilon^2 & \epsilon \end{pmatrix}, \quad (2.50)$$

where we have also introduced the appropriate orders of magnitude for the matrix elements  $(M_\ell)_{\mu e}$  and  $(M_\ell)_{\tau e}$  as well as for the ‘‘phenomenological’’ (in contrast to exact) texture zeros arising in Eqs. (2.45a) and (2.47a). Here,  $m_\ell$  is the absolute charged lepton mass scale. Note that a permutation of the second and third generations  $\ell_\mu \leftrightarrow \ell_\tau$ ,  $E_\mu \leftrightarrow E_\tau$  leads from one solution to another. Let us consider the first one for our remaining discussion.

## 2.5 Yukawa interactions of the neutrinos

We shall now consider the effective Yukawa coupling operators  $\mathcal{O}_{\alpha\beta}^\nu$  which generate the entries in the neutrino mass matrix  $M_\nu$  via the mass terms

$$\mathcal{L}_Y^\nu = \overline{\ell}_\alpha^c \frac{H^2}{M_2} \mathcal{O}_{\alpha\beta}^\nu \ell_\beta + \text{h.c.}, \quad (2.51)$$

where  $\alpha, \beta = e, \mu, \tau$  and  $M_2$  is the relevant high mass scale which is responsible for the smallness of the neutrino masses in comparison with the charged lepton masses. Since the SM singlet neutrinos as well as the Higgs doublet are  $\mathcal{D}_1$ -singlets, the presence of the fields  $\Phi_1, \Phi_2$ , and  $\Phi_3$  (which transform non-trivially under  $\mathcal{D}_1$ ) in the operators  $\mathcal{O}_{\alpha\beta}^\nu$  is forbidden. Hence, the only scalar fields that can be involved in the leading order operators  $\mathcal{O}_{\alpha\beta}^\nu$  are  $\Phi_4, \phi_9, \phi_{10}$ , and  $\theta$ .

### 2.5.1 Effective Yukawa interactions of the neutrinos

The operators  $\mathcal{O}_{\mu\mu}^\nu, \mathcal{O}_{\mu\tau}^\nu, \mathcal{O}_{\tau\mu}^\nu$ , and  $\mathcal{O}_{\tau\tau}^\nu$  must have the U(1) charge structure  $(0, -2, 0)$ . An example of the lowest dimensional operators which achieve this is

$$\sim \frac{\phi_9 \phi_{10} \theta}{(M_1)^5} \left[ (\phi_7^\dagger)^2 + (\phi_8^\dagger)^2 \right]. \quad (2.52)$$

Since the U(1) charge structure of the entry  $\mathcal{O}_{ee}^\nu$  is  $(-2, 0, 0)$ , the operator  $\mathcal{O}_{ee}^\nu$  is to leading order

$$\mathcal{O}_{ee}^\nu = Y_a^\nu \frac{\phi_9 \phi_{10} \theta}{(M_1)^3}, \quad (2.53)$$

where  $Y_a^\nu$  is an arbitrary order unity coefficient. Note that the operators of the type in Eq. (2.52) carry two units of mass dimension more than the operator  $\mathcal{O}_{ee}^\nu$ .



The operators  $\mathcal{O}_{e\mu}^\nu$  and  $\mathcal{O}_{e\tau}^\nu$  (as well as  $\mathcal{O}_{\mu e}^\nu$  and  $\mathcal{O}_{\tau e}^\nu$ ) must have the U(1) charge structure  $(-1, -1, 0)$ . Therefore, the lowest dimensional terms which contribute to these operators are  $\sim \phi_7/M_1$  and  $\sim \phi_8/M_1$ . The symmetries  $\mathcal{D}_2, \mathcal{D}_3$ , and  $\mathcal{D}_4$  then yield to leading order  $\mathcal{O}_{e\mu}^\nu = Y_b^\nu \phi_7/M_1$  and  $\mathcal{O}_{e\tau}^\nu = Y_b^\nu \phi_8/M_1$ , where  $Y_b^\nu$  is an arbitrary order unity coefficient. Note that  $\mathcal{O}_{ee}^\nu$  in Eq. (2.53) carries two units of mass dimension more than  $\mathcal{O}_{e\mu}^\nu \sim \phi_7/M_1$  and  $\mathcal{O}_{e\tau}^\nu \sim \phi_8/M_1$ . We will therefore not in detail consider the structure of the highly suppressed terms that appear in the 2-3-submatrix of the neutrino mass matrix.

In total, the most general effective Yukawa coupling matrix of the neutrinos ( $\mathcal{O}_{\alpha\beta}^\nu$ ) that is consistent with the symmetries of our model is to leading order given by

$$(\mathcal{O}_{\alpha\beta}^\nu) = \begin{pmatrix} A_2 & B_2 & B_3 \\ B_2 & 0 & 0 \\ B_3 & 0 & 0 \end{pmatrix}. \quad (2.54)$$

Here, the dimensionful coefficients  $A_2$ ,  $B_2$ , and  $B_3$  are identical with

$$A_2 = Y_a^\nu \frac{\phi_9 \phi_{10} \theta}{(M_1)^3}, \quad B_2 = Y_b^\nu \frac{\phi_7}{M_1}, \quad B_3 = Y_b^\nu \frac{\phi_8}{M_1}, \quad (2.55a)$$

where the quantity  $Y_b^\nu$  is an order unity coefficient. The leading order tree-level realizations of the higher-dimensional operators, which generate the neutrino masses, are shown in Figs. 2.4 and 2.5. Note that the coefficients  $B_2$  and  $B_3$  contain the same

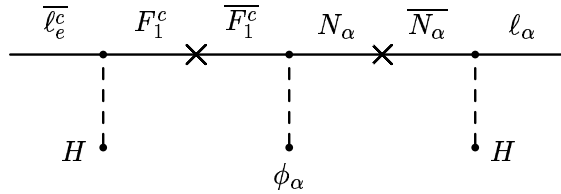


Figure 2.4: The dimension-six operator for  $\alpha = \mu, \tau$  and  $\phi_\mu \equiv \phi_7$ ,  $\phi_\tau \equiv \phi_8$  generating the  $e$ - $\mu$ - and  $e$ - $\tau$ -elements in the effective neutrino mass matrix.

Yukawa coupling constant  $Y_b^\nu$ . Furthermore, we point out that the texture zeros in the 2-3-submatrix of the effective neutrino Yukawa matrix should be understood as “phenomenological” ones, since they actually represent highly suppressed operators carrying two units of mass dimension more than the entry  $\mathcal{O}_{ee}^\nu$ .

## 2.5.2 The neutrino mass matrix

Inserting the VEV in Eq. (2.20) into the effective operators in Eqs. (2.55), we obtain from Eq. (2.54) the effective neutrino mass matrix (to leading order)

$$M_\nu = \frac{\langle H \rangle^2}{M_2} \begin{pmatrix} Y_a^\nu \epsilon^3 & Y_b^\nu \epsilon & \pm Y_b^\nu \epsilon \\ Y_b^\nu \epsilon & \epsilon^5 & \epsilon^5 \\ \pm Y_b^\nu \epsilon & \epsilon^5 & \epsilon^5 \end{pmatrix}, \quad (2.56)$$

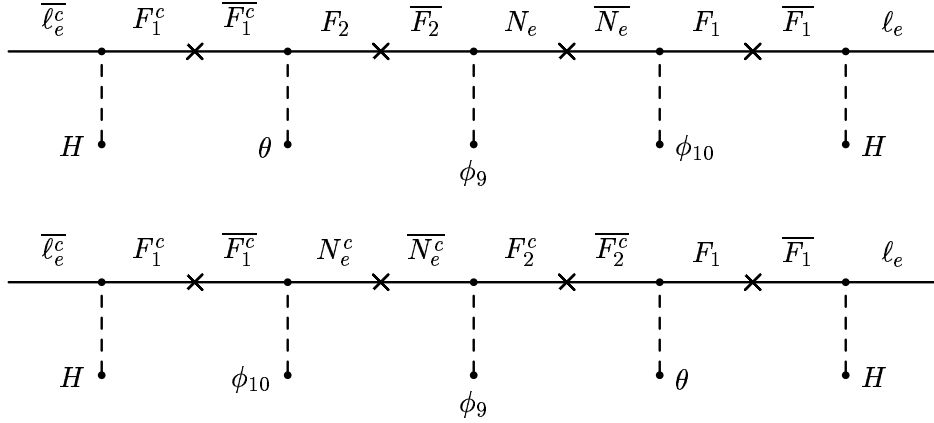


Figure 2.5: The dimension-eight operators generating the  $e$ - $e$ -element in the effective neutrino mass matrix.

where we have introduced the actual orders of magnitude of the higher-order corrections to the texture zeros in the 2-3-submatrix of the matrix in Eq. (2.54). Note that after SSB the symmetries determine the  $e$ - $\mu$ - and  $e$ - $\tau$ -elements to be exactly degenerate (up to a sign), giving rise to an atmospheric mixing angle which is close to maximal (higher-order corrections to exact maximal atmospheric mixing mainly come from the  $\mu$ - $\tau$ - and  $\tau$ - $\mu$ -elements of the charged lepton mass matrix). Introducing an absolute neutrino mass scale  $m_\nu$  and choosing  $Y_a^\nu/Y_b^\nu \simeq 1$ , we can write the neutrino mass matrix in Eq. (2.56) as

$$M_\nu \simeq m_\nu \begin{pmatrix} \epsilon^2 & 1 & -1 \\ 1 & \epsilon^4 & \epsilon^4 \\ -1 & \epsilon^4 & \epsilon^4 \end{pmatrix}, \quad (2.57)$$

where

$$m_\nu = \frac{\langle H \rangle^2}{M_2} Y_b^\nu \epsilon. \quad (2.58)$$

Note that we have chosen the minus signs for the  $e$ - $\tau$ - and  $\tau$ - $e$ -elements due to our freedom of absorbing the corresponding phase into the order unity coefficients in the charged lepton sector. Furthermore, it is important to keep in mind that the entries “1” and “-1” of the matrix in Eq. (2.57) indeed denote matrix elements, which are degenerate to a very high accuracy, whereas the other entries are only known up to their order unity coefficients.

## 2.6 Lepton masses and mixing angles

In the last two sections, we have found from the U(1) and discrete symmetries the effective charged lepton and neutrino mass matrix patterns

$$M_\ell \simeq m_\ell \begin{pmatrix} \epsilon^3 & \epsilon^2 & \epsilon^4 \\ \epsilon^3 & \epsilon & \epsilon^2 \\ \epsilon^3 & \epsilon^2 & 1 \end{pmatrix} \quad \text{and} \quad M_\nu \simeq m_\nu \begin{pmatrix} \epsilon^2 & 1 & -1 \\ 1 & \epsilon^4 & \epsilon^4 \\ -1 & \epsilon^4 & \epsilon^4 \end{pmatrix},$$

where  $m_\ell$  is the absolute charged lepton mass scale,  $m_\nu$  is the absolute neutrino mass scale,  $\epsilon \simeq 0.1$  is the small expansion parameter, and only the orders of magnitude of the  $\epsilon$ -suppressed matrix elements have been indicated. Note that  $M_\ell$  and  $M_\nu$  are both described by the same expansion parameter  $\epsilon$ . Now, the mixing angles and masses of the left-handed charged leptons are found by diagonalizing the matrix product  $M_\ell M_\ell^\dagger$ , which is a unitary matrix. Biunitary diagonalization of  $M_\ell$  gives  $U_\ell^\dagger M_\ell V_\ell = \mathcal{M}_\ell$ , where  $\mathcal{M}_\ell = \text{diag}(m_e, m_\mu, m_\tau)$  is the diagonalized charged lepton mass matrix containing the left-handed charged lepton masses and  $U_\ell$  and  $V_\ell$  are two unitary mixing matrices. Thus, we have  $\mathcal{M}_\ell \mathcal{M}_\ell^\dagger = U_\ell^\dagger M_\ell M_\ell^\dagger U_\ell$ , where  $U_\ell$  is the mixing matrix of the left-handed charged leptons. For simplicity, we will take  $M_\ell$  to be a real matrix, implying that  $\mathcal{M}_\ell \mathcal{M}_\ell^\dagger = \mathcal{M}_\ell \mathcal{M}_\ell^T = U_\ell^T M_\ell M_\ell^T U_\ell$ . Thus, it holds

$$\mathcal{M}_\ell \mathcal{M}_\ell^\dagger = (m_\ell)^2 \text{diag}(\epsilon^6 + \mathcal{O}(\epsilon^7), \epsilon^2 + \mathcal{O}(\epsilon^4), 1 + \mathcal{O}(\epsilon^4)) \quad (2.59)$$

and

$$U_\ell \equiv ((U_\ell)_{\alpha a}) \simeq \begin{pmatrix} -0.995 & -0.0997 & -0.000212 \\ 0.0997 & -0.995 & -0.0111 \\ -0.000897 & 0.0111 & -1.000 \end{pmatrix}, \quad (2.60)$$

such that  $U_\ell^\dagger U_\ell \simeq U_\ell U_\ell^\dagger \simeq 1_3$ , where  $\alpha = e, \mu, \tau$  and  $a = 1, 2, 3$ . Hence, the charged lepton masses are given by  $m_e = m_\ell \epsilon^3 (1 - \epsilon + \mathcal{O}(\epsilon^2))$ ,  $m_\mu = m_\ell \epsilon (1 + \frac{1}{2}\epsilon^2 + \mathcal{O}(\epsilon^3))$ , and  $m_\tau = m_\ell (1 + \epsilon^4 + \mathcal{O}(\epsilon^5))$ . This leads to the order-of-magnitude relations

$$m_e/m_\mu \simeq \epsilon^2 \simeq 10^{-2} \quad \text{and} \quad m_\mu/m_\tau \simeq \epsilon \simeq 10^{-1}, \quad (2.61)$$

which are to be compared with the experimentally observed values, *i.e.*,  $(m_e/m_\mu)_{\text{exp}} \simeq 4.8 \cdot 10^{-3}$  and  $(m_\mu/m_\tau)_{\text{exp}} \simeq 5.9 \cdot 10^{-2}$  [58]. Working in the standard parameterization, we find for the mixing angles of the left-handed charged leptons [61]

$$\theta_{12}^\ell \equiv \arctan \left| \frac{(U_\ell)_{e2}}{(U_\ell)_{e1}} \right| = \epsilon + \mathcal{O}(\epsilon^3), \quad (2.62a)$$

$$\theta_{13}^\ell \equiv \arcsin |(U_\ell)_{e3}| = 2\epsilon^2 + \mathcal{O}(\epsilon^5), \quad (2.62b)$$

$$\theta_{23}^\ell \equiv \arctan \left| \frac{(U_\ell)_{\mu 3}}{(U_\ell)_{\tau 3}} \right| = \epsilon^2 + \mathcal{O}(\epsilon^3). \quad (2.62c)$$

Substituting  $\epsilon \simeq 0.1$  into Eqs. (2.62), one obtains  $\theta_{12}^\ell \approx 6^\circ$ ,  $\theta_{13}^\ell \approx 0.01^\circ$ , and  $\theta_{23}^\ell \approx 0.6^\circ$ , *i.e.*, the mixing angles in the charged lepton sector are all small. The mixing angle

$\theta_{12}^l$  is the only one that is not negligible and will give a significant contribution to the leptonic mixing angles [59, 60].

To determine the leptonic mixing angles, it is necessary to diagonalize the effective neutrino mass matrix  $M_\nu$  as well. Since the Majorana mass matrix  $M_\nu$  is symmetric, one can always write  $U_\nu^T M_\nu U_\nu = \mathcal{M}_\nu$ , where  $\mathcal{M}_\nu = \text{diag}(m_{\nu_1}, m_{\nu_2}, m_{\nu_3})$  is the diagonalized neutrino mass matrix containing the neutrino mass eigenvalues and  $U_\nu$  is the unitary neutrino mixing matrix. For simplicity, we take  $M_\nu$  to be a real matrix. Hence, we obtain

$$\begin{aligned}\mathcal{M}_\nu &= m_\nu \text{diag} \left( \frac{1}{2} (\epsilon^2 + \sqrt{8 + \epsilon^4}), \frac{1}{2} (\epsilon^2 - \sqrt{8 + \epsilon^4}), 2\epsilon^4 \right) \\ &= m_\nu \text{diag} \left( \sqrt{2} + \frac{1}{2}\epsilon^2 + \mathcal{O}(\epsilon^4), -\sqrt{2} + \frac{1}{2}\epsilon^2 + \mathcal{O}(\epsilon^4), 2\epsilon^4 \right)\end{aligned}\tag{2.63}$$

and

$$U_\nu \equiv ((U_\nu)_{\alpha a}) \simeq \begin{pmatrix} 0.708 & 0.706 & 0 \\ 0.499 & -0.501 & \frac{1}{\sqrt{2}} \\ -0.499 & 0.501 & \frac{1}{\sqrt{2}} \end{pmatrix},\tag{2.64}$$

such that  $U_\nu^\dagger U_\nu \simeq U_\nu U_\nu^\dagger \simeq 1_3$ , where  $\alpha = e, \mu, \tau$  and  $a = 1, 2, 3$ . The (physical) neutrino masses are  $m_1 \equiv |m_{\nu_1}| \simeq \sqrt{2}m_\nu$ ,  $m_2 \equiv |m_{\nu_2}| \simeq \sqrt{2}m_\nu$ , and  $m_3 \equiv |m_{\nu_3}| = 2\epsilon^4 m_\nu \approx 0$ , *i.e.*, the neutrino mass spectrum is inverse hierarchical. For the neutrino mass squared differences  $\Delta m_{ab}^2 = m_a^2 - m_b^2$ , where  $m_a$  is the physical mass of the  $a$ th neutrino mass eigenstate, we find

$$\Delta m_{21}^2 = m_\nu^2 \left( -2\sqrt{2}\epsilon^2 + \mathcal{O}(\epsilon^6) \right),\tag{2.65a}$$

$$\Delta m_{32}^2 = m_\nu^2 \left( -2 + \sqrt{2}\epsilon^2 + \mathcal{O}(\epsilon^4) \right),\tag{2.65b}$$

$$\Delta m_{31}^2 = m_\nu^2 \left( -2 - \sqrt{2}\epsilon^2 + \mathcal{O}(\epsilon^4) \right).\tag{2.65c}$$

Thus, the solar and atmospheric neutrino mass squared differences are given by  $\Delta m_{\odot}^2 \equiv |\Delta m_{21}^2| \simeq 2\sqrt{2}\epsilon^2 m_\nu^2$  and  $\Delta m_{\text{atm}}^2 \equiv |\Delta m_{32}^2| \simeq |\Delta m_{31}^2| \simeq 2m_\nu^2$ , respectively. The presently preferred experimental values of these quantities are  $\Delta m_{\odot}^2 \simeq 7.5 \cdot 10^{-5} \text{ eV}^2$  (LMA-I) [14] and  $\Delta m_{\text{atm}}^2 \simeq 2.5 \cdot 10^{-3} \text{ eV}^2$  [11]. Therefore, one concludes that  $m_\nu \simeq 0.04 \text{ eV}$  and  $\epsilon \simeq 0.1$ , which is consistent with our used value for the small expansion parameter  $\epsilon$ . In addition, the neutrino masses are  $m_1 \simeq m_2 \simeq 0.05 \text{ eV}$  and  $m_3 \simeq 1 \cdot 10^{-5} \text{ eV} \approx 0$ . In the standard parameterization, the neutrino mixing angles are determined to be [61]

$$\theta_{12}^\nu \equiv \arctan \left| \frac{(U_\nu)_{e2}}{(U_\nu)_{e1}} \right| = \frac{\pi}{4} + \frac{1}{4\sqrt{2}}\epsilon^2 + \mathcal{O}(\epsilon^6),\tag{2.66a}$$

$$\theta_{13}^\nu \equiv \arcsin |(U_\nu)_{e3}| = 0,\tag{2.66b}$$

$$\theta_{23}^\nu \equiv \arctan \left| \frac{(U_\nu)_{\mu 3}}{(U_\nu)_{\tau 3}} \right| = \frac{\pi}{4}.\tag{2.66c}$$

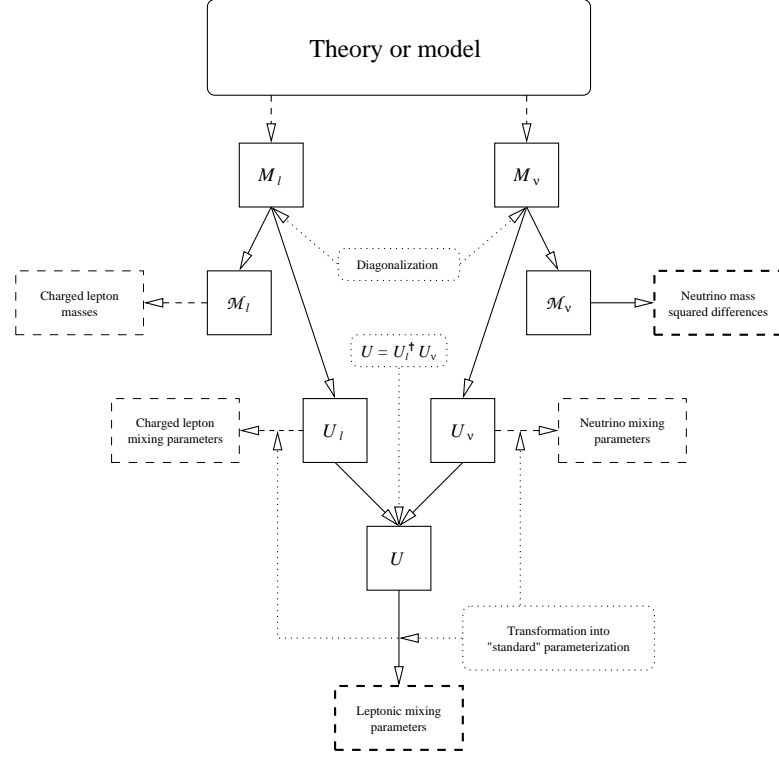


Figure 2.6: Scheme for calculating the leptonic mass and mixing parameters [60].

Substituting  $\epsilon \simeq 0.1$  into Eqs. (2.66), one arrives at  $\theta_{12}^\nu \simeq 45.1^\circ \approx 45^\circ$ ,  $\theta_{13}^\nu = 0$ , and  $\theta_{23}^\nu = 45^\circ$ , *i.e.*, the neutrinos exhibit a bimaximal mixing [62]. Note that the predictions for  $\theta_{13}^\nu$  and  $\theta_{23}^\nu$  are exact, since these values are exclusively determined by the entries in the third column of  $U_\nu$  in Eq. (2.64).

## 2.7 The leptonic mixing angles

The leptonic mixing matrix  $U$  is given by the charged lepton mixing matrix  $U_\ell$  and the neutrino mixing matrix  $U_\nu$  in terms of (see Fig 2.6):

$$U \equiv U_\ell^\dagger U_\nu. \quad (2.67)$$

The matrix  $U$  [ $U_{ab} = (U_\ell^\dagger U_\nu)_{ab} = \sum_{\alpha=e,\mu,\tau} (U_\ell^\dagger)_{a\alpha} (U_\nu)_{\alpha b} = \sum_{\alpha=e,\mu,\tau} (U_\ell)_{\alpha a}^* (U_\nu)_{\alpha b}$ ] can be viewed as the messenger between the mass eigenstate bases of the charged leptons and the neutrinos. Substituting the matrices in Eqs. (2.60) and (2.64) into Eq. (2.67), it follows that

$$U \equiv (U_{ab}) \simeq \begin{pmatrix} -0.655 & -0.753 & 0.0699 \\ -0.573 & 0.434 & -0.696 \\ 0.493 & -0.495 & -0.715 \end{pmatrix}, \quad (2.68)$$

which approximately satisfies the condition  $U^\dagger U = U U^\dagger = 1_3$ . In the standard parameterization, the leptonic mixing angles are identical with [61]:

$$\theta_{12} \equiv \arctan \left| \frac{U_{12}}{U_{11}} \right|, \quad \theta_{13} \equiv \arcsin |U_{13}|, \quad \theta_{23} \equiv \arctan \left| \frac{U_{23}}{U_{33}} \right|. \quad (2.69)$$

Here, substituting the appropriate matrix elements of the matrix  $U$  expressed in terms of  $\epsilon$  in Eq. (2.67) into Eq. (2.69), one concludes

$$\theta_{12} = \frac{\pi}{4} - \frac{1}{\sqrt{2}}\epsilon + \frac{1}{4\sqrt{2}}\epsilon^2 + \mathcal{O}(\epsilon^3), \quad (2.70a)$$

$$\theta_{13} = \frac{1}{\sqrt{2}}\epsilon + \mathcal{O}(\epsilon^3), \quad (2.70b)$$

$$\theta_{23} = \frac{\pi}{4} - \frac{5}{4}\epsilon^2 + \mathcal{O}(\epsilon^3). \quad (2.70c)$$

Here, it is important to note that the first correction to the atmospheric mixing angle  $\theta_{23}$  is of second order in  $\epsilon$ , and it is therefore very small, *i.e.*, the atmospheric mixing angle stays nearly maximal. In contrast to this, the first corrections to the solar mixing angle  $\theta_{12}$  and the reactor (or CHOOZ) mixing angle  $\theta_{13}$  are both of first order in  $\epsilon$  and they are of the same size, but with opposite sign. This leads to the relation

$$\theta_{12} = \frac{\pi}{4} - \theta_{13} + \mathcal{O}(\epsilon^2), \quad (2.71)$$

between the solar and the reactor mixing angle. Now, inserting  $\epsilon \simeq 0.1$  in Eqs. (2.70), one obtains the leptonic mixing angles

$$\theta_{12} \approx 41^\circ, \quad \theta_{13} \approx 4^\circ, \quad \text{and} \quad \theta_{23} \approx 44^\circ, \quad (2.72)$$

which means that we have bilarge leptonic mixing. These values of the leptonic mixing angles lie within the 99.73% C.L. contour line of the MSW LMA solution [14] and lie within the ranges preferred by atmospheric neutrino data [11] (close to maximal atmospheric mixing), and CHOOZ reactor neutrino data. Although the obtained value for the solar mixing angle  $\theta_{12}$  implies a significant deviation from maximal solar mixing, the expected solar mixing angle  $41^\circ$  is still too close to maximal to be within the 99% C.L. region of the MSW LMA solution [14].

Let us now give an impression of the robustness of the above calculated leptonic mixing angles under variation of the involved order unity coefficients. For example, changing the ratio  $Y_b^\ell/Y_d^\ell$  from 1 to 2 leads to

$$\theta_{12} \simeq 37^\circ, \quad \theta_{13} \simeq 8^\circ, \quad \text{and} \quad \theta_{23} \simeq 44^\circ, \quad (2.73)$$

where the new value for  $\theta_{12}$  lies within the 90% C.L. region of the MSW LMA solution [14] while the value for  $\theta_{13}$  still remains below the CHOOZ upper bound. Note that  $\theta_{23}$  has practically not changed as compared with Eq. (2.72). At the same time, the

exact values of the charged lepton masses can be accommodated by choosing the values  $Y_a^\ell = 0.5$ ,  $Y_c^\ell = 1.8$ , and  $Y_d^\ell = 1.0$  for the order unity coefficients. Thus, the model is in agreement with the MSW LMA solution and can accommodate the spectrum of charged lepton masses.

In this chapter, we have analyzed a model for inverse hierarchical neutrino masses, which gives bilarge leptonic mixing in agreement with the MSW LMA solution. Here, the atmospheric mixing angle is maximal due to some non-Abelian symmetry and a vacuum-alignment mechanism generates the splitting  $m_\mu \ll m_\tau$  between the muon and tau mass. The vacuum alignment mechanism is essentially based on an enlarged sector of replicated scalar representations transforming non-trivially under the non-Abelian discrete symmetry. Recently, replicated scalar representations in conjunction with discrete symmetries were also used to solve the doublet-triplet splitting problem in models inspired by dimensional deconstruction. Motivated by this fact, we will in the next chapter use deconstruction as a tool for organizing the horizontal charges in a normal hierarchical neutrino mass model, which gives the MSW LMA solution within the 90% C.L. contour line without any tuning of parameters.

# Chapter 3

## Hierarchies from Mooses

In the last chapter, we have seen that an enlarged symmetry structure with an extended set of scalar fields can predict maximal atmospheric mixing and the hierarchical splitting  $m_e \ll m_\mu \ll m_\tau$  of charged lepton masses. In this chapter, we will use deconstruction as an elegant organizing principle for the collection of symmetries and scalar variables to comfortably obtain the MSW LMA solution for a normal neutrino mass hierarchy. This chapter extends and modifies the treatment in Ref. [63].

### 3.1 Deconstruction

In this section, we will first briefly review the deconstruction setup [34, 35] for two relevant cases: the “periodic model” and the “aliphatic model” for fermions. These models describe a latticized fifth dimension which is compactified either on the circle  $\mathcal{S}^1$  or on the orbifold  $\mathcal{S}^1/Z_2$ .

#### 3.1.1 The periodic model

Consider a 4D gauge-invariant field theory for deconstructed or latticized extra dimensions [34, 35]. Let the field theory be described by a product  $G = \prod_{i=1}^N G_i$  of  $SU(m)$  gauge groups  $G_i$ , where  $N$  is the total number of “sites” corresponding to  $G$ . In the “periodic model” [34], one associates with each pair of groups  $G_i \times G_{i+1}$  a (fundamental or effective) link-Higgs field  $Q_i$ , which transforms according to the bi-fundamental representation  $(m_i, \bar{m}_{i+1})$  under  $G_i \times G_{i+1}$ , where the index  $i$  is periodically identified with  $i + N$ . Each link field  $Q_i$  can be represented by a complex  $m \times m$  matrix where the group  $SU(m)_i$  acts on the columns and the group  $SU(m)_{i+1}$  acts on the rows of the matrix. This field theory is conveniently represented by the “moose” [64] or “quiver” [65] diagram in Fig. 3.1. Each circle in Fig. 3.1 represents a gauge group  $SU(m)_i$  and each line corresponds to a link-Higgs field  $Q_i$  which transforms under the two adjacent gauge groups  $SU(m)_i$  and  $SU(m)_{i+1}$  associated with the corresponding sites (see Fig. 3.2). Here, a line directed away from a site denotes



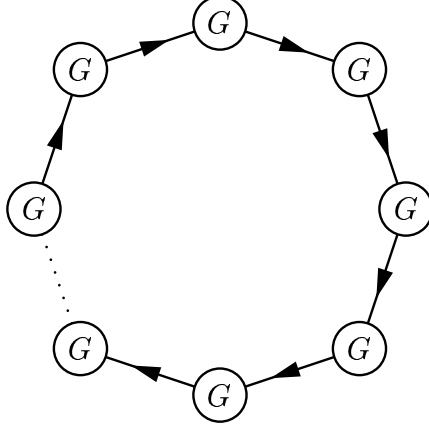


Figure 3.1: Moose (or quiver) diagram for the periodic  $G^N$  model.

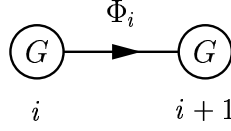


Figure 3.2: View at one line of the polygon in Fig. 3.1. The link field  $\Phi_i$  transforms as the bi-fundamental representation  $(m_i, \bar{m}_{i+1})$  under the adjacent gauge groups  $G_i$  and  $G_{i+1}$ .

the transformation of the field under the fundamental representation, while a line pointing towards a site denotes the transformation under the complex-conjugate of the fundamental representation. The Lagrangian of the periodic model is given by

$$\mathcal{L} = -\frac{1}{4} \sum_{i=1}^N \text{Tr} (F_{i\mu\nu}^a F^{i\mu\nu a}) + \sum_{i=1}^N \text{Tr} \left( (D_\mu Q_i)^\dagger D^\mu Q_i \right), \quad (3.1)$$

where  $F_{i\mu\nu}^a = \partial_\mu A_{i\nu}^a - \partial_\nu A_{i\mu}^a + g_i f^{abc} A_{i\mu}^b A_{i\nu}^c$  is the 4D field strength of the gauge group  $SU(m)_i$  and the covariant derivative is defined by

$$D_\mu Q_i = (\partial_\mu - ig_i A_{i\mu}^a T^a + ig_{i+1} A_{(i+1)\mu}^a T^a) Q_i, \quad (3.2)$$

where  $g_i$  is the dimensionless coupling constant of the gauge group  $G_i$  and  $T^a$  ( $a = 1, \dots, m^2 - 1$ ) are the  $SU(m)$  generators (normalized by  $\text{Tr} (T^a T^b) = \delta^{ab}/2$ ). For simplicity, we assume a cyclic symmetry which ensures universal gauge couplings,

$$g_1 = g_2 = \dots = g_N \equiv g. \quad (3.3)$$

Since we work here with fundamental link-Higgs fields, the Lagrangian of the model actually includes a renormalizable potential

$$V(Q_i) = \sum_{i=1}^N \left[ -M^2 \text{Tr} \left( Q_i^\dagger Q_i \right) + \lambda_1 \text{Tr} \left( Q_i^\dagger Q_i \right)^2 + \lambda_2 \left( \text{Tr} \left( Q_i^\dagger Q_i \right) \right)^2 + M' \left( e^{i\theta} \det(Q_i) + \text{h.c.} \right) \right], \quad (3.4)$$

where the term in the 2nd line is absent if  $m > 4$ . For zero gauge couplings, the link-Higgs sector would exhibit an  $SU(m)^N \times SU(m)^N$  chiral global symmetry under which the link fields transform as  $Q_i \rightarrow L_i Q_i R_{i+1}^\dagger$ , where  $L_i$  and  $R_i$  are independent elements of  $SU(m)$  [36]. If the gauge couplings are switched on, only the  $SU(m)^N$  subgroup of the chiral symmetry is preserved, where  $L_i = R_i$ . In Eq. (3.4), one can choose the parameters in such a way, that after SSB the link-Higgs fields become non-linear sigma model fields [35],

$$Q_i \rightarrow v \exp(i\pi_i^a T^a / v), \quad (3.5)$$

with universal VEVs  $v$  for all  $i = 1, \dots, N$ . As a consequence, the chiral symmetry is spontaneously broken  $SU(m)^N \times SU(m)^N \rightarrow SU(m)^N$  which leaves  $N$  Nambu-Goldstone boson multiplets, each of which transforms according to the adjoint representation of  $SU(m)$ . At the same time, the full  $SU(m)^N$  gauge symmetry is broken down to the diagonal subgroup  $SU(m)_{\text{diag}}$ , thereby generating  $(N-1)(m^2-1)$  massive spin-1 vector states by eating  $N-1$  of the would-be Nambu-Goldstone boson multiplets via the Higgs mechanism. Thus, one massless scalar  $\phi = (\pi_1 + \pi_2 + \dots + \pi_N) / \sqrt{N}$  remains in the spectrum, which transforms under the adjoint representation of  $SU(m)_{\text{diag}}$ . The classically massless  $\phi$  is a pseudo-Nambu Goldstone boson and acquires at the quantum level a mass which is protected against divergencies by the  $SU(m)^N$  gauge symmetries [36, 37].

Actually, the Lagrangian in Eq. (3.1) describes a 4+1 dimensional  $SU(m)$  gauge theory on a flat background, where only the fifth dimension has been latticized. The lattice spacing  $a$  and circumference  $R$  of the fifth dimension are  $a = 1/(gv)$  and  $R = N/(gv)$ , whereas the 5D gauge coupling  $g_5$  is given by  $1/g_5^2 = 1/(ag^2)$  [34, 66]. (In the model with free boundary conditions [35] generic gauge couplings and non-universal VEVs introduce an overall non-trivial warp factor [37, 40], resulting, *e.g.*, in a Randall-Sundrum model [67].) The field  $\phi$  corresponds to the zero mode  $\tilde{A}_5^{(0)}$  of the continuum 5D  $SU(m)$  gauge theory and could be projected out by suitable boundary conditions. Implicitly, we identify the link-Higgs fields with the continuum Wilson lines

$$Q_i(x^\mu) = \exp \left( i \int_{ia}^{(i+1)a} dx^5 A_5^b(x^\mu, x^5) T^b \right), \quad (3.6)$$

where  $(x^\mu, x^5)$  are the bulk coordinates and  $A_5^b$  is the fifth component of the bulk gauge field associated with the gauge group  $G$ . The gauge boson mass matrix takes

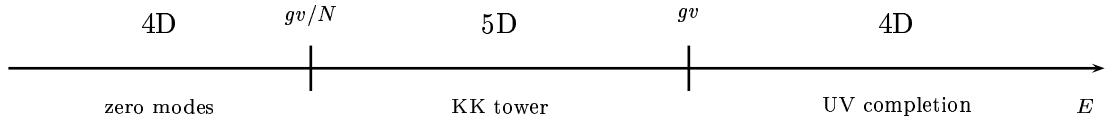


Figure 3.3: Deconstruction picture for the dynamical generation of a fifth dimension. At energy scales below  $gv/N$ , we have a 4D theory with zero modes. For energies  $\gtrsim gv/N$ , the physics is that of a 5D gauge theory with KK excitations. At high energies  $\gtrsim gv$ , the fifth dimension “melts away” leaving a 4D UV complete theory with enlarged gauge symmetry.

the form

$$\sum_{i=1}^N g^2 v^2 (A_{i\mu}^a - A_{(i+1)\mu}^a)^2 \quad (3.7)$$

and is of the type of a nearest neighbor coupled oscillator Hamiltonian. Explicitly, the  $N \times N$  gauge boson mass matrix reads

$$g^2 v^2 \begin{pmatrix} 2 & -1 & 0 & 0 & 0 & \cdots & -1 \\ -1 & 2 & -1 & 0 & 0 & \cdots & 0 \\ 0 & -1 & 2 & -1 & 0 & \cdots & 0 \\ \vdots & \ddots & \ddots & \ddots & \ddots & \ddots & \vdots \\ 0 & \cdots & 0 & 0 & -1 & 2 & -1 \\ -1 & \cdots & 0 & 0 & 0 & -1 & 2 \end{pmatrix}. \quad (3.8)$$

The matrix in Eq. (3.8) yields a mass spectrum labeled by an integer  $k$  satisfying  $-N/2 < k \leq N/2$  [34],

$$M_k^2 = 4g^2 v^2 \sin^2 \left( \frac{\pi k}{N} \right) \equiv \left( \frac{2}{a} \right)^2 \sin^2 \left( \frac{p_5 a}{2} \right), \quad (3.9)$$

where  $p_5 \equiv 2\pi k/R$  is the discrete 5D momentum. For small  $|k|$ , the masses are

$$M_k \simeq |p_k| = \frac{2\pi|k|}{R}, \quad |k| \ll N/2, \quad (3.10)$$

which is exactly the KK spectrum<sup>1</sup> of a 5D gauge theory compactified on  $\mathcal{S}^1$  with circumference  $R = N/(gv)$ . The zero mode corresponds to the unbroken group  $SU(m)_{\text{diag}}$ . Hence, at energies  $E \ll gv/N$  we observe an ordinary 4D gauge theory, in the range  $gv/N < E < gv$  the physics is that of an extra dimension, and for  $E \gg gv$  an unbroken  $SU(m)^N$  gauge theory in four dimensions is recovered (see Fig. 3.3).

<sup>1</sup>Note here the doubling of KK modes.

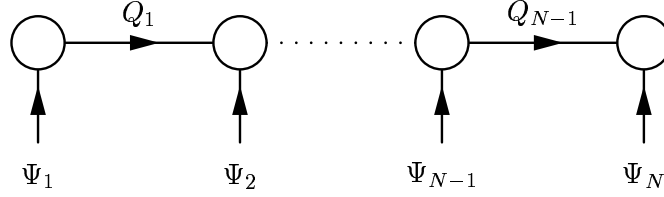


Figure 3.4: Moose diagram for bulk vector fields and fermions in the aliphatic model.

### 3.1.2 The aliphatic model for fermions

The “aliphatic model” [35] for the product gauge group  $G$ , as defined in Sec. 3.1.1, is obtained from the periodic model by setting  $Q_N = 0$ , which yields a linear system with free boundary conditions. For this type of latticization, we will consider  $N$  SM singlet Dirac fermions  $\Psi_n$  ( $n = 1, \dots, N$ ), each of which transforms under the complex-conjugate representation  $\bar{m}_n$  of the fundamental representation of  $SU(m)_n$ . The SM singlet Higgs fields  $Q_n$  ( $n = 1, \dots, N$ ) which transform under  $G_n \times G_{n+1}$  as the bi-fundamental representation  $(m_n, \bar{m}_{n+1})$  specify the allowed couplings between the fermions. The moose diagram for the aliphatic model is shown in Fig. 3.4. In contrast to the periodic model in Sec. 3.1.1, we now have only a  $SU(m)^{N-1} \times SU(m)^{N-1}$  chiral global symmetry in the scalar sector. When the link fields acquire their VEVs as in Eq. (3.5), the global symmetry is spontaneously broken  $SU(m)^{N-1} \times SU(m)^{N-1} \rightarrow SU(m)^{N-1}$  leaving  $N - 1$  Nambu-Goldstone multiplets. The  $SU(m)^N$  gauge symmetry is broken down to the diagonal subgroup  $SU(m)_{\text{diag}}$ , thereby eating  $N - 1$  of the would-be Nambu-Goldstone multiplets. Hence, no scalar zero mode remains in the spectrum, which corresponds exactly to the compactification of a  $SU(m)$  gauge theory on an orbifold  $\mathcal{S}^1/Z_2$ , where unwanted vector field strengths in the 4D theory are projected out by suitable boundary conditions.

We will denote by  $\Psi_{nL}$  and  $\Psi_{nR}$  the left- and right-handed chiral components of  $\Psi_n$  respectively. To engineer chiral fermion zero modes from compactification of the 5th dimension, one can impose discretized versions of the Neumann and Dirichlet boundary conditions  $\Psi_{NL} - (Q_{N-1}/v)\Psi_{(N-1)L} = 0$  and  $\Psi_{1R} = \Psi_{NR} = 0$  which explicitly break the Lorentz group  $SO(4, 1)$  in five dimensions. In the moose diagram in Fig. 3.4, the Neumann boundary condition corresponds to removing the variable  $\Psi_N$  from the last site, while the Dirichlet boundary condition replaces  $\Psi_1 \rightarrow \Psi_{1L}$  on the first site. Using the transverse lattice technique [68, 69] the relevant mass and mixing terms of  $\Psi_{nL}$  and  $\Psi_{mR}$  then read [35, 37]

$$\begin{aligned} \mathcal{L}_1 = & M_f \sum_{n=2}^{N-1} \left[ \bar{\Psi}_{nL} \left( \frac{Q_n^\dagger}{v} \Psi_{(n+1)R} - \Psi_{nR} \right) - \bar{\Psi}_{nR} \left( \Psi_{nL} - \frac{Q_{n-1}}{v} \Psi_{(n-1)L} \right) \right] \\ & + M_f \bar{\Psi}_{1L} \frac{Q_1^\dagger}{v} \Psi_{2R} + \text{h.c.}, \end{aligned} \quad (3.11)$$

where  $\langle Q_n \rangle \equiv v \mathbb{1}_m$  for  $n = 1, \dots, N - 1$ , *i.e.*, we have universal VEVs proportional

to the unit matrix. In fact, Eq. (3.11) is the Wilson-Dirac action [70] for a transverse extra dimension which reproduces the 5D continuum theory in the limit of vanishing lattice spacing. Clearly, this tacitly presupposes a specific functional measure for the link variables in question which may, however, no longer be a necessary choice when the lattice spacing is finite [69]. In App. A, we explicitly demonstrate the transverse lattice technique leading to the Wilson-Dirac action as in Eq. (3.11). After SSB, the mixed mass terms of the chiral fermions are

$$\begin{aligned} \mathcal{L}_{\text{mass}} &= M_f \sum_{n=2}^{N-1} [\bar{\Psi}_{nL}(\Psi_{(n+1)R} - \Psi_{nR}) - \bar{\Psi}_{nR}(\Psi_{nL} - \Psi_{(n-1)L})] \\ &\quad + M_f \bar{\Psi}_{1L} \Psi_{2R} + \text{h.c.} \\ &= (\bar{\Psi}_{1L}, \dots, \bar{\Psi}_{(N-1)L})^T \mathcal{M}_1 (\Psi_{2R}, \dots, \Psi_{(N-1)R}) + \text{h.c.}, \end{aligned} \quad (3.12)$$

where the  $(N-1) \times (N-2)$  fermion mass matrix  $\mathcal{M}_1$  is on the form

$$\mathcal{M}_1 = M_f \begin{pmatrix} 1 & 0 & 0 & \cdots & 0 & 0 \\ -1 & 1 & 0 & \cdots & 0 & 0 \\ \vdots & \vdots & \vdots & & \vdots & \vdots \\ 0 & 0 & 0 & \cdots & -1 & 1 \\ 0 & 0 & 0 & \cdots & 0 & -1 \end{pmatrix}. \quad (3.13)$$

Now, the masses of the right- and left-handed fermions are determined from the matrices  $\mathcal{M}_1^\dagger \mathcal{M}_1$  and  $\mathcal{M}_1 \mathcal{M}_1^\dagger$ , respectively. Diagonalizing the  $(N-2) \times (N-2)$  matrix  $\mathcal{M}_1^\dagger \mathcal{M}_1$  gives for the mass eigenvalues of the right-handed fermions

$$M_{nR} = 2M_f \sin\left(\frac{n\pi}{2(N-1)}\right), \quad n = 1, 2, \dots, N-2, \quad (3.14)$$

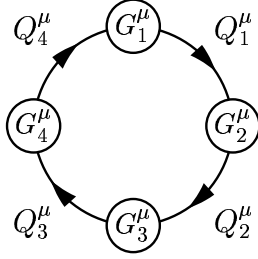
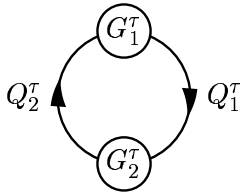
whereas diagonalization of the  $(N-1) \times (N-1)$  matrix  $\mathcal{M}_1 \mathcal{M}_1^\dagger$  yields the masses for the left-handed fermions,

$$M_{nL} = 2M_f \sin\left(\frac{n\pi}{2(N-1)}\right), \quad n = 0, 1, \dots, N-2, \quad (3.15)$$

which are identical with the gauge boson masses [35]. Setting  $M_f = \frac{N-1}{R}$  and taking the limit  $n \ll N$ , the linear KK spectrum of a 5D fermion in an orbifold extra dimension  $\mathcal{S}^1/Z_2$  is reproduced. Up to an overall scale factor of 2, the periodic and the aliphatic model generate identical KK mass spectra for bulk vector fields, with the number of KK modes doubled in the periodic case [71].

## 3.2 Enlarged gauge symmetries

In 5D continuum theories, hierarchical Yukawa coupling matrix textures have been successfully generated [72]. Hierarchical Yukawa matrices have also been obtained in

Figure 3.5: Moose diagram for the gauge group  $G^\mu = \Pi_{i=1}^4 G_i^\mu$ .Figure 3.6: Moose diagram for the gauge group  $G^\tau = \Pi_{i=1}^2 G_i^\tau$ .

deconstructed warped geometries [45]. Let us now consider an extension of the SM where the mass matrix patterns of the charged leptons and the neutrinos originate in four dimensions from two mechanisms which have an extra-dimensional correspondence. For this purpose, we assume that the masses in the charged lepton sector are generated by Wilson-line type effective operators of deconstructed 5D  $SU(m)$  gauge symmetries compactified on  $\mathcal{S}^1$ . In the neutrino sector, on the other hand, we suppose that the solar neutrino parameters reflect the separation between the compactification radius and the fundamental scale of a latticized orbifold extra dimension  $\mathcal{S}^1/Z_2$ , which is experienced by an extra SM singlet bulk-neutrino. To be specific, we associate with the muon a product gauge group  $G^\mu = \Pi_{i=1}^4 G_i^\mu$  of four  $SU(m)$  gauge groups  $G_i^\mu$  ( $i = 1, 2, 3, 4$ ) and with the tau a product  $G^\tau = \Pi_{i=1}^2 G_i^\tau$  of two  $SU(m)$  gauge groups  $G_i^\tau$  ( $i = 1, 2$ ). Within each of the gauge groups  $G^\mu$  and  $G^\tau$ , neighboring  $SU(m)$  symmetries are connected by bi-fundamental link-Higgs variables transforming as  $Q_i^\alpha \subset (m_i, \bar{m}_{i+1})$  under  $G_i^\alpha \times G_{i+1}^\alpha$ , where  $\alpha = \mu, \tau$  and  $i = i + 4$  for  $\alpha = \mu$  and  $i = i + 2$  for  $\alpha = \tau$ . The corresponding moose diagrams are given in Figs. 3.5 and 3.6. Note that in  $G^\alpha$  the periodic identifications  $i + 4 = i$  for  $\alpha = \mu$  and  $i + 2 = i$  for  $\alpha = \tau$  yield two closed lattice geometries. Next, we put the bulk-neutrino on a deconstructed  $\mathcal{S}^1/Z_2$  orbifold extra dimension by employing the aliphatic model for a product  $G^\nu = \Pi_{i=1}^N G_i^\nu$  of  $SU(m)$  gauge symmetries  $G_i^\nu$  ( $i = 1, 2, \dots, N$ ). At this stage, we allow the number of lattice sites  $N$  to be large but leave it yet unspecified. In fact, it will prove later that  $N$  parameterizes the solar mass squared difference  $\Delta m_\odot^2$  and  $N$  will be determined in Sec. 3.7.4 from the presently preferred solar neutrino parameters. In the aliphatic model, the bulk neutrino is described by a set of  $N$  Dirac fermions  $\Psi_n$  ( $n = 1, \dots, N$ ) which transform according to the corresponding

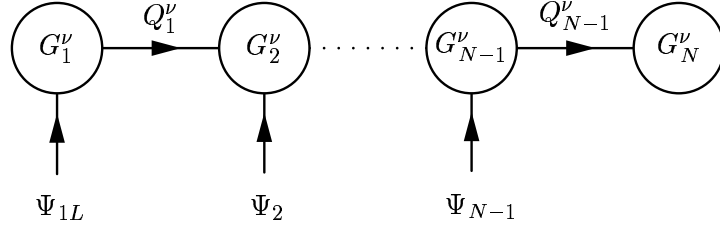


Figure 3.7: Moose diagram for the bulk-neutrino in the orbifold extra dimension associated with the gauge group  $G^\nu$ . Note that the boundary conditions leave on the first site only the left-handed field  $\Psi_{1L}$  and remove  $\Psi_N$  from the last site.

anti-fundamental representation  $\bar{m}_n$  of the gauge group  $G_n^\nu$ . Appropriate application of the Dirichlet and Neumann boundary conditions on the lattice projects out the right-handed component  $\Psi_{1R}$  of  $\Psi_1$  as well as both chiral components of the Dirac spinor  $\Psi_N$  on the  $N$ th lattice site (see Sec. 3.1.2). The corresponding moose diagram is given in Fig. 3.7. For the generation of lepton masses, it is sufficient to assume the electroweak scalar sector of the SM to consist only of the SM Higgs doublet  $H$ . In order to account for the neutrino masses, we will introduce three SM singlet scalar fields  $\xi_0, \xi_1$ , and  $\xi_2$ , as well as three heavy SM singlet Dirac neutrinos  $F_e, F_\mu, F_\tau$ , and a massless left-handed Weyl spinor  $\eta_L$ . Since the Dirac neutrinos are supposed to have masses of the order of the GUT scale  $\simeq 10^{15}$  GeV, they can yield small masses of the active neutrinos via the seesaw mechanism [20–22].

## 3.3 Discrete horizontal symmetries

### 3.3.1 Abelian charges

The extra degrees of freedom which correspond to the field theories summarized by the moose diagrams in Figs. 3.5, 3.6, and 3.7 can be related to a realistic low-energy phenomenology of lepton masses and mixing angles by appropriate discrete Abelian symmetries. In models of inverted neutrino mass hierarchy, for example, a small reactor mixing angle  $\theta_{13}$  may be understood in terms of a softly broken  $L_e - L_\mu - L_\tau$  lepton number [73]. Analogously, we assume that our example field theory contains a product  $Z_8 \times Z'_8$  of two discrete  $Z_8$  symmetries which distinguish the 1st generation from the 2nd and 3rd generations. In addition, the  $Z_8 \times Z'_8$  symmetry acts also on  $\xi_0, \xi_1, \xi_2$ , and the link fields  $Q_1^\mu, Q_4^\mu, Q_1^\tau$ , and  $Q_2^\tau$ . The complete  $Z_8 \times Z'_8$  charge assignment is shown in table 3.1. We assume that the charges of the product groups  $Z_8 \times Z'_8$ ,  $G^\mu$ , and  $G^\tau$  are approximately conserved in the charged lepton sector, implying the generation of hierarchical charged lepton mass terms via the Froggatt-Nielsen mechanism. Furthermore, we suppose that the heavy Froggatt-Nielsen states generating the charged lepton masses are put only on the first site  $G_1^\nu$  as site variables in the fundamental or anti-fundamental representation of  $G_1^\nu$  while carrying zero  $G_i^\nu$

	$Z_8 \times Z'_8$
$\ell_e$	$(+2, -2)$
$E_e, F_e, \xi_0$	$(-2, +2)$
$\ell_\mu, \ell_\tau, Q_1^\mu, Q_1^\tau, \xi_1$	$(+1, 0)$
$\xi_2$	$(+3, 0)$
$F_\mu, F_\tau$	$(-1, 0)$
$E_\mu, E_\tau$	$(0, +1)$
$Q_4^\mu, Q_2^\tau$	$(0, -1)$
$\eta_L$	$(-4, 0)$

Table 3.1: Assignment of the horizontal  $Z_8 \times Z'_8$  charges to the different fields. The fields not shown here transform trivially under  $Z_8 \times Z'_8$ .

charges for  $i = 2, 3, \dots, N$ . Then, the orbifold extra dimension described by the moose diagram in Fig. 3.7 is (at tree-level) completely decoupled from the charged leptons and can only be experienced by the neutrinos.

In addition, let us assume that the scalars  $\xi_0, \xi_1, \xi_2$ , and the SM singlet neutrinos transform under a  $Z_2$  symmetry as

$$Z_2 \quad : \quad \eta_L \longrightarrow -\eta_L, \quad \Psi_{1L} \longrightarrow -\Psi_{1L}, \quad \Psi_n \longrightarrow -\Psi_n, \quad \xi_i \longrightarrow -\xi_i, \quad (3.16)$$

where  $n = 2, \dots, N - 1$ , and  $i = 0, 1, 2$ . All other fields, including the fundamental Froggatt-Nielsen messenger states of the charged lepton sector, which are not displayed in Eq. (3.16) are taken to be even under the  $Z_2$  symmetry. As a consequence, the fields  $\xi_0, \xi_1$ , and  $\xi_2$  can be discarded in the discussion of the generation of the charged lepton masses (see also Sec. 3.7.1).

### 3.3.2 Non-Abelian charges

Among the discrete symmetries that have been proposed in the context of the MSW LMA solution as a possible origin of an approximately maximal atmospheric mixing angle  $\theta_{23}$  are the symmetric groups  $S_2$  and  $S_3$  acting on the 2nd and 3rd generations of leptons [28, 29]. While this can indeed give an approximately maximal  $\nu_\mu$ - $\nu_\tau$ -mixing, the hierarchical charged lepton mass spectrum is typically not produced in these types of models, since they rather yield masses of the muon and tau that are of the same order of magnitude. However, when we add to the regular representation of  $S_2$  in the  $\mu$ - $\tau$ -flavor basis the generator  $\text{diag}(-1, 1)$ , one obtains the vector representation of the dihedral group  $\mathcal{D}_4$ , which is non-Abelian (see App. B). Since the generator  $\text{diag}(-1, 1)$  distinguishes between  $\ell_\mu$  and  $\ell_\tau$ , it may serve as a possible source for the charged lepton mass hierarchy, which breaks the permutation symmetry  $S_2 \subset \mathcal{D}_4$  characterizing the  $\nu_\mu$ - $\nu_\tau$ -sector. Clearly, if the charged lepton masses arise from the



Froggatt-Nielsen mechanism, we will have to expect that the underlying symmetry is actually equivalent to a group *extension*<sup>2</sup> of some subgroup of  $\mathcal{D}_4$ , presumably a suitable subgroup of some replicated product of  $\mathcal{D}_4$ -factors.

Motivated by these general observations, we will take here the view, that an approximately maximal atmospheric mixing angle  $|\theta_{23} - \frac{\pi}{4}| \ll 1$  is due to a non-Abelian discrete symmetry  $\mathcal{G}$  which is a group extension based on the generators of the dihedral group  $\mathcal{D}_4$  under which the leptons of the 2nd and 3rd generation, the scalars  $\xi_1, \xi_2$ , and the scalar link variables of the deconstructed extra-dimensional gauge symmetries  $G^\mu = \prod_{i=1}^4 G_i^\mu$  and  $G^\tau = \prod_{i=1}^2 G_i^\tau$  transform non-trivially. Specifically, we suppose that in the defining representation  $\mathcal{D}$  the group  $\mathcal{G}$ , which is a subgroup of the four-fold (external) product group  $\mathcal{D}_4 \times \mathcal{D}_4 \times \mathcal{D}_4 \times \mathcal{D}_4$ , can be written as a sequence

$$\mathcal{D}(g) \equiv \text{diag} [D_1(g), D_2(g), D_3(g), D_4(g)] \quad g \in \mathcal{G}, \quad (3.17)$$

where each element  $g \in \mathcal{G}$  is associated with four<sup>3</sup> (in general different)  $2 \times 2$  charge operators  $D_i(g)$  ( $i = 1, 2, 3, 4$ ) which have values in the vector representation of  $\mathcal{D}_4$ . Clearly, for given  $i = 1, 2, 3, 4$  the set of all operators  $\{D_i(g) : g \in \mathcal{G}\}$  forms a subrepresentation of  $\mathcal{G}$  which we will call  $D_i$ . Now, using the notation of App. B we suppose that  $\mathcal{G}$  is represented by four generators with following  $\mathcal{D}_4$ -charge structure

$$\mathcal{D}(a_1) \equiv \text{diag} [D(C_b), D(E), D(C_{b'}), D(C_{b'})], \quad (3.18a)$$

$$\mathcal{D}(a_2) \equiv \text{diag} [D(C_{b'}), D(C_{b'}), D(C_b), D(E)], \quad (3.18b)$$

$$\mathcal{D}(a_3) \equiv \text{diag} [D(E), D(E), D(C_b), D(C_b)], \quad (3.18c)$$

$$\mathcal{D}(a_4) \equiv \text{diag} [D(C_b), D(C_b), D(E), D(E)], \quad (3.18d)$$

where  $a_1, a_2, a_3, a_4 \in \mathcal{G}$  are the corresponding abstract generators. We will call  $e$  the identity element of  $\mathcal{G}$ . Note that the operators in Eqs. (3.18) are characterized by a one-to-one-correspondence  $\mathcal{D}(a_1) \leftrightarrow \mathcal{D}(a_2)$  and  $\mathcal{D}(a_3) \leftrightarrow \mathcal{D}(a_4)$  under the permutation of the upper-left and the lower-right  $4 \times 4$ -matrices. As will be shown in Sec. 3.3.3, by factoring the subrepresentation  $D_i$  for any  $i = 1, 2, 3, 4$  with respect to its kernel  $\mathcal{N}_i$  we obtain a representation of the factor group  $\mathcal{G}/\mathcal{N}_i$  that is isomorphic with  $\mathcal{D}_4$ . This implies, of course, that all four subrepresentations  $D_1, D_2, D_3$ , and  $D_4$  are two-dimensional irreps of  $\mathcal{G}$ . From App. B it is seen, that in an appropriate basis,

---

<sup>2</sup>An *extension* of a group  $N$  by a group  $H$  is an embedding of  $N$  into some group  $E$  such that  $N$  is normal in  $E$  and  $H \simeq E/N$ .

<sup>3</sup>Since each element  $g \in \mathcal{G}$  is associated with four (in general) different operators  $D_1(g), D_2(g), D_3(g)$ , and  $D_4(g)$ , one may view in a discretized picture  $\mathcal{D}$  as a 4-valued representation of  $\mathcal{D}_4$  with  $\mathcal{G}$  as the corresponding (universal) covering group.

the generators of Eqs. (3.18) can be explicitly written as

$$\mathcal{D}(a_1) \equiv \text{diag} \left[ \begin{pmatrix} -1 & 0 \\ 0 & 1 \end{pmatrix}, \begin{pmatrix} 1 & 0 \\ 0 & 1 \end{pmatrix}, \begin{pmatrix} 0 & 1 \\ 1 & 0 \end{pmatrix}, \begin{pmatrix} 0 & 1 \\ 1 & 0 \end{pmatrix} \right], \quad (3.19a)$$

$$\mathcal{D}(a_2) \equiv \text{diag} \left[ \begin{pmatrix} 0 & 1 \\ 1 & 0 \end{pmatrix}, \begin{pmatrix} 0 & 1 \\ 1 & 0 \end{pmatrix}, \begin{pmatrix} -1 & 0 \\ 0 & 1 \end{pmatrix}, \begin{pmatrix} 1 & 0 \\ 0 & 1 \end{pmatrix} \right], \quad (3.19b)$$

$$\mathcal{D}(a_3) \equiv \text{diag} \left[ \begin{pmatrix} 1 & 0 \\ 0 & 1 \end{pmatrix}, \begin{pmatrix} 1 & 0 \\ 0 & 1 \end{pmatrix}, \begin{pmatrix} -1 & 0 \\ 0 & 1 \end{pmatrix}, \begin{pmatrix} -1 & 0 \\ 0 & 1 \end{pmatrix} \right], \quad (3.19c)$$

$$\mathcal{D}(a_4) \equiv \text{diag} \left[ \begin{pmatrix} -1 & 0 \\ 0 & 1 \end{pmatrix}, \begin{pmatrix} -1 & 0 \\ 0 & 1 \end{pmatrix}, \begin{pmatrix} 1 & 0 \\ 0 & 1 \end{pmatrix}, \begin{pmatrix} 1 & 0 \\ 0 & 1 \end{pmatrix} \right]. \quad (3.19d)$$

With respect to  $\mathcal{D}$ , we will combine the left- and right-handed SM leptons as well as the Dirac neutrinos of the 2nd and 3rd generations into the  $\mathcal{G}$ -doublets  $\mathbf{2}_\ell \equiv (\ell_\mu, \ell_\tau)^T$ ,  $\mathbf{2}_E \equiv (E_\mu, E_\tau)^T$ , and  $\mathbf{2}_F \equiv (F_\mu, F_\tau)^T$ , respectively. The fermionic doublets  $\mathbf{2}_\ell$  and  $\mathbf{2}_F$  as well as the scalars  $\xi_1 \equiv (\xi_{1a}, \xi_{1b})^T$  and  $\xi_2 \equiv (\xi_{2a}, \xi_{2b})^T$  are all put into the doublet representation  $D_1$ . Next, the generalized Wigner-Eckart theorem tells us that the effective Yukawa interaction matrix spanned by  $\mathbf{2}_\ell$  and  $\mathbf{2}_E$  in the  $\mu$ - $\tau$ -subsector of the charged leptons is identical with a linear combination of sets of irreducible Yukawa tensor operators. If the irreducible Yukawa tensor operators take their values in the vector representation of  $\mathcal{D}_4$ , it is clear from App. B, that the hierarchy  $m_\mu \ll m_\tau$  is only possible if  $\mathbf{2}_E$  transforms according to an irrep of  $\mathcal{G}$  which is inequivalent<sup>4</sup> with  $D_1$ . We will therefore put  $\mathbf{2}_E$  into the irrep  $D_2$  which is inequivalent with  $D_1$  and note that the large subgroup of  $\mathcal{G}$  generated by  $\mathcal{D}(a_2)$ ,  $\mathcal{D}(a_3)$ , and  $\mathcal{D}(a_4)$  acts diagonally on  $\mathbf{2}_\ell$  and  $\mathbf{2}_E$ .

Now, if the Wilson loops  $\text{Tr}(\Pi_{i=1}^4 Q_i^\mu)$  and  $\text{Tr}(\Pi_{i=1}^2 Q_i^\tau)$  are non-singlet representations of  $\mathcal{G}$ , a non-trivial Yukawa matrix structure in the  $\mu$ - $\tau$ -subsector of the charged leptons can be generated at the non-renormalizable level. Although the irreps  $D_1$  and  $D_2$  already determine the overall transformation properties of the Wilson loops under  $\mathcal{G}$  via the generalized Wigner-Eckart theorem, there is still some ambiguity in the individual  $\mathcal{G}$ -charge assignment to the link-fields  $Q_1^\mu, Q_2^\mu, Q_3^\mu, Q_4^\mu$ , and  $Q_1^\tau, Q_2^\tau$ . Here, it is appealing to assume that all the scalar link fields of  $G^\mu$  and  $G^\tau$  transform according to some doublet subrepresentation of  $\mathcal{G}$ , which has the property that its lift is isomorphic with  $\mathcal{D}_4$ . Since each of the Wilson loops  $\text{Tr}(\Pi_{i=1}^4 Q_i^\mu)$  and  $\text{Tr}(\Pi_{i=1}^2 Q_i^\tau)$  involves an even number of (two or four) link fields, we find from the multiplication rules in App. B that this can only be the case if each of the sets  $\{Q_1^\mu, Q_2^\mu, Q_3^\mu, Q_4^\mu\}$  and  $\{Q_1^\tau, Q_2^\tau\}$  contains at least two inequivalent irreps. This can be simply realized by putting, *e.g.*, the 1st ( $i = 1$ ) link fields  $Q_1^\mu$  and  $Q_1^\tau$  into the doublet representation  $D_3$  while the remaining link fields  $Q_2^\mu, Q_3^\mu, Q_4^\mu$ , and  $Q_2^\tau$  all transform as doublets under  $D_4$  (see Fig. 3.8). Note again, that both  $D_3$  and  $D_4$  are characterized by a large common subgroup generated by  $\mathcal{D}(a_1)$ ,  $\mathcal{D}(a_3)$ , and  $\mathcal{D}(a_4)$ , which acts diagonally

<sup>4</sup>Similarity transformations allow only mappings within one class, which would yield  $m_\mu =$

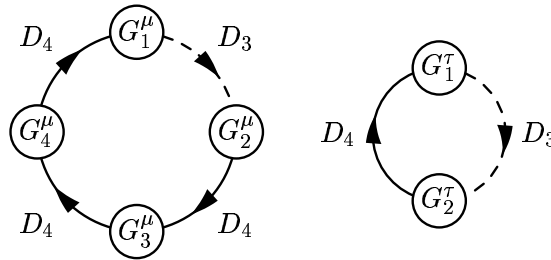


Figure 3.8: “Space-dependent” transformation properties of the link variables of the product gauge groups  $G^\mu$  (left panel) and  $G^\tau$  (right panel) under the discrete group  $\mathcal{G}$ . The link-fields connecting the 1st with the 2nd site (in this direction) are in the irrep  $D_3$  (dashed arrows). The remaining link fields are in the irrep  $D_4$  (solid arrows).

$I$	$D_1$	$D_2$	$D_3$	$D_4$
$\mathbf{1}_\ell, \mathbf{1}_E, \mathbf{1}_F, \xi_0$	$\mathbf{2}_\ell, \mathbf{2}_F, \xi_1, \xi_2$	$\mathbf{2}_E$	$Q_1^\mu, Q_1^\tau$	$Q_2^\mu, Q_3^\mu, Q_4^\mu, Q_2^\tau$

Table 3.2: Assignment of the fermionic and scalar fields to the irreps  $D_1, D_2, D_3, D_4$ , and  $I$ . Note that the scalar link fields transform according to their position in the “index space” of gauge groups (see Fig. 3.8).

on all of the link fields. In component-form, the scalar  $\mathcal{G}$ -doublets will be written as  $Q_i^\mu \equiv (q_{ia}^\mu, q_{ib}^\mu)^T$ , where  $i = 1, 2, 3, 4$ , and  $Q_i^\tau \equiv (q_{ia}^\tau, q_{ib}^\tau)^T$ , where  $i = 1, 2$ . To complete the  $\mathcal{G}$ -charge assignment, we suppose that the first generation fields  $\ell_e, E_e$ , and  $F_e$ , as well as the scalar  $\xi_0$  transform only trivially under  $\mathcal{G}$ , *i.e.*, they are all put into the identity representation  $I$  of  $\mathcal{G}$ . For the fermionic  $\mathcal{G}$ -singlets  $\ell_e, E_e$ , and  $F_e$  we will equivalently choose the notation  $\mathbf{1}_\ell \equiv \ell_e$ ,  $\mathbf{1}_E \equiv E_e$ , and  $\mathbf{1}_F \equiv F_e$ . The assignment of the fields to the irreps  $D_i$  and  $I$  is summarized in table 3.2.

In this section, we have presented the non-Abelian group  $\mathcal{G}$  in terms of its generators which are motivated by phenomenology. In the following subsection we will examine in some more detail the structure of  $\mathcal{G}$  through a descending series of normal subgroups which define the *normal structure* of  $\mathcal{G}$ .

### 3.3.3 Normal structure

In Sec. 3.3.2, the discrete group  $\mathcal{G}$  has been constructed from the generators of the dihedral group  $\mathcal{D}_4$ . A standard way of gaining further information about  $\mathcal{G}$  is to analyze a series of subgroups of  $\mathcal{G}$ , where each term is either normal in  $\mathcal{G}$  or at least normal in the previous term. In general, if a subgroup  $N$  of some group  $G$  is normal in  $G$ , we will write  $N \trianglelefteq G$ . Moreover, we call  $\text{Aut}(N)$  the automorphism group of

---

$m_\tau$  after SSB. Note also that different transformation properties of left-handed and right-handed fermions under horizontal symmetries are used in models of “neutrino democracy” [74].

$N$ , *i.e.*, the group of bijective endomorphisms of  $N$ .

We will denote by  $\mathcal{K}_1$  the collection of all elements  $g \in \mathcal{G}$  which obey  $D_1(g) = \mathbb{1}_2$ , where  $\mathbb{1}_2$  is the  $2 \times 2$  unit matrix. Accordingly, we will define  $\mathcal{K}_2$  as the set of all elements  $g \in \mathcal{G}$  which obey  $D_1(g) = D_2(g) = \mathbb{1}_2$ , and  $\mathcal{K}_3$  as the set of all elements  $g \in \mathcal{G}$  which obey  $D_1(g) = D_2(g) = D_3(g) = \mathbb{1}_2$ . We therefore have the sequence

$$\mathcal{K}_3 \subset \mathcal{K}_2 \subset \mathcal{K}_1 \subset \mathcal{G}, \quad (3.20)$$

where each subset is a group, actually an invariant subgroup of the embedding groups, for if  $a \in \mathcal{K}_i$  ( $i = 1, 2, 3$ ) is homomorphically mapped on the identity of the operator group  $D_1 \oplus \dots \oplus D_i$ , then so are all elements in its class. We therefore have  $\mathcal{K}_{i+1} \trianglelefteq \mathcal{K}_i$  and  $\mathcal{K}_i \trianglelefteq \mathcal{G}$  for every  $i$ , *i.e.*, the subgroup series in Eq. (3.20) is in fact a *normal series*. From Eqs. (3.19) we find that for any  $k \in \mathcal{K}_2$  the factorization of  $\mathcal{D}(k)$  into a product of the operators  $\mathcal{D}(a_i)$  ( $i = 1, 2, 3, 4$ ) necessarily involves each of the factors  $\mathcal{D}(a_1)$ ,  $\mathcal{D}(a_2)$ , and  $\mathcal{D}(a_4)$  an even number of times. In turn, this implies that the operators  $D_3(k)$  and  $D_4(k)$  are on diagonal form and can take their values only in the classes  $E, C_4^2$ , and  $C_2(2)$  of the dihedral group  $\mathcal{D}_4$  (see App. B). Since the number of elements in the classes  $E, C_4^2$ , and  $C_2(2)$  is four, we conclude that the order of  $\mathcal{K}_2$ , which we will denote by  $|\mathcal{K}_2|$ , obeys  $|\mathcal{K}_2| \leq 4$ . Indeed, besides the unity  $e$ , we find the three distinct elements  $b_1 = a_1 a_3 a_1$ ,  $b_2 = a_3$ , and  $b_3 = (a_1 a_3)^2$  which form  $\mathcal{K}_2 = \{e, b_1, b_2, b_3\}$ . Hence,  $|\mathcal{K}_2| = 4$  and we have

$$\mathcal{D}(b_1) = \text{diag} [D(E), D(E), D(C_a), D(C_a)], \quad (3.21a)$$

$$\mathcal{D}(b_2) = \text{diag} [D(E), D(E), D(C_b), D(C_b)], \quad (3.21b)$$

$$\mathcal{D}(b_3) = \text{diag} [D(E), D(E), D(C_4^2), D(C_4^2)]. \quad (3.21c)$$

Since  $\mathcal{K}_3 \trianglelefteq \mathcal{K}_2$ , the group  $\mathcal{K}_3$  is trivial  $\mathcal{K}_3 = e$ , as inspection of Eqs. (3.21) shows. Moreover, from Eqs. (3.21) we find that  $\mathcal{K}_2$  describes a 2-fold axis with a system of two 2-fold axes at right angle to it. Hence,  $\mathcal{K}_2$  is isomorphic with the *Klein group*  $Z_2 \times Z_2 \simeq \mathcal{K}_2$ . In fact, the Klein group is one of the dihedral groups  $Z_2 \times Z_2 \simeq \mathcal{D}_2$  (see App. B) and is one of the two only possible distinct structures for abstract groups of order 4. Since  $\mathcal{D}_2 \subset \mathcal{D}_4$ , we have expressed in Table 3.3 the multiplication table of  $\mathcal{D}_2$  in terms of the elements of the classes  $E, C_4^2$ , and  $C_2(2)$  of  $\mathcal{D}_4$ , which generate  $\mathcal{D}_2$ . With  $\mathcal{K}_2$  explicitly given in Eqs. (3.21), we can now easily construct a representation of the group  $\mathcal{K}_1 \supseteq \mathcal{K}_2$ . First, note that for any  $k \in \mathcal{K}_1$  the factorization of the operator  $\mathcal{D}(k)$  into a product of the generators in Eq. (3.19) must involve  $\mathcal{D}(a_2)$  an even number of times. Hence,  $D_2(k)$  is necessarily on diagonal form and can take its values only in the classes  $E, C_4^2$ , and  $C_2(2)$  of  $\mathcal{D}_4$ . This implies that the index  $|\mathcal{K}_1 : \mathcal{K}_2|$  of  $\mathcal{K}_2$  under  $\mathcal{K}_1$  (*i.e.*, the number of cosets of  $\mathcal{K}_2$  in  $\mathcal{K}_1$ ) is at most four. In

	$(E, e)$	$(C_a, c_1)$	$(C_b, c_2)$	$(C_4^2, c_3)$
$(E, e)$	$(E, e)$	$(C_a, c_1)$	$(C_b, c_2)$	$(C_4^2, c_3)$
$(C_a, c_1)$	$(C_a, c_1)$	$(E, e)$	$(C_4^2, c_3)$	$(C_b, c_2)$
$(C_b, c_2)$	$(C_b, c_2)$	$(C_4^2, c_3)$	$(E, e)$	$(C_a, c_1)$
$(C_4^2, c_3)$	$(C_4^2, c_3)$	$(C_b, c_2)$	$(C_a, c_1)$	$(E, e)$

Table 3.3: Multiplication table of the Klein group  $Z_2 \times Z_2 \simeq \mathcal{D}_2$  expressed in terms of the elements of the classes  $E$ ,  $C_4^2$ , and  $C_2(2)$  of  $\mathcal{D}_4$  (see App. B). The brackets indicate the homomorphism between  $\mathcal{D}_2$  and the right transversal  $T_2 = \{e, c_1, c_2, c_3\}$  for  $\mathcal{K}_2$  (see text). Note that the group table is symmetric about the main diagonal since  $\mathcal{D}_2$  is Abelian.

fact, the group  $\mathcal{K}_1$  can be decomposed into (right) cosets<sup>5</sup> in terms of<sup>6</sup>

$$\mathcal{K}_1 \simeq \mathcal{K}_2 + \sum_{i=1}^3 \mathcal{K}_2 c_i, \quad (3.22)$$

where we can choose the different coset representatives to be  $c_1 = a_2 a_1 a_4 a_2$ ,  $c_2 = a_1 a_4$ , and  $c_3 = c_1 c_2$ . In other words, four elements of  $\mathcal{K}_1$  are mapped on each element of the operator group corresponding to the representation of  $\mathcal{K}_1$  *subduced* by  $D_2$  which we write as<sup>7</sup>  $D_2 \downarrow \mathcal{K}_1$ . The coset representatives in Eq. (3.22) can be combined into the right transversal  $T_2 = \{e, c_1, c_2, c_3\}$  for  $\mathcal{K}_2$  and we explicitly have

$$\mathcal{D}(c_1) = \text{diag} [D(E), D(C_a), D(C_{a'}), D(C_b)], \quad (3.23a)$$

$$\mathcal{D}(c_2) = \text{diag} [D(E), D(C_b), D(C_{b'}), D(C_{b'})], \quad (3.23b)$$

$$\mathcal{D}(c_3) = \text{diag} [D(E), D(C_4^2), D(C_4^2), D(E)]. \quad (3.23c)$$

Since the subgroup  $\mathcal{K}_2 \trianglelefteq \mathcal{K}_1$  is the kernel of  $D_2 \downarrow \mathcal{K}_1$ , the operators  $D_2(c_i)$  ( $i = 1, 2, 3$ ) from the (right) transversal allow us to identify the lift of  $D_2 \downarrow \mathcal{K}_1$  as the Klein group  $Z_2 \times Z_2$ . Also, upon identifying  $e \rightarrow E$ ,  $c_1 \rightarrow C_a$ ,  $c_2 \rightarrow C_b$ , and  $c_3 \rightarrow C_4^2$ , it is shown in Table 3.3 that  $T_2 \simeq Z_2 \times Z_2$ . Hence, we conclude that  $\mathcal{K}_1$  is a semi-direct product  $\mathcal{K}_1 = \mathcal{K}_2 \rtimes T_2$  or *split extension* of  $\mathcal{K}_2$  by  $T_2$  which can equivalently be written as

$$\mathcal{K}_1 \simeq (Z_2 \times Z_2) \rtimes_{\varphi} (Z_2 \times Z_2), \quad (3.24)$$

<sup>5</sup>Since the subgroup  $\mathcal{K}_2$  is invariant, left and right cosets are identical.

<sup>6</sup>Here “+” denotes the summation of sets, *i.e.*, the group  $\mathcal{K}_1$  contains all the elements in  $\mathcal{K}_2$  and all the elements in the sets  $\mathcal{K}_2 c_i$  ( $i = 1, 2, 3$ ). Note that, in this instance, the sets  $\mathcal{K}_2, \mathcal{K}_2 c_1, \dots$  are all disjoint.

<sup>7</sup>This is usually also called the *subduced representation*.

where  $\varphi : T_2 \rightarrow \text{Aut}(\mathcal{K}_2)$  is the conjugation homomorphism describing the interaction of the two  $Z_2 \times Z_2$  subgroups inside  $\mathcal{G}$ . On  $\mathcal{K}_2 \times T_2$ , the semi-direct product in Eq. (3.24) defines a binary operation by

$$(k_1, t_1)(k_2, t_2) = (k_1\varphi(t_1)(k_2), t_1t_2), \quad (3.25)$$

where  $k_1, k_2 \in \mathcal{K}_2$  and  $t_1, t_2 \in T_2$ . In Eq. (3.25), the conjugation of  $k_2$  by  $t_1$  reads

$$\varphi(t_1)(k_2) = t_1k_2t_1^{-1}, \quad (3.26)$$

and maps  $\mathcal{K}_2$  to  $\mathcal{K}_2$  since  $\mathcal{K}_2$  is normal in  $\mathcal{K}_1$ . In this way, the semi-direct product in Eq. (3.24) yields a prescription of how to perform the group operations of  $\mathcal{K}_1$  in terms of the group operations of the subgroups  $\mathcal{K}_2$  and  $T_2$  via the homomorphism  $\varphi$ . Assume that  $\varphi : T_2 \rightarrow \text{Aut}(\mathcal{K}_2)$  were the trivial automorphism. Then it would hold  $ktk^{-1} = k\varphi(t)(k^{-1})t = kk^{-1}t = t$  for any  $t \in T_2$  and  $k \in \mathcal{K}_2$  implying that  $T_2 \trianglelefteq \mathcal{K}_1$ . Therefore,  $\mathcal{K}_1 = T_2 \times \mathcal{K}_2$  and  $\mathcal{K}_1$  would be Abelian. In our case, however, the coset representatives  $c_i \in T_2$  ( $i = 1, 2, 3$ ) don't commute with the elements  $b_i \in \mathcal{K}_2$  ( $i = 1, 2, 3$ ) and hence the conjugation homomorphism  $\varphi$  in Eq. (3.26) is actually non-trivial and  $\mathcal{K}_1$  non-Abelian. Now,  $|\mathcal{K}_1| = |\mathcal{K}_2| \cdot |T_2| = 16$ , *i.e.*,  $\mathcal{K}_1$  contains 16 elements.

The coset graph of  $\mathcal{K}_1$  with respect to the subgroups  $\mathcal{K}_2$  and  $T_2$  is given in Fig. 3.9. Each coset of  $\mathcal{K}_2$  and  $T_2$  in  $\mathcal{K}_1$  is represented by one vertex and each edge represents the elements belonging to both the cosets associated with the vertices which are connected by the edge. Since  $\mathcal{K}_2$  and  $T_2$  generate  $\mathcal{K}_1$ , the coset graph is simply connected (for a discussion of coset graphs see, *e.g.*, Ref. [75]). Here, the 16 edges can be isomorphically mapped on the 16 elements of  $\mathcal{K}_1$ . In this plane configuration, two distinct vertices are contained in at most one line. Also, given an edge  $l$  and a vertex  $p$  not on  $l$ , there is at most one edge  $k$  through  $p$  that intersects  $l$ . Hence, the coset graph satisfies the axioms for a *generalized quadrangle* of order  $(1, 4)$  and describes the complete bipartite graph on 8 vertices.<sup>8</sup> As can be seen in Fig. 3.9, it has valency 2, diameter 2 and girth 4. The associated incidence graph, which contains the complete information about the coset graph, has 24 vertices. The coset graph can also be modeled in three dimensions on the cube by taking as its points the 8 vertices of the cube and as its lines the 12 sides and 4 main diagonals of the cube. The decomposition of  $\mathcal{G}$  into right cosets with respect to  $\mathcal{K}_1$  reads

$$\mathcal{G} \simeq \mathcal{K}_1 + \sum_{i=1}^7 \mathcal{K}_1 d_i, \quad (3.27)$$

where we can choose for the coset representatives  $d_1 = a_2a_1$ ,  $d_2 = a_1a_2$ ,  $d_3 = (a_1a_2)^2$ ,  $d_4 = a_2a_1a_2$ ,  $d_5 = a_1$ ,  $d_6 = a_1a_2a_1$ , and  $d_7 = a_2$ . The coset representatives are

---

<sup>8</sup>We call a graph *complete* if any two of its vertices are connected by an edge.

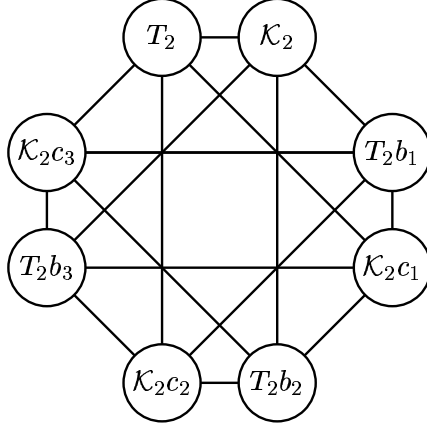


Figure 3.9: Coset graph of  $\mathcal{K}_1 = \mathcal{K}_2 \rtimes T_2$  with respect to  $\mathcal{K}_2$  and  $T_2$ .

combined into the right transversal  $T_1 = \{e, d_1, \dots, d_7\}$  and explicitly read

$$\mathcal{D}(d_1) = \text{diag} [D(C_4), D(C_{b'}), D(C_4^3), D(C_{b'})], \quad (3.28a)$$

$$\mathcal{D}(d_2) = \text{diag} [D(C_4^3), D(C_{b'}), D(C_4), D(C_{b'})], \quad (3.28b)$$

$$\mathcal{D}(d_3) = \text{diag} [D(C_4^2), D(E), D(C_4^2), D(E)], \quad (3.28c)$$

$$\mathcal{D}(d_4) = \text{diag} [D(C_a), D(E), D(C_{a'}), D(C_{b'})], \quad (3.28d)$$

$$\mathcal{D}(d_5) = \text{diag} [D(C_b), D(E), D(C_{b'}), D(C_{b'})], \quad (3.28e)$$

$$\mathcal{D}(d_6) = \text{diag} [D(C_{a'}), D(C_{b'}), D(C_a), D(E)], \quad (3.28f)$$

$$\mathcal{D}(d_7) = \text{diag} [D(C_{b'}), D(C_{b'}), D(C_b), D(E)], \quad (3.28g)$$

from which we conclude that  $\mathcal{G}/\mathcal{K}_1 \simeq \mathcal{D}_4$ . Moreover, Table B.3 in App. B shows that the right transversal  $T_1$  forms a group which is isomorphic with  $\mathcal{D}_4$ . Using Eq. (3.22), it follows that  $\mathcal{G}$  is a split extension

$$\mathcal{G} \simeq (Z_2 \times Z_2) \rtimes_{\varphi} (Z_2 \times Z_2) \rtimes_{\psi} \mathcal{D}_4, \quad (3.29)$$

where, in analogy with Eq. (3.24), the mapping  $\psi : T_1 \rightarrow \text{Aut}(\mathcal{K}_1)$  is the conjugation homomorphism describing the interaction of  $\mathcal{D}_4$  with the involved  $Z_2 \times Z_2$  subgroups inside  $\mathcal{G}$ . The corresponding splitting map is specified by the generators in Eqs. (3.28). Again, the seven coset representatives don't commute with the elements of  $\mathcal{K}_1$ , which shows that  $\psi$  cannot be the trivial homomorphism. Here, the irrep

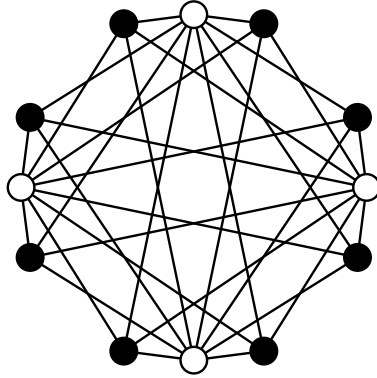


Figure 3.10: Coset graph of  $T_2 \rtimes T_1 \simeq (Z_2 \times Z_2) \rtimes \mathcal{D}_4$  with respect to  $T_1$  and  $T_2$ . The coset graph is a subgraph of the complete bipartite graph on 16 vertices, *i.e.*, the generalized quadrangle of order  $(1, 8)$ .

$D_1$  maps 16 elements of  $\mathcal{G}$  onto each element of  $\mathcal{D}_4$  and hence  $|\mathcal{G}| = |T_1| \cdot |\mathcal{K}_1| = 128$ . The coset graph of  $T_2 \rtimes T_1 \simeq (Z_2 \times Z_2) \rtimes \mathcal{D}_4$  with respect to  $T_1$  and  $T_2$  is shown in Fig. 3.10. Each solid (open) vertex corresponds to one coset of  $T_1$  ( $T_2$ ) in  $T_2 \rtimes T_1$ . This coset graph is a subgraph of the complete bipartite graph on 16 vertices and can be constructed as follows. First, label the vertices of a regular 16-gon (in a natural way) from 0 to 15. Then, connect two vertices  $i$  and  $j$  if and only if  $i - j$  is an odd number. This defines the complete bipartite graph on 16 vertices (or generalized quadrangle of order  $(1, 8)$ ). Now, remove each line pencil<sup>9</sup> which is carried by a vertex  $i$  obeying  $i \bmod 4 = 2$  and one arrives at the coset graph in Fig. 3.10. In a similar way, one can construct the coset graph of  $\mathcal{G} = \mathcal{K}_1 \rtimes T_1$  with respect to  $\mathcal{K}_1$  and  $T_1$  by starting with the complete bipartite graph on 32 vertices.

From Eqs. (3.28) it is obvious that the operator group associated with the irrep  $D_1$  has  $\mathcal{K}_1$  as its kernel. In other words, by factoring  $D_1$  with respect to the subgroup  $\mathcal{K}_1$  we see that the lift of  $D_1$  is isomorphic with  $\mathcal{D}_4$ . Furthermore, by replacing  $\mathcal{D}(a_1) \rightarrow \mathcal{D}(a_1)\mathcal{D}(a_4)$ , it is seen that the irreps  $D_1$  and  $D_2$  change their rôles in the above considerations. Taking, in addition, the exchange symmetry between  $\mathcal{D}(a_1) \leftrightarrow \mathcal{D}(a_2)$  and  $\mathcal{D}(a_3) \leftrightarrow \mathcal{D}(a_4)$  under permutation of the  $4 \times 4$  submatrices on the diagonal into account (see Sec. 3.3.2), we generally conclude that the lift of every subrepresentation  $D_i$  ( $i = 1, 2, 3, 4$ ) is isomorphic with  $\mathcal{D}_4$ .

In this subsection we have analyzed the structure of the group  $\mathcal{G}$  and its relation to the dihedral groups  $\mathcal{D}_2$  and  $\mathcal{D}_4$ . Specifically, we have seen that the lift of any irrep  $D_i$  ( $i = 1, 2, 3, 4$ ) is isomorphic with  $\mathcal{D}_4$ . This will allow us in the next section to apply the decomposition and multiplication rules of  $\mathcal{D}_4$  in order to find the relevant  $\mathcal{G}$ -singlets in product representations.

<sup>9</sup>A *line pencil* corresponding to a set of points of a geometry is the set of all edges which contain all the points in the set.



### 3.4 Construction of the scalar potential

We will denote by  $\Phi$  and  $\Omega$  two arbitrary scalar  $\mathcal{G}$ -doublets which are listed in table 3.2 and write them in component-form as

$$\Phi \equiv (\phi_a, \phi_b)^T, \quad \Omega \equiv (\omega_a, \omega_b)^T, \quad (3.30)$$

where  $\Phi, \Omega \in \{\xi_1, \xi_2, Q_1^\mu, Q_2^\mu, Q_3^\mu, Q_4^\mu, Q_1^\tau, Q_2^\tau\}$ . For definiteness, we will assume that  $\Phi$  is put into the irrep  $D_i$  and  $\Omega$  is put into the irrep  $D_j$ , where  $i, j = 1, 3, 4$ . Invariance under the product groups  $G^\mu \times G^\tau \times G^\nu$  and  $Z_8 \times Z'_8$  tells us that any renormalizable term in the scalar potential which involves, *e.g.*, the field  $\Phi$  must actually contain the tensor product  $\Phi \otimes \Phi^\dagger$ . The lowest-dimensional  $\mathcal{G}$ -invariant operator-products of  $\Phi$  in the multi scalar potential are therefore

$$V_0(\Phi) \equiv \Phi \otimes \Phi^\dagger|_{1_A} = A_0 (|\phi_a|^2 + |\phi_b|^2), \quad (3.31)$$

where  $\Phi$  transforms under any of the irreps  $D_i$  ( $i = 1, 3, 4$ ) and  $A_0$  is a real-valued number. Note that three-fold products of  $\Phi$  and  $\Phi^\dagger$  in the potential are forbidden by both the  $SU(m)$  charge assignment as well as by  $\mathcal{G}$ -invariance. Accordingly, any invariant term in the scalar potential which mixes the doublets  $\Phi$  and  $\Omega$  must be contained in the product representation  $\Phi \otimes \Phi^\dagger \otimes \Omega \otimes \Omega^\dagger$ . Since the liftings of the irreps  $D_i$  and  $D_j$  are isomorphic with  $\mathcal{D}_4$  (see Sec. 3.3.3), the  $\mathcal{G}$ -invariant mixed terms of  $\Phi$  and  $\Omega$  are found by considering all combinations of the one-dimensional irreps of  $\mathcal{D}_4$  in the product

$$\Phi \otimes \Phi^\dagger \otimes \Omega \otimes \Omega^\dagger = [\mathbf{1}_A^i + \mathbf{1}_B^i + \mathbf{1}_C^i + \mathbf{1}_D^i] \otimes [\mathbf{1}_A^j + \mathbf{1}_B^j + \mathbf{1}_C^j + \mathbf{1}_D^j], \quad (3.32)$$

where each of the sets  $\mathbf{1}_A^i, \mathbf{1}_B^i, \mathbf{1}_C^i, \mathbf{1}_D^i$ , and  $\mathbf{1}_A^j, \mathbf{1}_B^j, \mathbf{1}_C^j, \mathbf{1}_D^j$  respectively denotes the  $\mathcal{D}_4$ -singlet representations associated with  $D_i$  and  $D_j$  (see App. B). In component-form, the singlet representations are explicitly given in Eq. (B.3). In order to extract from Eq. (3.32) the relevant dimension-four terms, we will first suppose that  $\Phi$  and  $\Omega$  are put into the same irrep  $D_i = D_j$ . Then, the decomposition of the product representations in Eq. (B.2) in conjunction with the multiplication rules in table B.2 yield that the invariant mixed terms of  $\Phi$  and  $\Omega$  are in this case

$$\begin{aligned} V_1(\Phi, \Omega) &\equiv (\Phi \otimes \Phi^\dagger) \otimes (\Omega \otimes \Omega^\dagger)|_{1_A} \\ &= A_1 (|\phi_a|^2 + |\phi_b|^2) (|\omega_a|^2 + |\omega_b|^2) \\ &\quad + B_1 (\phi_a \phi_b^\dagger - \phi_a^\dagger \phi_b) (\omega_a \omega_b^\dagger - \omega_a^\dagger \omega_b) \\ &\quad + C_1 (|\phi_a|^2 - |\phi_b|^2) (|\omega_a|^2 - |\omega_b|^2) \\ &\quad + D_1 (\phi_a \phi_b^\dagger + \phi_a^\dagger \phi_b) (\omega_a \omega_b^\dagger + \omega_a^\dagger \omega_b), \end{aligned} \quad (3.33a)$$

where we have labeled the real-valued coefficients  $A_1, B_1, C_1$ , and  $D_1$  of the invariants according to the sequence of products  $(\mathbf{1}_A)^2, (\mathbf{1}_B)^2, (\mathbf{1}_C)^2$ , and  $(\mathbf{1}_D)^2$ . Let us now turn

to the case, when  $\Phi$  and  $\Omega$  belong to different irreps  $D_i \neq D_j$ . First, suppose that  $\Phi$  transforms under  $D_3$  and  $\Omega$  transforms under  $D_4$ . Application of the generators  $\mathcal{D}(a_1), \mathcal{D}(a_2)$ , and  $\mathcal{D}(a_3)$  yields that in Eq. (3.32) for  $i = 3$  and  $j = 4$  only the combinations  $\mathbf{1}_{\mathbf{A}}^i \otimes \mathbf{1}_{\mathbf{A}}^j$  and  $\mathbf{1}_{\mathbf{C}}^i \otimes \mathbf{1}_{\mathbf{C}}^j$  are  $\mathcal{G}$ -invariants. Hence, the most general invariant mixed term of  $\Phi$  and  $\Omega$  reads

$$V_2(\Phi, \Omega) \equiv A_2 (|\phi_a|^2 + |\phi_b|^2) (|\omega_a|^2 + |\omega_b|^2) + C_2 (|\phi_a|^2 - |\phi_b|^2) (|\omega_a|^2 - |\omega_b|^2), \quad (3.33b)$$

where  $\Phi \in \{Q_1^\tau, Q_1^\mu\}$ ,  $\Omega \in \{Q_2^\tau, Q_2^\mu, Q_3^\mu, Q_4^\mu\}$  and the coefficients  $A_2, C_2$  are real-valued numbers. Now, suppose that  $\Phi$  transforms under  $D_1$  and  $\Omega$  transforms under one of the irreps  $D_3$  or  $D_4$ . In this case, subsequent application of the operators  $\mathcal{D}(a_i)$  ( $i = 1, 2, 3, 4$ ) to Eq. (3.32) readily yields that the most general mixed term of the fields  $\Phi$  and  $\Omega$  is given by  $\mathbf{1}_{\mathbf{A}}^i \otimes \mathbf{1}_{\mathbf{A}}^j$  and hence

$$V_3(\Phi, \Omega) \equiv A_3 (|\phi_a|^2 + |\phi_b|^2) (|\omega_a|^2 + |\omega_b|^2), \quad (3.33c)$$

where  $\Phi \in \{\xi_1, \xi_2\}$ ,  $\Omega \in \{Q_1^\tau, Q_2^\tau, Q_1^\mu, Q_2^\mu, Q_3^\mu, Q_4^\mu\}$  and the coefficient  $A_3$  is a real-valued number. Putting everything together, the most general multi scalar potential  $V$  of the SM singlet scalar fields decomposes into the terms  $V_0(\Phi), V_1(\Phi, \Omega), V_2(\Phi, \Omega)$ , and  $V_3(\Phi, \Omega)$  of Eqs. (3.33), as follows

$$\begin{aligned} V \equiv & \sum_{i,j,k} [V_0(\xi_i) + V_0(Q_j^\tau) + V_0(Q_k^\mu)] + \sum_{i_1, i_2=1,2} V_1(\xi_{i_1}, \xi_{i_2}) \\ & + \sum_{X,Y=Q_1^\tau, Q_1^\mu} V_1(X, Y) + \sum_{j_1, j_2=2}^4 [V_1(Q_2^\tau, Q_{j_1}^\mu) + V_1(Q_{j_1}^\mu, Q_{j_2}^\mu)] \\ & + V_1(Q_2^\tau, Q_2^\tau) + \sum_{X=Q_1^\tau, Q_1^\mu} \sum_{j_1=2}^4 [V_2(X, Q_2^\tau) + V_2(X, Q_{j_1}^\mu)] \\ & + \sum_{i,j,k} [V_3(\xi_i, Q_j^\tau) + V_3(\xi_i, Q_k^\mu)], \end{aligned} \quad (3.34)$$

where  $i = 1, 2$ ;  $j = 1, 2$ , and  $k = 1, 2, 3, 4$ . In Eq. (3.34), we have omitted  $\xi_0$  and the  $SU(2)$  Higgs doublet  $H$ . Actually, in any renormalizable terms of the full multi-scalar potential which mix the  $\mathcal{G}$ -singlets with the  $\mathcal{G}$ -doublets, the  $\mathcal{G}$ -singlet fields  $\xi_0$  and  $H$  are only allowed to appear in terms of their absolute squares  $|\xi_0|^2$  and  $|H|^2$ . This is an immediate consequence of the  $Z_8 \times Z'_8$  charge of  $\xi_0$  and the electroweak quantum numbers of  $H$ . As a result, there exists a range of parameters in the multi-scalar potential where the vacuum alignment of the  $\mathcal{G}$ -doublet scalars is essentially independent from the details of the VEVs  $\langle \xi_0 \rangle$  and  $\langle H \rangle$ . Specifically, we can assume the standard electroweak symmetry breaking and allow the field  $\xi_0$  to acquire an arbitrary VEV of the order  $|\langle \xi_0 \rangle| \simeq 10^2$  GeV. It is therefore sufficient to restrict our considerations concerning the vacuum alignment of the  $\mathcal{G}$ -doublet scalars

to the potential  $V$  in Eq. (3.34), in order to determine the range of parameters which leads to realistic lepton masses and mixing angles. This analysis will be carried out in the following section.

### 3.5 The vacuum alignment mechanism

We will now determine the vacuum structure emerging after SSB from the potential  $V$  by individually minimizing each of the potentials  $V_1(\Phi, \Omega)$  and  $V_2(\Phi, \Omega)$  which appear in Eq. (3.34) (see App. C). For this purpose, it is suitable to parameterize the VEVs of the doublets  $\Phi$  and  $\Omega$  like in Eqs. (2.13) as

$$\langle \Phi \rangle = \begin{pmatrix} \langle \phi_a \rangle \\ \langle \phi_b \rangle \end{pmatrix} = v_1 \begin{pmatrix} e^{i\varphi_1} \cos \alpha \\ e^{i\varphi'_1} \sin \alpha \end{pmatrix} \equiv v_1 \begin{pmatrix} e^{i\varphi_1} c_\alpha \\ e^{i\varphi'_1} s_\alpha \end{pmatrix}, \quad (3.35a)$$

$$\langle \Omega \rangle = \begin{pmatrix} \langle \omega_a \rangle \\ \langle \omega_b \rangle \end{pmatrix} = v_2 \begin{pmatrix} e^{i\varphi_2} \cos \beta \\ e^{i\varphi'_2} \sin \beta \end{pmatrix} \equiv v_2 \begin{pmatrix} e^{i\varphi_2} c_\beta \\ e^{i\varphi'_2} s_\beta \end{pmatrix}, \quad (3.35b)$$

where  $v_1, v_2$  are positive numbers and  $\varphi_1, \varphi'_1, \varphi_2, \varphi'_2$  denote the phases of the VEVs. For convenience, we will work with the relative phases  $\varphi \equiv \varphi'_1 - \varphi_1$  and  $\psi \equiv \varphi'_2 - \varphi_2$ . In all potentials  $V_0(\Phi)$  which appear in Eq. (3.34), we take the quadratic couplings  $A_0$ , defined in Eq. (3.31), to be negative. Furthermore, we assume for all potentials  $V_3(\Phi, \Omega)$  in Eq. (3.34) the quartic couplings  $A_3$ , defined in Eq. (3.33c), to be positive and sufficiently large compared with the remaining quartic couplings in Eq. (3.34). This ensures non-vanishing VEVs  $v_1, v_2 \neq 0$  and vacuum stability. Then, the possible physical vacua can be analyzed using the parameterization of Eqs. (3.35) where  $v_1$  and  $v_2$  are kept fixed, *i.e.*, one can treat each of the fields  $\Phi$  and  $\Omega$  as a non-linear sigma model field and restrict the analysis to the  $(\alpha, \beta, \varphi, \psi)$ -parameter-subspace. Then, following Sec. 2.3.2, we observe in Eqs. (3.35), that the pairs of parameters  $(\alpha, \varphi)$  and  $(\beta, \psi)$  actually describe global accidental  $SU(2)_{\text{acc}}$  symmetries. Note in Eqs. (3.31) and (3.33c) that the potentials  $V_0(\Phi)$  and  $V_3(\Phi, \Omega)$  indeed exhibit these  $SU(2)_{\text{acc}}$  symmetries. As a consequence, the potentials  $V_0(\Phi)$  and  $V_3(\Phi, \Omega)$  which appear in Eq. (3.34) will have no influence on the vacuum alignment of the SM singlet scalars in  $\mathcal{G}$ -space. Therefore, we can without loss of generality discard them for the rest of our discussion.

Assume first that the fields  $\Phi$  and  $\Omega$  both transform according to the same irrep  $D_i$  ( $i = 1, 3, 4$ ). For the most general potential involving only these fields, we will denote by  $V_\Delta(\Phi, \Omega)$  the part which breaks the  $SU(2)_{\text{acc}}$  symmetry. From Eq. (3.33a) we find that  $V_\Delta(\Phi, \Omega)$  can be organized as a sum  $V_\Delta(\Phi, \Omega) = V_A(\Phi, \Omega) + V_B(\Phi, \Omega)$  of

two potentials which explicitly read

$$\begin{aligned}
V_A(\Phi, \Omega) &\equiv d_1 |\phi_a^\dagger \phi_b|^2 + d_2 |\omega_a^\dagger \omega_b|^2 + d_3 (|\phi_a|^2 - |\phi_b|^2)(|\omega_a|^2 - |\omega_b|^2), \\
V_B(\Phi, \Omega) &\equiv d_4 \left[ (\phi_a^\dagger \phi_b)^2 + (\phi_b^\dagger \phi_a)^2 \right] + d_5 \left[ (\omega_a^\dagger \omega_b)^2 + (\omega_b^\dagger \omega_a)^2 \right] \\
&\quad + d_6 (\phi_a^\dagger \phi_b + \phi_b^\dagger \phi_a)(\omega_a^\dagger \omega_b + \omega_b^\dagger \omega_a) \\
&\quad + d_7 (\phi_a^\dagger \phi_b - \phi_b^\dagger \phi_a)(\omega_a^\dagger \omega_b - \omega_b^\dagger \omega_a),
\end{aligned} \tag{3.36}$$

where the coefficients  $d_1, \dots, d_7$  are some real-valued numbers. The potential  $V_A(\Phi, \Omega)$  depends only on the angles  $\alpha$  and  $\beta$  whereas  $V_B(\Phi, \Omega)$  is, in addition, also a function of  $\varphi$  and  $\psi$ . If the fields satisfy  $\Phi \in \{Q_1^\tau, Q_1^\mu\}$  and  $\Omega \in \{Q_2^\tau, Q_2^\mu, Q_3^\mu, Q_4^\mu\}$  the analogous  $SU(2)_{\text{acc}}$  symmetry breaking term  $V_B(\Phi, \Omega)$  must have  $d_6 = d_7 = 0$ . In this case, the relative phases  $\varphi$  and  $\psi$  are not correlated in the lowest energy state. In Eq. (3.34), we will assume for each of the different  $SU(2)_{\text{acc}}$  symmetry breaking parts  $V_A(\Phi, \Omega)$  that  $d_1, d_2 < 0$  and that the condition

$$d_1 d_2 > 4d_3^2, \tag{3.37a}$$

is satisfied. Additionally, we assume that for all possible terms  $V_B(\Phi, \Omega)$  in Eq. (3.34) the coefficients  $d_4$  and  $d_5$  are negative and that they also obey the constraint

$$(-2d_4 v_1^4 + |d_6| v_1^2 v_2^2)(-2d_5 v_2^4 + |d_6| v_1^2 v_2^2) > d_7^2 v_1^4 v_2^4. \tag{3.37b}$$

As shown in Appendix C, the conditions formulated in Eqs. (3.37) enforce the nonzero VEVs of the component fields to satisfy the relations

$$\langle \xi_{ia} \rangle = \pm \langle \xi_{ib} \rangle \quad (i = 1, 2), \tag{3.38a}$$

$$\langle q_{ja}^\tau \rangle = \pm \langle q_{jb}^\tau \rangle \quad (j = 1, 2), \tag{3.38b}$$

$$\langle q_{ka}^\mu \rangle = \pm \langle q_{kb}^\mu \rangle \quad (k = 1, 2, 3, 4), \tag{3.38c}$$

*i.e.*, within each of the scalar  $\mathcal{G}$ -doublets the VEVs of the component fields are relatively real and exactly degenerate (up to a possible relative sign).<sup>10</sup> Note that all terms in the potentials  $V_B(\Phi, \Omega)$  which are multiplied by the coefficient  $d_7$  must vanish in the lowest energy state and, hence, cannot contribute to the minimization of the scalar potential. For the potential  $V$  we furthermore choose in both of the terms  $V_B(Q_1^\tau, Q_1^\mu)$  and  $V_B(\xi_1, \xi_2)$  the corresponding coefficients  $d_6$  to be positive. In contrast to this, the non-vanishing coefficients  $d_6$  in all of the remaining terms  $V_B(\Phi, \Omega)$  of  $V$  are all assumed to be negative. Then, the absolute minimum of the multi scalar

---

<sup>10</sup>We consider here only the tree-level approximation.

potential is in addition to Eqs. (3.38) furthermore characterized by the relations

$$\frac{\langle \xi_{1a} \rangle}{\langle \xi_{1b} \rangle} = -\frac{\langle \xi_{2a} \rangle}{\langle \xi_{2b} \rangle}, \quad (3.39a)$$

$$\frac{\langle q_{1a}^\tau \rangle}{\langle q_{1b}^\tau \rangle} = -\frac{\langle q_{1a}^\mu \rangle}{\langle q_{1b}^\mu \rangle}, \quad (3.39b)$$

$$\frac{\langle q_{2a}^\tau \rangle}{\langle q_{2b}^\tau \rangle} = \frac{\langle q_{2a}^\mu \rangle}{\langle q_{2b}^\mu \rangle} = \frac{\langle q_{3a}^\mu \rangle}{\langle q_{3b}^\mu \rangle} = \frac{\langle q_{4a}^\mu \rangle}{\langle q_{4b}^\mu \rangle}, \quad (3.39c)$$

*i.e.*, the relative orientation of the VEVs of the component fields within a specific doublet is equal for all doublets transforming under the irrep  $D_4$  and opposite for the pairs of doublets transforming under  $D_1$  or  $D_3$ .<sup>11</sup> We suppose that the VEVs of the fields  $\xi_0, \xi_1$ , and  $\xi_2$ , which are responsible for the generation of the neutrino masses, are all of the order of the electroweak scale

$$|\langle \xi_0 \rangle| \simeq |\langle \xi_{1a} \rangle| \simeq |\langle \xi_{2a} \rangle| \simeq 10^2 \text{ GeV}. \quad (3.40)$$

In contrast to this, we assume that the link fields of the deconstructed extra-dimensional gauge symmetries  $G^\mu$  and  $G^\tau$  all acquire VEVs of the same order at some high mass scale somewhat below the fundamental scale  $M_f$  and thereby give rise to a small expansion parameter

$$\lambda \simeq \frac{|\langle q_{ja}^\tau \rangle|}{M_f} \simeq \frac{|\langle q_{ka}^\mu \rangle|}{M_f} \simeq 0.22, \quad (3.41)$$

where  $j = 1, 2$ , and  $k = 1, 2, 3, 4$ . Small hierarchies of this type can emerge from large hierarchies in supersymmetric theories when the scalar fields acquire their VEVs along a D-flat direction [57]. Note in Eq. (3.41) that  $\lambda$  is given by the Wolfenstein parameter [76] which approximately describes the mass ratios and CKM mixing angles in the down-quark sector [77] as well as the mass ratios in the charged lepton sector [58].<sup>12</sup> The mass and mixing parameters of the charged leptons are determined in the next section.

## 3.6 The charged lepton mass matrix

Consider the Yukawa interactions of the charged leptons

$$\mathcal{L}_Y^\ell = \bar{\ell}_\alpha H \mathcal{O}_{\alpha\beta}^\ell E_\beta + \text{h.c.}, \quad (3.42)$$

<sup>11</sup>The terms associated with the coefficients  $d_6$  actually represent a spin-spin-interaction in a version of the Ising-model, known from ferromagnetism. The topology here is of course unfamiliar since all “spins” couple with equal strength.

<sup>12</sup>An Ansatz where the Wolfenstein parameter is also used to describe neutrino mixing and leptogenesis has recently been presented in Ref. [78].

		$E_e$	$E_\mu$	$E_\tau$
	$Z_8 \times Z'_8$	$(-2, 2)$	$(0, 1)$	$(0, 1)$
$\overline{\ell_e}$	$(-2, 2)$	$(-4, 4)$	$(-2, 3)$	$(-2, 3)$
$\overline{\ell_\mu}$	$(-1, 0)$	$(-3, 2)$	$(-1, 1)$	$(-1, 1)$
$\overline{\ell_\tau}$	$(-1, 0)$	$(-3, 2)$	$(-1, 1)$	$(-1, 1)$

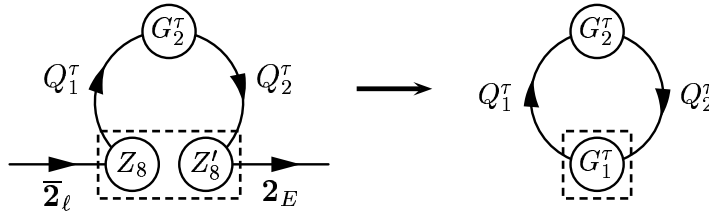
Table 3.4:  $Z_8 \times Z'_8$  charge structure of the charged lepton-antilepton pairs.

Figure 3.11: Contour in theory space which generates the leading-order dimension-six mass operator in the  $\mu$ - $\tau$ -subsector of the charged leptons by connecting  $\mathbf{2}_\ell$  and  $\mathbf{2}_E$  via the link fields of  $G^\tau$  (left panel). Formal contraction of the open fermion lines and  $Z_8 \times Z'_8$  into  $G_1^\tau$  (dashed boxes) exhibits the full  $G^\tau$  gauge-invariance of the corresponding effective Yukawa couplings (right panel).

where  $\mathcal{O}_{\alpha\beta}^\ell$  denotes an effective Yukawa operator and  $\alpha, \beta = e, \mu, \tau$ . Since the horizontal  $Z_8 \times Z'_8$  symmetry is assumed to be approximately conserved in the charged lepton sector (see Sec. 3.3.1), the  $Z_8 \times Z'_8$  charge structure of the charged lepton-antilepton pairs will determine the types of Yukawa operators  $\mathcal{O}_{\alpha\beta}^\ell$  which are generated via the Froggatt-Nielsen mechanism by the link fields of the gauge groups  $G^\mu$  and  $G^\tau$ . The  $Z_8 \times Z'_8$  transformation properties of the charged lepton-antilepton pairs is shown in Table 3.4. Now, taking the discrete charges of the fundamental scalars given in Table 3.1 into account, we find that one of the possible lowest-dimensional contributions to the operator  $\mathcal{O}_{ee}^\ell$  is given by

$$\mathcal{O}_{ee}^\ell \simeq (Q_1^\tau Q_2^\tau)^4 / (M_f)^8, \quad (3.43)$$

since it yields an invariant under both the symmetries  $Z_8 \times Z'_8$  and  $\mathcal{G}$ . Furthermore, invariance under application of the operator  $\mathcal{D}(a_4)$  requires  $\mathcal{O}_{e\mu}^\ell = \mathcal{O}_{\mu e}^\ell = 0$ . Since the transformation  $\mathcal{D}(a_2)$  permutes  $\mathcal{O}_{e\mu}^\ell \leftrightarrow \pm \mathcal{O}_{e\tau}^\ell$  and  $\mathcal{O}_{\mu e}^\ell \leftrightarrow \pm \mathcal{O}_{\tau e}^\ell$  (a sign flip is possible due to  $D_3(a_2) = D(C_b)$ ) it follows that  $\mathcal{O}_{e\tau}^\ell = \mathcal{O}_{\tau e}^\ell = 0$ , *i.e.*, in the first row and column of the charged lepton mass matrix only the (1, 1)-element is non-vanishing.

The lowest-dimensional mass operators in the  $\mu$ - $\tau$ -subsector of the charged leptons are dimension-six and dimension-eight terms, the Yukawa operators  $\mathcal{O}_{\alpha\beta}$  ( $\alpha, \beta = \mu, \tau$ ) of which can be represented by contours in theory space: The dimension-six and dimension-eight mass terms correspond to the Wilson-loops around the plaquettes associated with the gauge symmetries  $G^\tau$  (Fig. 3.11) and  $G^\mu$  (Fig. 3.12), respectively.

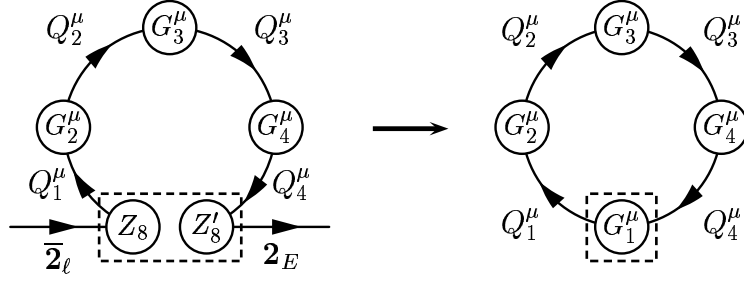


Figure 3.12: Contour in theory space which generates the next-to-leading-order dimension-eight mass operator in the  $\mu$ - $\tau$ -subsector of the charged leptons by connecting  $\mathbf{2}_\ell$  and  $\mathbf{2}_E$  via the link fields of  $G^\mu$  (left panel). Formal contraction of the open fermion lines and  $Z_8 \times Z'_8$  into  $G_1^\mu$  (dashed boxes) exhibits the full  $G^\mu$  gauge-invariance of the corresponding effective Yukawa couplings (right panel).

Note in Figs. 3.11 and 3.12, that the moose notation (see Sec. 3.1.1) has been generalized for the discrete  $Z_8 \times Z'_8$  charges in a straightforward and obvious way. The generalized Wigner-Eckart theorem implies that each of these Wilson loops is identified in  $\mathcal{G}$ -space with a set of irreducible Yukawa tensor operators spanned by the irreps  $\mathbf{2}_\ell$  and  $\mathbf{2}_E$ . These operators can be quickly determined by first noting that under  $\mathcal{D}(a_4)$  the effective couplings  $\mathcal{O}_{\mu\tau}^\ell$  and  $\mathcal{O}_{\tau\mu}^\ell$  undergo a sign flip whereas all link fields of  $\Pi_{i=1}^4 G_i^\mu$  and  $\Pi_{i=1}^2 G_i^\tau$  transform trivially. As a result, we have  $\mathcal{O}_{\mu\tau}^\ell = \mathcal{O}_{\tau\mu}^\ell = 0$ , *i.e.*, the charged lepton mass matrix is diagonal. Then, testing for invariance under the action of  $a_1, a_2, a_3 \in \mathcal{G}$  gives that each set of irreducible Yukawa tensor operators transforms according to a representation  $D_5$  of  $\mathcal{G}$  which is in matrix-form defined by the generators

$$D_5(a_1) = \begin{pmatrix} 0 & 1 \\ 1 & 0 \end{pmatrix}, \quad D_5(a_2) = \begin{pmatrix} -1 & 0 \\ 0 & 1 \end{pmatrix}, \quad D_5(a_3) = D_5(a_4) = \mathbb{1}_2. \quad (3.44)$$

To leading order, the generators in Eq. (3.44) act on five independent doublets  $(\psi_a^{(i)}, \psi_b^{(i)})^T$  of product functions  $\psi_a^{(i)}$  and  $\psi_b^{(i)}$ , where  $i = 0, 1, \dots, 4$ , which form the basis of five distinct carrier spaces  $V^{(i)}$ . Here, the  $\mathcal{G}$ -doublets  $(\psi_a^{(i)}, \psi_b^{(i)})^T$  correspond for  $i = 0$  and  $i \geq 1$  to the Wilson loops around the plaquettes associated with  $G^\tau$  and  $G^\mu$ , respectively. The basis functions for the different carrier spaces of  $D_5$  are given in table 3.5. The allowed types of basis functions in table 3.5 follow from invariance under application of the transformations  $\mathcal{D}(a_3)$  and  $\mathcal{D}(a_1)$ . First, application of  $\mathcal{D}(a_3)$  yields that in each basis function the number of the  $a$ -components is even. Second, for given  $i = 0, 1, \dots, 4$ , invariance under the transformation  $\mathcal{D}(a_1)$  requires the index structure of the basis functions  $\psi_a^{(i)}$  and  $\psi_b^{(i)}$  to be of such a form that  $\psi_a^{(i)}$  and  $\psi_b^{(i)}$  get interchanged when the indices  $a$  and  $b$  are permuted. Then, expressed in terms of the sets of irreducible Yukawa tensor operators, the effective

$V^{(i)}$	$\psi_a^{(i)}$	$\psi_b^{(i)}$
$V^{(0)}$	$q_{1a}^\tau q_{2a}^\tau$	$q_{1b}^\tau q_{2b}^\tau$
$V^{(1)}$	$q_{1a}^\mu q_{2a}^\mu q_{3a}^\mu q_{4a}^\mu$	$q_{1b}^\mu q_{2b}^\mu q_{3b}^\mu q_{4b}^\mu$
$V^{(2)}$	$q_{1a}^\mu q_{2a}^\mu q_{3b}^\mu q_{4b}^\mu$	$q_{1b}^\mu q_{2b}^\mu q_{3a}^\mu q_{4a}^\mu$
$V^{(3)}$	$q_{1a}^\mu q_{2b}^\mu q_{3a}^\mu q_{4b}^\mu$	$q_{1b}^\mu q_{2a}^\mu q_{3b}^\mu q_{4a}^\mu$
$V^{(4)}$	$q_{1a}^\mu q_{2b}^\mu q_{3b}^\mu q_{4a}^\mu$	$q_{1b}^\mu q_{2a}^\mu q_{3a}^\mu q_{4b}^\mu$

Table 3.5: The basis functions  $\psi_a^{(i)}$  and  $\psi_b^{(i)}$  ( $i = 0, 1, \dots, 4$ ) of the leading-order set of irreducible Yukawa tensor operators ( $\mathcal{O}_{kl}^\ell$ ), where  $k, l = \mu, \tau$ , in terms of the component fields of  $Q_i^\tau = (q_{ia}^\tau, q_{ib}^\tau)^T$  ( $i = 1, 2$ ) and  $Q_i^\mu = (q_{ia}^\mu, q_{ib}^\mu)^T$  ( $i = 1, 2, 3, 4$ ).

Yukawa coupling matrix in the  $\mu$ - $\tau$ -subsector of the charged leptons reads

$$(\mathcal{O}_{kl}^\ell) = \sum_{i=0}^4 Y_{\text{eff}}^{(i)} \left[ \begin{pmatrix} 1 & 0 \\ 0 & 1 \end{pmatrix} \psi_a^{(i)} + \begin{pmatrix} -1 & 0 \\ 0 & 1 \end{pmatrix} \psi_b^{(i)} \right], \quad (3.45a)$$

where  $k, l = \mu, \tau$  and  $Y_{\text{eff}}^{(i)}$  for  $i = 0, 1, \dots, 4$  denotes the effective Yukawa couplings

$$Y_{\text{eff}}^{(i)} = \left\{ \begin{array}{ll} Y^{(0)}/(M_f)^2 & (i = 0) \\ Y^{(i)}/(M_f)^4 & (i = 1, 2, 3, 4) \end{array} \right\}, \quad (3.45b)$$

where  $Y^{(i)}$  ( $i = 0, 1, \dots, 4$ ) are dimensionless order unity Yukawa couplings. The  $2 \times 2$  diagonal matrices in Eq. (3.45a) summarizing symmetry-related geometric factors, are the Clebsch-Gordan coefficients of the effective Yukawa coupling matrix ( $\mathcal{O}_{kl}^\ell$ ). Furthermore, the effective Yukawa couplings  $Y_{\text{eff}}^{(i)}$ , characterized by the outer multiplicity label  $i$ , are the reduced matrix elements of the Clebsch-Gordan coefficients and parameterize further information about the physics at the fundamental scale  $M_f$ . From Eqs. (3.38) we find that after SSB the vacuum alignment mechanism of Sec. 3.5 ensures that the VEVs of the basis functions in table 3.5 are - up to a possible relative sign - pairwise exactly degenerate

$$\langle \psi_a^{(i)} \rangle = \pm \langle \psi_b^{(i)} \rangle, \quad (3.46a)$$

where  $i = 0, 1, \dots, 4$ . In addition, Eqs. (3.39) relate the orientations of the VEVs by

$$\langle \psi_a^{(0)} \rangle / \langle \psi_b^{(0)} \rangle = - \langle \psi_a^{(i)} \rangle / \langle \psi_b^{(i)} \rangle, \quad (3.46b)$$

where  $i = 1, 2, 3, 4$ . Substituting Eqs. (3.46) into Eqs. (3.45), we observe that after SSB the set of irreducible Yukawa tensor operators ( $\mathcal{O}_{kl}^\ell$ ) can take one of the following two forms

$$(\mathcal{O}_{kl}^\ell) \rightarrow Y^{(0)} \lambda^2 \left[ \begin{pmatrix} 1 & 0 \\ 0 & 1 \end{pmatrix} \pm \begin{pmatrix} -1 & 0 \\ 0 & 1 \end{pmatrix} \right] + \sum_{i=1}^4 Y^{(i)} \lambda^4 \left[ \begin{pmatrix} 1 & 0 \\ 0 & 1 \end{pmatrix} \mp \begin{pmatrix} -1 & 0 \\ 0 & 1 \end{pmatrix} \right], \quad (3.47)$$



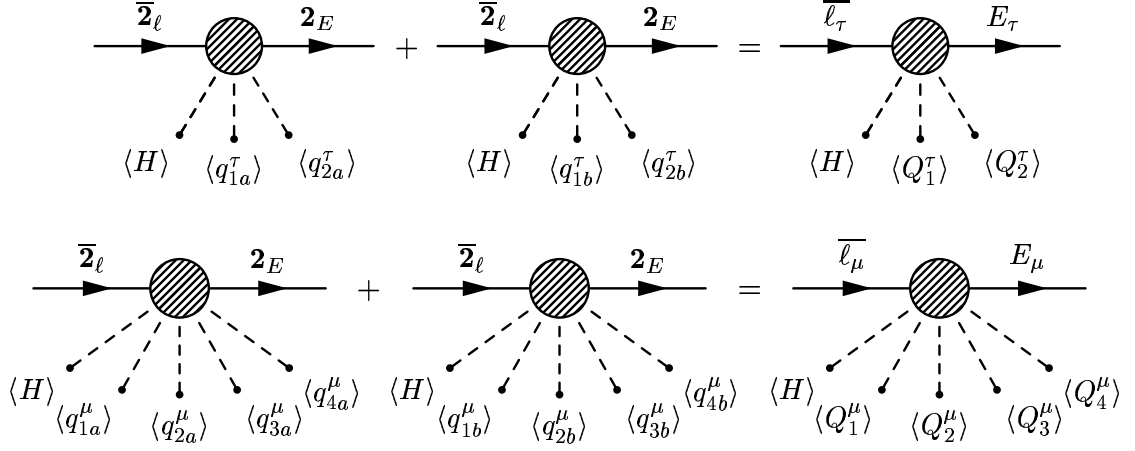


Figure 3.13: Froggatt-Nielsen-type diagrams for the lowest-dimensional Yukawa interactions generating  $m_\mu \ll m_\tau$ . The dimension-six operators add up to  $\sim m_\tau \bar{\ell}_\tau E_\tau$  (top panel). The dimension-eight operators add up to  $\sim m_\mu \bar{\ell}_\mu E_\mu$  (bottom panel).

where  $k, l = \mu, \tau$  and the expansion parameter  $\lambda \simeq 0.22$  of Eq. (3.41) has been used. In Eq. (3.47), it is important to note that the Clebsch-Gordan coefficients are added or subtracted depending on their outer multiplicity label: if the Clebsch-Gordan coefficients are added (subtracted) for  $i = 0$  then they are necessarily subtracted (added) for  $i = 1, 2, 3, 4$ . As a result, Eq. (3.47) shows that the vacuum alignment mechanism generates a hierarchical pattern in the  $\mu$ - $\tau$ -subsector of the charged leptons via a cancellation of some of the Clebsch-Gordan coefficients in the lowest energy state. The corresponding Froggatt-Nielsen-type diagrams for this cancellation mechanism are shown in Fig. 3.13. For definiteness, let us choose in Eq. (3.47) the solution with the signs “+” for  $i = 0$  and “−” for  $i = 1, 2, 3, 4$ . Taking everything into account, the full leading-order charged lepton mass matrix  $\mathcal{M}_\ell$  emerging after SSB is given by

$$\mathcal{M}_\ell \simeq m_\tau \begin{pmatrix} \lambda^6 & 0 & 0 \\ 0 & \lambda^2 & 0 \\ 0 & 0 & 1 \end{pmatrix}, \quad (3.48)$$

where only the orders of magnitude of the matrix elements have been indicated. As for the mass matrix in Eq. (3.48) is given at tree-level, we have to expect sub-leading corrections to its form and hence the “0”-entries in Eq. (3.48) should rather be viewed as “phenomenological” (in contrast to “exact”) texture zeros. From Eq. (3.48) we read off the charged lepton mass ratios

$$\frac{m_e}{m_\tau} \simeq \lambda^6, \quad \frac{m_\mu}{m_\tau} \simeq \lambda^2, \quad (3.49)$$

which approximately fit the experimentally observed values [58]. Since the mixing angles of the charged leptons practically vanish, the large leptonic mixing must stem from the neutrino sector. The neutrino mass and mixing parameters will be determined in the next section.

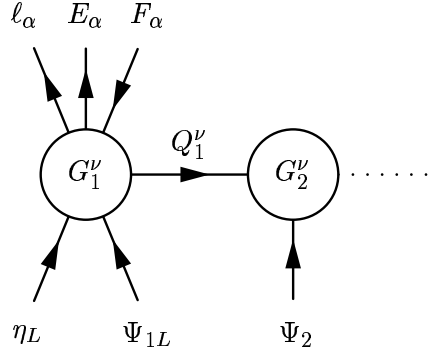


Figure 3.14: View on the first two sites of the moose diagram of the gauge group  $G^\nu$ . Since  $\alpha$  runs over the three flavors  $\alpha = e, \mu, \tau$ , all SM leptons, heavy Dirac neutrinos and the Weyl spinor  $\eta_L$  are located on the brane corresponding to the first site.

## 3.7 The neutrino mass matrix

### 3.7.1 Aliphatic model for neutrinos

So far, we have examined the connection between dynamically generated extra dimensions compactified on  $\mathcal{S}^1$  and the hierarchical Yukawa coupling matrix of the charged leptons. In this approach, a small expansion parameter in the charged lepton mass matrix was introduced through the mixing with heavy Froggatt-Nielsen states. This has the advantage that only a small number of lattice sites is needed to account for phenomenologically viable mass matrix patterns. On the other hand, however, the dynamical origin of the small expansion parameter remains unclear. Let us therefore consider for the generation of neutrino masses a different mechanism which relies on the presence of a large number of lattice sites and hence exhibits a closer 5D correspondence. We assume that for all flavors  $\alpha = e, \mu, \tau$  the SM leptons  $\ell_\alpha$  and  $E_\alpha$  transform according to the fundamental representation  $m$  of  $G_1^\nu$  and the right-handed Dirac neutrinos  $F_\alpha$  as well as the massless Weyl spinor  $\eta_L$  transform according to the anti-fundamental representation  $\bar{m}$  of  $G_1^\nu$  (see Sec. 3.2). The corresponding moose diagram is shown in Fig. 3.14. Note that since these fields carry zero  $G_i^\nu$  charges for  $i = 2, 3, \dots, N$ , they are localized on the boundary of the latticized  $\mathcal{S}^1/Z_2$  orbifold.

### 3.7.2 The one-generation-case

Let us first examine the case of a single generation by considering the coupling of the  $\mathcal{G}$ -singlet neutrino  $\nu_e$  to the fermionic site variables of the orbifold extra dimension. From Table 3.1 we conclude that invariance under the  $Z_8 \times Z'_8$ -symmetry and the  $Z_2$ -parity in Eq. (3.16) requires the relevant effective Yukawa interaction of the electron lepton doublet  $\mathbf{1}_\ell$  with the bulk-fermion to be of the type

$$\mathcal{L}_2 = Y_1 \bar{\mathbf{1}}_\ell^c H \mathbf{1}_{FL} + Y_2 \bar{\mathbf{1}}_{FR} \xi_0 \Psi_{1L} + M_{1F} \bar{\mathbf{1}}_{FR} \mathbf{1}_{FL} + \text{h.c.}, \quad (3.50)$$

where  $Y_1$  and  $Y_2$  are dimensionless order unity coefficients and  $M_{1F} \simeq 10^{15}$  GeV denotes the seesaw scale. The Lagrangian for the bulk and brane fields is given by  $\mathcal{L}_1 + \mathcal{L}_2$ , where  $\mathcal{L}_1$  has been defined in Eq. (3.11). As a result, the  $N \times N$  mass matrix which emerges from  $\mathcal{L}_1 + \mathcal{L}_2$  after SSB is given by

$$\begin{array}{c} \overline{\mathbf{1}}_\ell^c \\ \overline{\mathbf{1}}_{FR} \\ \overline{\Psi}_{2R} \\ \overline{\Psi}_{3R} \\ \vdots \end{array} \begin{pmatrix} \mathbf{1}_{FL} & \Psi_{1L} & \Psi_{2L} & \Psi_{3L} & \cdots \\ h_1 & 0 & 0 & 0 & \cdots \\ M_{1F} & h_2 & 0 & 0 & \cdots \\ 0 & M_f & -M_f & 0 & \cdots \\ 0 & 0 & M_f & -M_f & \cdots \\ \vdots & \vdots & \vdots & \vdots & \ddots \end{pmatrix}, \quad (3.51)$$

where we have introduced the VEVs  $h_1 \equiv Y_1 \langle H \rangle$ ,  $h_2 \equiv Y_2 \langle \xi_0 \rangle$ , and use  $h_1 \simeq h_2 \simeq 10^2$  GeV, *i.e.*, the associated mass terms are generated at the electroweak scale. Note that the mass matrix in Eq. (3.51) has been displayed in a basis where the active neutrinos have right-handed chirality. Integrating out the heavy  $\mathcal{G}$ -singlet  $\mathbf{1}_F$ , yields the effective  $(N-1) \times (N-1)$  mass matrix

$$\mathcal{M}_2 \equiv \begin{pmatrix} m_\nu & 0 & 0 & \cdots \\ M_f & -M_f & 0 & \cdots \\ 0 & M_f & -M_f & \cdots \\ \vdots & \vdots & \vdots & \ddots \end{pmatrix}, \quad (3.52)$$

where  $m_\nu = h_1 h_2 / M_{1F} \simeq 10^{-3}$  eV denotes the absolute neutrino mass scale. The mass  $m_\nu$  lifts the zero eigenvalue in the KK mass spectrum of the left-handed fields to a small but non-vanishing value which can be determined by diagonalizing the  $(N-1) \times (N-1)$  matrix

$$\mathcal{M}_2 \mathcal{M}_2^\dagger = \begin{pmatrix} m_\nu^2 & m_\nu M_f & 0 & \cdots \\ m_\nu M_f & 2M_f^2 & -M_f^2 & \cdots \\ 0 & -M_f^2 & 2M_f^2 & \cdots \\ \vdots & \vdots & \vdots & \ddots \end{pmatrix}. \quad (3.53)$$

From Eq. (3.53) it is readily seen that the mixing of  $\mathbf{1}_\ell^c$  with the right-handed fields  $\Psi_{nR}$  is described by angles  $\simeq m_\nu / M_f$  which vanish in the limit  $M_f \rightarrow \infty$ . For  $m_\nu \ll M_f$  the non-zero heavy masses are approximately given by the KK spectrum in Eq. (3.15) where  $n = 1, \dots, N-2$ . The lightest eigenvalue  $(m_0)^2$  of  $\mathcal{M}_2 \mathcal{M}_2^\dagger$  can be determined by integrating out the invertible heavy  $(N-2) \times (N-2)$  submatrix in the down-right corner of  $\mathcal{M}_2 \mathcal{M}_2^\dagger$  in Eq. (3.53). Taking into account that the  $(1,1)$ -element of the inverse of this submatrix is equal to  $\frac{N-2}{N-1} M_f^{-2}$ , we obtain in the limit  $m_\nu \ll M_f$  for the lightest mass eigenvalue

$$m_0 = m_\nu / \sqrt{N-1} = m_\nu / \sqrt{M_f R}, \quad (3.54)$$

where the second equation matches onto the continuum limit. In the classical 5D continuum theory the mass (or volume) suppression factor  $\sim \sqrt{M_f R}$  emerges from the normalization of the wave-function of the right-handed neutrino propagating in the bulk [83, 84].

### 3.7.3 Adding the 2nd and 3rd generation

The full neutrino mass matrix emerges by inclusion of the  $SU(2)$  lepton doublets of the 2nd and 3rd generation, which are combined into the  $\mathcal{G}$ -doublet  $\mathbf{2}_\ell$ . Actually, invariance under  $Z_8 \times Z'_8$  allows for the fields  $\xi_2$  and  $\xi_3$  Yukawa interactions with  $\mathbf{2}_\ell$  which read

$$\mathcal{L}_3 = Y_3 \overline{\mathbf{2}}_l^e H \mathbf{2}_{FL} + Y_4 \overline{\mathbf{2}}_{FR} \xi_1 \Psi_{1L} + Y_5 \overline{\mathbf{2}}_{FR} \xi_2 \eta_L + M_{2F} \overline{\mathbf{2}}_{FR} \mathbf{2}_{FL} + \text{h.c.}, \quad (3.55)$$

where  $Y_3, Y_4$ , and  $Y_5$  denote dimensionless order unity Yukawa couplings,  $\langle \xi_1 \rangle \simeq \langle \xi_2 \rangle \simeq 10^2 \text{ GeV}$ , and  $M_{2F} \simeq 10^{15} \text{ GeV}$ . Here, it is important to note, that the  $Z_8 \times Z'_8$  charge of the Weyl spinor  $\eta_L$  forbids any further Yukawa interactions or mass terms with the other fermions. In complete analogy to the calculation of the light mass  $m_0$  in Sec. 3.7.2, one can in the combined system  $\mathcal{L}_1 + \mathcal{L}_2 + \mathcal{L}_3$  integrate out the heavy vectorlike degrees of freedom. As a consequence, in the basis where the VEVs of  $\xi_1$  and  $\xi_2$  are described by Eqs. (3.38a) and (3.39a), the resulting  $3 \times 2$  light Dirac neutrino mass matrix can be written as

$$\mathcal{M}_D = m_\nu \begin{pmatrix} \rho\epsilon & 0 \\ \epsilon & 1 \\ -\epsilon & 1 \end{pmatrix}, \quad (3.56)$$

where the neutrino expansion parameter  $\epsilon \simeq 1/\sqrt{N-1}$  and the order unity Yukawa coupling  $\rho = \mathcal{O}(1)$  are both real quantities and  $m_\nu$  denotes the absolute neutrino mass scale. In Eq. (3.56), all phases have been absorbed into the right-handed neutrino and charged lepton sectors. The Dirac neutrino mass matrix  $\mathcal{M}_D$  in Eq. (3.56) has the important property that within each column the flavor symmetry  $\mathcal{G}$  enforces the 2nd and 3rd elements to be relatively real and exactly degenerate in their magnitudes. Thus,  $\mathcal{M}_D$  describes an exactly maximal  $\nu_\mu$ - $\nu_\tau$ -mixing.

### 3.7.4 Neutrino masses and mixing angles

The neutrino masses and leptonic mixing angles are determined from Eq. (3.56) by diagonalizing the matrix

$$\mathcal{M}_D \mathcal{M}_D^\dagger = m_\nu^2 \begin{pmatrix} \rho^2 \epsilon^2 & \rho \epsilon^2 & -\rho \epsilon^2 \\ \rho \epsilon^2 & 1 + \epsilon^2 & 1 - \epsilon^2 \\ -\rho \epsilon^2 & 1 - \epsilon^2 & 1 + \epsilon^2 \end{pmatrix}. \quad (3.57)$$

The matrix in Eq. (3.57) is diagonalized in two steps. First, a rotation of the active neutrino fields in the 2-3-plane through an angle  $\theta_{23} = \pi/4$  brings  $\mathcal{M}_D \mathcal{M}_D^\dagger$  to the form

$$\mathcal{M}_D \mathcal{M}_D^\dagger \longrightarrow m_\nu^2 \begin{pmatrix} \rho^2 \epsilon^2 & \sqrt{2} \rho \epsilon^2 & 0 \\ \sqrt{2} \rho \epsilon^2 & 2 \epsilon^2 & 0 \\ 0 & 0 & 2 \end{pmatrix}, \quad (3.58)$$

from which we observe that the reactor mixing angle is exactly zero, *i.e.*,  $\theta_{13} = 0$  in agreement with the CHOOZ reactor neutrino data which sets the upper bound  $|\theta_{13}| \lesssim 9.2^\circ$  [15]. Second, the matrix in Eq. (3.58) is brought on diagonal form by a rotation in the 1-2-plane through an angle

$$\theta_{12} = \arctan \left[ (2\sqrt{2})^{-1} \left( \rho^2 - 2 + \sqrt{(2-\rho)^2 + 8} \right) \right]. \quad (3.59)$$

The neutrino masses exhibit the normal hierarchy

$$m_1 = 0, \quad m_2 = m_\nu \epsilon \sqrt{2 + \rho^2}, \quad m_3 = \sqrt{2} m_\nu, \quad (3.60)$$

which gives for the solar and atmospheric neutrino mass squared differences

$$\Delta m_\odot^2 = m_\nu^2 \epsilon^2 (2 + \rho^2), \quad \Delta m_{\text{atm}}^2 = 2m_\nu^2 - \Delta m_\odot^2. \quad (3.61)$$

Using the upper bound  $\Delta m_\odot^2 \lesssim 1.9 \times 10^{-4} \text{ eV}^2$  [14] and the best-fit value  $\Delta m_{\text{atm}}^2 \simeq 2.5 \times 10^{-3} \text{ eV}^2$  [11] we obtain  $m_\nu \simeq 0.04 \text{ eV}$ . Without tuning of parameters, we have  $\rho = 1$  and  $\epsilon = 1/\sqrt{N-1}$  which gives for the solar neutrino parameters the values

$$\Delta m_\odot^2 \simeq \frac{3}{2} \frac{\Delta m_{\text{atm}}^2}{N-1}, \quad \theta_{12} = \arctan \frac{1}{\sqrt{2}} \simeq 35^\circ, \quad (3.62)$$

where we have used in the first equation the hierarchy  $\Delta m_\odot^2 \ll \Delta m_{\text{atm}}^2$ . At  $3\sigma$ , the combined solar and KamLAND neutrino data allows for  $\Delta m_\odot^2$  the two regions  $5.1 \times 10^{-5} \text{ eV}^2 \lesssim \Delta m_\odot^2 \lesssim 9.7 \times 10^{-5} \text{ eV}^2$  (LMA-I) and  $1.2 \times 10^{-4} \text{ eV}^2 \lesssim \Delta m_\odot^2 \lesssim 1.9 \times 10^{-4} \text{ eV}^2$  (LMA-II) [14]. Matching onto these values requires

$$N = 57 \pm 17 \quad \text{LMA-I}, \quad N = 27 \pm 6 \quad \text{LMA-II}, \quad (3.63)$$

where we have set in Eq. (3.62) the atmospheric mass squared difference equal to the best-fit value  $\Delta m_{\text{atm}}^2 = 2.5 \times 10^{-3} \text{ eV}^2$ . In short, the presently allowed ratios  $\Delta m_\odot^2 / \Delta m_{\text{atm}}^2$  implied by the LMA-I and LMA-II solutions already significantly discriminate between the associated radii  $N/(2\pi g v)$  of the dynamically generated  $\mathcal{S}^1/Z_2$  orbifold. At this level, the neutrino expansion parameter is  $0.12 \lesssim \epsilon \lesssim 0.16$  (LMA-I) or  $0.18 \lesssim \epsilon \lesssim 0.23$  (LMA-II), which is comparable with the Wolfenstein parameter  $\lambda \simeq 0.22$ . For the non-fine-tuned solar mixing angle  $\theta_{12} = \arctan 1/\sqrt{2}$  in Eq. (3.62) we find from Ref. [14] that a number of

$$55 \pm 8 \quad \text{LMA-I (@ 90\% C.L.)} \quad (3.64)$$

lattice sites yields the MSW LMA-I solution within the 90% confidence level region. In general, for both the LMA-I and the LMA-II solution, the dynamical generation of the solar mass squared difference  $\Delta m_{\odot}^2$  via deconstruction in a flat background requires a relatively fine-grained latticization of the associated  $\mathcal{S}^1/Z_2$  orbifold with roughly  $10^1 - 10^2$  lattice sites.

# Chapter 4

## Latticized Geometries

In the previous chapter, we employed deconstruction as a tool for a predictive model of lepton masses based on a non-Abelian discrete symmetry. Specifically in the neutrino sector, a large number of lattice sites was used to express the solar mass squared difference in terms of the “volume” of a dynamically generated orbifold extra dimension. In this chapter, we will further generalize this approach to lepton masses by restricting to a small number of lattice sites. With this, the inverse lattice spacing can be identified with the seesaw scale  $1/a \simeq 10^{15}$  GeV or may even naturally be as small as  $1/a \simeq 10^{-3}$  eV through a replicated seesaw mechanism. The first three sections of this chapter follow the results of Ref. [79].

### 4.1 The two-site model

#### 4.1.1 Charge assignment

We consider a  $G = SU(m)_1 \times SU(m)_2$  gauge theory for deconstructed extra dimensions where a bi-fundamental scalar link field  $\Phi \subset (m_1, \bar{m}_2)$  connects the adjacent  $SU(m)_i$  ( $i = 1, 2$ ) groups [34, 35]. For the present, let us restrict here to the case of only two flavors  $\alpha, \beta \in \{e, \mu, \tau\}$ ,  $\alpha \neq \beta$  (in Secs. 4.2 and 4.3 this basic two-site model will then be embedded into various realistic three-flavor scenarios). We assume that the leptons  $\ell_\beta$  and  $E_\beta$  transform according to the fundamental representation  $m_2$  under  $SU(m)_2$  and the fields  $\ell_\alpha$  and  $E_\alpha$  transform according to the complex conjugate representation  $\bar{m}_1$  under  $SU(m)_1$ . In addition, we introduce for each of the active flavors, the right-handed neutrinos  $N_\alpha$  and  $N_\beta$ , where  $N_\alpha$  transforms as  $\bar{m}_1$  under  $SU(m)_1$  while  $N_\beta$  transforms as  $m_2$  under  $SU(m)_2$ . Note that  $N_\alpha$  and  $N_\beta$  are two-component Weyl spinors. The moose diagram of this representation content is succinctly shown in Fig. 4.1. It is also obvious from Fig. 4.1 that the product gauge group  $G$  is free from chiral anomalies since the left- and right-handed states form vector-like representations with respect to  $SU(m)_1$  and  $SU(m)_2$ . The most general

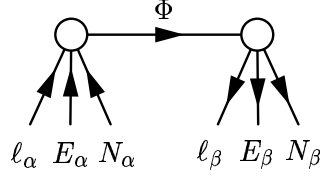


Figure 4.1: Moose diagram for the two-site model.

renormalizable Yukawa interactions for the leptons are then given by

$$\mathcal{L}_Y = Y_\alpha^E \bar{\ell}_\alpha H E_\alpha + Y_\beta^E \bar{\ell}_\beta H E_\beta + Y_\alpha^\nu \bar{\ell}_\alpha \tilde{H} N_\alpha + Y_\beta^\nu \bar{\ell}_\beta \tilde{H} N_\beta + f \bar{N}_\alpha^c \Phi N_\beta + \text{h.c.}, \quad (4.1)$$

where  $Y_\alpha^E, Y_\beta^E, Y_\alpha^\nu, Y_\beta^\nu, f$  are complex Yukawa couplings of order unity. Note that in Eq. (4.1) bare Dirac and Majorana mass terms of the types  $\sim \bar{N}_\alpha^c N_\beta$  and  $\sim \bar{N}_\alpha^c N_\alpha$  or  $\sim \bar{N}_\beta^c N_\beta$  are forbidden<sup>1</sup> by invariance under  $G$ . The gauge-sector of this system is governed by the Lagrangian

$$\mathcal{L}_\Phi = -\frac{1}{4} \sum_{i=1}^2 F_{i\mu\nu}^a F^{i\mu\nu a} + \sum_{i=1}^2 (D_\mu \Phi)^\dagger (D^\mu \Phi), \quad (4.2)$$

where the covariant derivative is  $D_\mu \Phi = (\partial_\mu - ig_1 A_{1\mu}^a T_a + ig_2 A_{2\mu}^a T_a) \Phi$ , in which  $g_1$  and  $g_2$  denote the dimensionless gauge couplings of  $SU(m)_1$  and  $SU(m)_2$ , respectively. One can always arrange the scalar potential such that  $\Phi$  naturally acquires a VEV  $\langle \Phi \rangle = M_x$ . Here,  $M_x$  is identified with the deconstruction scale at which the  $SU(m)_1 \times SU(m)_2$  symmetry is broken down to the diagonal subgroup  $SU(m)_{\text{diag}}$ , thereby eating  $m^2 - 1$  Nambu-Goldstone bosons in the process. For  $g_1, g_2 \simeq \mathcal{O}(1)$ , the corresponding lattice spacing  $a$  of the deconstructed theory is set by the inverse scale  $a \simeq 1/M_x$ . After SSB, the neutrino mass matrix takes the form

$$\begin{array}{c} \bar{\nu}_\alpha \\ \bar{\nu}_\beta \\ \bar{N}_\alpha^c \\ \bar{N}_\beta^c \end{array} \begin{pmatrix} \nu_\alpha^c & \nu_\beta^c & N_\alpha & N_\beta \\ 0 & 0 & Y_\alpha^\nu \epsilon & 0 \\ 0 & 0 & 0 & Y_\beta^\nu \epsilon \\ Y_\alpha^\nu \epsilon & 0 & 0 & f M_x \\ 0 & Y_\beta^\nu \epsilon & f M_x & 0 \end{pmatrix}, \quad (4.3)$$

where  $\epsilon \equiv \langle H \rangle \simeq 10^2 \text{ GeV}$  is the electroweak scale. The light effective  $2 \times 2$  Majorana mass matrix is

$$\mathcal{M}_\nu = Y_\alpha^\nu Y_\beta^\nu \frac{\epsilon^2}{f M_x} \begin{pmatrix} 0 & 1 \\ 1 & 0 \end{pmatrix}, \quad (4.4)$$

which we identify for an inverse lattice spacing  $M_x \simeq 10^{15} \text{ GeV}$  with the usual dimension-five seesaw operator [20–22]. Hence, for length scales  $r \gg a \simeq 1/M_x$ ,

<sup>1</sup>The term  $\bar{N}_\alpha^c N_\beta$  is charged under both  $SU(m)$  groups and the products  $\bar{N}_\alpha^c N_\alpha$  and  $\bar{N}_\beta^c N_\beta$  contain only irreps with dimensions  $\frac{1}{2}m(m-1)$  and  $\frac{1}{2}m(m+1)$ .



the renormalizable and gauge invariant Yukawa interactions in Eq. (4.1) reproduce upon dimensional deconstruction the effects of the fifth dimension. For shorter length scales  $r \ll a$ , we recover again the renormalizable 4D interactions as given in Eq. (4.1). Moreover, contrary to the conventional seesaw operator, dimensional deconstruction can provide a rationale for maximal leptonic mixing between the active flavors  $\alpha$  and  $\beta$  since the charged lepton mass matrix is strictly diagonal. This feature of maximal mixing can be easily understood once we realize that the link field  $\Phi$  mediates a symmetry between each of the right-handed neutrinos  $N_\alpha$  and  $N_\beta$  which are placed at different lattice sites. This symmetry can be interpreted as an interaction which conserves a charge  $L_\alpha - L_\beta$  and produces the texture-zeros in the mass matrix of the right-handed neutrinos. Below the deconstruction scale, the conserved charge  $L_\alpha - L_\beta$  is reflected by the fact that  $\ell_\beta, E_\beta$ , and  $N_\beta$  transform according to the fundamental representation of  $SU(m)_{\text{diag}}$  whereas  $\ell_\alpha, E_\alpha$ , and  $N_\alpha$  transform according to the anti-fundamental representation of  $SU(m)_{\text{diag}}$ . The unbroken group  $SU(m)_{\text{diag}}$  is associated with a zero mode in the gauge sector. This can be seen in the kinetic term in Eq. (4.2) which gives a mass squared matrix to the gauge bosons

$$M_G^2 = \frac{1}{2} M_x^2 (g_1 A_{1\mu}^a - g_2 A_{2\mu}^a)^2. \quad (4.5)$$

In the basis  $(A_{1\mu}^a, A_{2\mu}^a)$  we have

$$M_G^2 = \frac{1}{2} M_x^2 \begin{pmatrix} g_1^2 & -g_1 g_2 \\ -g_1 g_2 & g_2^2 \end{pmatrix}, \quad (4.6)$$

with the (normalized) zero mode wave function

$$A_\mu^{a(0)} = \frac{1}{\sqrt{g_1^2 + g_2^2}} (g_2 A_{1\mu}^a + g_1 A_{2\mu}^a). \quad (4.7)$$

In our setup, we generally observe that the Dirac sector of the model remains diagonal as a result of placing the flavors  $\alpha$  and  $\beta$  on different lattice sites. Therefore, maximal leptonic mixing is exclusively introduced by the heavy Majorana sector of the resulting seesaw operator. In Sec. 4.2, we will see that the qualitative features of this system are not altered even if one allows for both the fermions and scalars to be link variables. As a passing remark, we find from Eq. (4.4) that the resulting light neutrinos are in opposite  $\mathcal{CP}$  parities and there is no explicit leptonic  $\mathcal{CP}$  violation.

### 4.1.2 General properties of the two-site model

Let us now examine in how far the two-site model is generic by considering the phenomenological implications of other  $SU(m)$  charge assignments to the leptons. Actually, if we require the lepton fields to be either in the fundamental or anti-fundamental representation of one of the gauge groups  $SU(m)_1$  or  $SU(m)_2$ , one can have essentially three possible modifications to the moose diagram shown in Fig. 4.1.

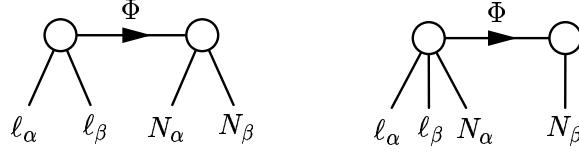


Figure 4.2: Moose diagrams for cases (i) (left panel) and (ii) (right panel).

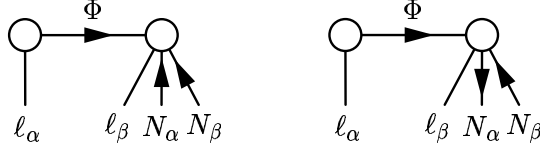


Figure 4.3: Moose diagram for cases (iii) a (left panel) and (iii) b (right panel).

These are, case (i) both leptonic doublets are at a single lattice site while the right-handed neutrinos are grouped at the second lattice site or, case (ii) both leptonic doublets are at a single site along with any one of the right-handed neutrinos (see Fig. 4.2) or, case (iii) both right-handed neutrinos are located at the same site while the doublets are at different sites (see Fig. 4.3). In Figs. 4.2 and 4.3 we have adopted the convention that undirected links denote transformations under either the fundamental or anti-fundamental representation of the corresponding gauge group. In case (i), one can have Majorana mass terms for the right-handed neutrinos but in the Dirac sector only non-renormalizable Yukawa interactions of the types  $\sim \bar{\ell}_\alpha \tilde{H} \Phi N_\beta$  are possible. A priori, however, these suppressed non-renormalizable interactions do not lead to large mixings. In case (ii), on the other hand, the neutrinos can have the renormalizable Yukawa interactions

$$\mathcal{L}_Y^\nu = Y_\alpha^\nu \bar{\ell}_\alpha \tilde{H} N_\alpha + Y_\beta^\nu \bar{\ell}_\beta \tilde{H} N_\alpha + f \bar{N}_\alpha^c \Phi N_\beta + \text{h.c.}, \quad (4.8)$$

leading in the basis of Eq. (4.3) to the neutrino mass matrix

$$M_\nu = \begin{pmatrix} 0 & 0 & Y_\alpha^\nu \epsilon & 0 \\ 0 & 0 & Y_\beta^\nu \epsilon & 0 \\ Y_\alpha^\nu \epsilon & Y_\beta^\nu \epsilon & 0 & f M_x \\ 0 & 0 & f M_x & 0 \end{pmatrix}, \quad (4.9)$$

which has two vanishing neutrino mass eigenvalues and two heavy mass eigenvalues of the order  $\simeq M_x$ . Hence, in case (ii) no seesaw mechanism is operative at the renormalizable level. In case (iii) a (see Fig. 4.3) one can envisage the Yukawa interaction

$$\mathcal{L}_Y^\nu = Y_\alpha^\nu \bar{\ell}_\beta \tilde{H} N_\alpha + Y_\beta^\nu \bar{\ell}_\beta \tilde{H} N_\beta + \text{h.c.}, \quad (4.10)$$

which gives the usual Dirac masses with arbitrary mixings but no seesaw suppression of the active neutrino masses since mass terms for the right-handed neutrinos are

forbidden. Bare Majorana masses for the right-handed neutrinos are allowed in case (iii) b (see Fig. 4.3) which is characterized by the Yukawa interactions

$$\mathcal{L}_Y^\nu = Y_\alpha^\nu \bar{\ell}_\beta \tilde{H} N_\alpha + f M_x \bar{N}_\alpha^c N_\beta + \text{h.c.} \quad (4.11)$$

The  $4 \times 4$  neutrino mass matrix corresponding to Eq. (4.11) is similar to  $M_\nu$  in Eq. (4.9) with  $Y_\beta^\nu = 0$  and hence, also in this case, there is no seesaw mechanism. Moreover, the presence of the bare mass term in Eq. (4.11) is in contrast to Eq. (4.1) where the theory before symmetry breaking is massless.

Altogether, we observe from the different cases (i)-(iii) a pattern for the allowed fermion masses which is in a way restrictive and does not allow for an effective seesaw mechanism. Furthermore, in the cases (i)-(iii) chiral anomalies may possibly be present since the left- and right-handed states are treated in an asymmetric manner. This contrasts with Eq. (4.1), where each of the right-handed neutrinos has a mass term in the Dirac and the Majorana mass matrix, thereby maximizing the nature of the Yukawa sector. In this respect, the two-site model is a fairly natural setup which automatically predicts seesaw suppressed neutrino masses with maximal mixing. The basic geometric structure of Eq. (4.1) is expected to be borne out in a realistic phenomenological application. In Sec. 4.2, we show this property by considering a model on a moose mesh and also give in Sec. 4.3 other realizations.

## 4.2 Four-site model

We examine now a generalization of the basic two-site model described in Sec. 4.1 to the case of a *moose mesh* [80] in which all fermion and scalar fields are treated as bi-fundamental representations. As a result, we will find that this scenario can provide a realistic description of neutrino mass and mixing parameters.

### 4.2.1 Non-renormalizable Yukawa interactions

Consider a  $\prod_{i=1}^4 SU(m)_i$  gauge theory containing five scalar link variables  $\Phi_i$  ( $i = 1, \dots, 5$ ) which transform under the  $SU(m)$  gauge groups as  $\Phi_1 \subset (m_1, \bar{m}_2)$ ,  $\Phi_2 \subset (m_2, \bar{m}_3)$ ,  $\Phi_3 \subset (m_3, \bar{m}_4)$ ,  $\Phi_4 \subset (m_4, \bar{m}_1)$ , and  $\Phi_5 \subset (m_2, \bar{m}_4)$ . We will combine the fields  $\ell_\alpha, E_\alpha$ , and  $N_\alpha$  of identical flavor  $\alpha = e, \mu, \tau$  into the set  $\Psi_\alpha \equiv \{\ell_\alpha, E_\alpha, N_\alpha\}$  of leptons. Here,  $\Psi_\alpha$  combines  $\ell_\alpha, E_\alpha$ , and  $N_\alpha$  with exactly these chiralities and no charge conjugates of these fields (like  $\ell^c$ ) are included. In our scheme, all the leptons associated with  $\Psi_\alpha$  carry the same  $SU(m)_i$  charge and connect the different gauge groups as bi-fundamental representations. Hence, all fermions and scalars are treated on the same footing as link variables. Specifically, we make the choice  $\Psi_e \subset (m_2, \bar{m}_4)$ ,  $\Psi_\mu \subset (m_4, \bar{m}_3)$ , and  $\Psi_\tau \subset (m_4, \bar{m}_1)$ . The link field content is given in Table 4.1. Graphically, the scalar and fermionic fields can be represented as a moose mesh which is depicted in Fig. 4.4. Up to mass dimension seven, the leading-order

	$\Phi_1$	$\Phi_2$	$\Phi_3$	$\Phi_4$	$\Phi_5$	$\Psi_e$	$\Psi_\mu$	$\Psi_\tau$
$SU(m)_1$	$\square$	1	1	$\overline{\square}$	1	1	1	$\overline{\square}$
$SU(m)_2$	$\overline{\square}$	$\square$	1	1	$\square$	$\square$	1	1
$SU(m)_3$	1	$\overline{\square}$	$\square$	1	1	1	$\overline{\square}$	1
$SU(m)_4$	1	1	$\overline{\square}$	$\square$	$\overline{\square}$	$\overline{\square}$	$\square$	$\square$

Table 4.1: Transformation properties of the scalar and fermionic link variables.

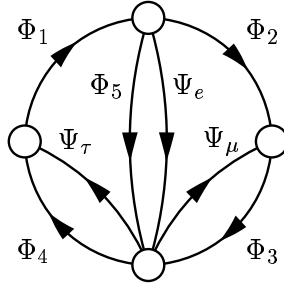


Figure 4.4: Moose mesh for the four-site model.

Yukawa interactions of the model are

$$\mathcal{L}_Y = \mathcal{L}_{\text{ren}} + \mathcal{L}_{\text{dim } 5}^M + \mathcal{L}_{\text{dim } 6}^D + \dots, \quad (4.12)$$

where  $\mathcal{L}_{\text{ren}}$  denotes the renormalizable Yukawa interactions,  $\mathcal{L}_{\text{dim } 5}^M$  are the dimension-five terms of the right-handed Majorana neutrinos and  $\mathcal{L}_{\text{dim } 6}^D$  are the dimension-six terms in the Dirac mass matrices. In Eq. (4.12), the dots represent non-renormalizable higher-order Yukawa interactions of the leptons with effective scalar operators which involve only the Higgs doublet  $H$  and/or the link fields  $\Phi_i$  ( $i = 1, \dots, 5$ ). The renormalizable Yukawa interactions are

$$\mathcal{L}_{\text{ren}} = \sum_{\alpha=e,\mu,\tau} \left( Y_\alpha^E \overline{\ell}_\alpha H E_\alpha + Y_\alpha^\nu \overline{\ell}_\alpha \tilde{H} N_\alpha \right) + f_1 \overline{N}_e^c \Phi_2^* N_\mu + f_2 \overline{N}_e^c \Phi_1 N_\tau + \text{h.c.}, \quad (4.13)$$

where  $Y_\alpha^E, Y_\alpha^\nu$  ( $\alpha = e, \mu, \tau$ ), and  $f_1, f_2$  denote complex Yukawa couplings of order unity. From Eq. (4.13), we observe that the charged lepton mass matrix and the Dirac neutrino mass matrix emerging after SSB from  $\mathcal{L}_{\text{ren}}$  are on diagonal form. However,  $\mathcal{L}_{\text{ren}}$  generates off-diagonal entries in the Majorana mass matrix thereby leading to a large mixing of the right-handed neutrinos. Note that  $\mathcal{L}_{\text{ren}}$  yields in the Majorana sector the most general mass terms consistent with the linear combination  $\overline{L} = L_e - L_\mu - L_\tau$  of the individual lepton numbers  $L_e, L_\mu$ , and  $L_\tau$ . The right-handed Majorana mass matrix consistent with this symmetry has a vanishing determinant and would therefore lead to a singular seesaw mechanism. A non-zero determinant, however, becomes possible when taking the dimension-five terms into account. All of the dimension-five Yukawa interactions allowed by gauge invariance appear in the

right-handed neutrino sector and read

$$\begin{aligned} \mathcal{L}_{\text{dim } 5}^M = & f_3 \frac{\Phi_3 \Phi_3}{\Lambda} \overline{N}_\mu^c N_\mu + f_4 \frac{\Phi_4^* \Phi_4^*}{\Lambda} \overline{N}_\tau^c N_\tau + f_5 \frac{\Phi_3 \Phi_4^*}{\Lambda} \overline{N}_\mu^c N_\tau \\ & + f_6 \frac{\Phi_5^* \Phi_5^*}{\Lambda} \overline{N}_e^c N_e + \text{h.c.}, \end{aligned} \quad (4.14)$$

where  $f_3, f_4, f_5$ , and  $f_6$  are complex Yukawa couplings of order unity and  $\Lambda \gg \langle \Phi_i \rangle$  ( $i = 1, \dots, 5$ ) denotes the mass scale at which the higher-order terms are generated. As an effective field theory, the interactions may become again fully renormalizable in the UV limit (*i.e.*, at small distances  $\ll 1/\Lambda$ ) and could, *e.g.*, be explicitly realized in terms of the Froggatt-Nielsen mechanism. Note that the  $\overline{L}$  symmetry characteristic of  $\mathcal{L}_{\text{ren}}$  is broken by the interactions in  $\mathcal{L}_{\text{dim } 5}^M$ . In the Majorana sector, all higher-order corrections of mass dimension  $\geq 6$  can be absorbed into the Yukawa couplings  $f_1, \dots, f_6$ . In the same way, one can treat by an appropriate redefinition of the Yukawa couplings the higher-order corrections to  $Y_\alpha^E$  and  $Y_\alpha^\nu$  ( $\alpha = e, \mu, \tau$ ). Hence, the relevant dimension-six mass terms for the neutrinos can be written as

$$\begin{aligned} \mathcal{L}_{\text{dim } 6}^D \supset & Y_{e\mu}^\nu \frac{\Phi_3 \Phi_5}{\Lambda^2} \overline{\ell}_e \tilde{H} N_e + Y_{e\tau}^\nu \frac{\Phi_4^* \Phi_5}{\Lambda^2} \overline{\ell}_e \tilde{H} N_\tau + Y_{\mu e}^\nu \frac{\Phi_3^* \Phi_5^*}{\Lambda^2} \overline{\ell}_\mu \tilde{H} N_e \\ & + Y_{\tau e}^\nu \frac{\Phi_4 \Phi_5^*}{\Lambda^2} \overline{\ell}_\tau \tilde{H} N_e + \left( Y_{\mu\tau}^\nu \frac{\Phi_1 \Phi_2}{\Lambda^2} + Y_{\mu\tau}^{\nu'} \frac{\Phi_3^* \Phi_4^*}{\Lambda^2} \right) \overline{\ell}_\mu \tilde{H} N_\tau \\ & + \left( Y_{\tau\mu}^\nu \frac{\Phi_1^* \Phi_2^*}{\Lambda^2} + Y_{\tau\mu}^{\nu'} \frac{\Phi_3 \Phi_4}{\Lambda^2} \right) \overline{\ell}_\mu \tilde{H} N_\tau + \text{h.c.}, \end{aligned} \quad (4.15)$$

where  $Y_{\alpha\beta}^\nu$  and  $Y_{\alpha\beta}^{\nu'}$  ( $\alpha, \beta = e, \mu, \tau$ ) are complex Yukawa couplings of order unity. In Eq. (4.15) only the off-diagonal neutrino mass terms are shown. The corresponding expression for the charged leptons is found by replacing  $\tilde{H} \rightarrow H$ ,  $N_\alpha \rightarrow E_\alpha$  ( $\alpha = e, \mu, \tau$ ), and  $\nu \rightarrow E$ . When the link fields acquire universal VEVs  $\langle \Phi_i \rangle \equiv M_x$  ( $i = 1, \dots, 5$ ) the Dirac and Majorana mass matrices of the neutrinos take the forms

$$M_D = \epsilon \begin{pmatrix} Y_e^\nu & \lambda^2 & \lambda^2 \\ \lambda^2 & Y_\mu^\nu & \lambda^2 \\ \lambda^2 & \lambda^2 & Y_\tau^\nu \end{pmatrix}, \quad M_R = M_x \begin{pmatrix} \lambda f_6 & f_1 & f_2 \\ f_1 & \lambda f_3 & \lambda f_5 \\ f_2 & \lambda f_5 & \lambda f_4 \end{pmatrix}, \quad (4.16)$$

where  $\lambda \equiv M_x/\Lambda \ll 1$  is a small dimensionless expansion parameter and only the order of magnitude of the terms with mass dimension  $\geq 6$  has been indicated<sup>2</sup>. Note in Eq. (4.16), that the patterns for the Dirac and Majorana mass matrices are similar to the ones following from Eq. (4.1). This is a consequence of the lattice geometry which prefers a diagonal Dirac fermion sector while the Majorana sector carries the  $\overline{L}$  symmetry in terms of the link variables. At the deconstruction scale, the  $\overline{L}$  symmetry is softly broken by the suppressed  $\mathcal{O}(\lambda)$  terms in the Majorana sector. It might be of interest to note that, similar to our two-site example, this system exhibits a

<sup>2</sup>The charged lepton mass matrix has a structure analogous to  $M_D$ .

$\mathcal{CP}$  symmetry once we set  $\lambda \rightarrow 0$ . In this case, we can perform a complete phase redefinition of the right-handed fields such that the Yukawa couplings,  $f_1$  and  $f_2$  become real. We wish to repeat that the diversity of the lattice geometry reproduces the same qualitative features even if one promotes both the fermions and scalars to link variables<sup>3</sup>.

### 4.2.2 Neutrino masses and mixing angles

Let us now consider Eq. (4.16) for the special case in which all mass terms are real and take  $f_1 = -f_2 = f_3 = f_4 = f_5 \equiv f$ . Suppressing the small off-diagonal terms in  $M_D$  and setting  $Y_\mu^\nu \simeq Y_\tau^\nu$  the effective light neutrino mass matrix up to  $\mathcal{O}(\lambda^3)$  is evaluated to be

$$M_\nu \simeq \frac{Y_\mu^\nu \epsilon^2}{4f^2 M_x} \begin{pmatrix} 0 & 2\lambda Y_e^\nu f & -2\lambda Y_e^\nu f \\ 2\lambda Y_e^\nu f & Y_\mu^\nu (\lambda^2 f_6 - f) & -Y_\mu^\nu (\lambda^2 f_6 + f) \\ -2\lambda Y_e^\nu f & -Y_\mu^\nu (\lambda^2 f_6 + f) & Y_\mu^\nu (\lambda^2 f_6 - f) \end{pmatrix} + \mathcal{O}(\lambda^3), \quad (4.17)$$

where we have already applied a phase redefinition  $\ell_e \rightarrow -\ell_e$ . Since the mass matrix of the charged leptons is nearly diagonal and on strictly hierarchical form, we can neglect the mixing coming from the charged leptons. Notice that this kind of pattern of lepton mass matrices is already familiar from scenarios for softly broken lepton numbers in the heavy Majorana sector [28]. Application of a rotation in the 2-3-plane through an angle  $\theta_{23} = \pi/4$  yields the matrix

$$\mathcal{M}'_\nu \simeq \frac{Y_\mu^\nu \epsilon^2}{2f^2 M_x} \begin{pmatrix} 0 & \sqrt{2}\lambda Y_e^\nu f & 0 \\ \sqrt{2}\lambda Y_e^\nu f & \lambda^2 Y_\mu^\nu f_6 & 0 \\ 0 & 0 & -Y_\mu^\nu f \end{pmatrix} + \mathcal{O}(\lambda^3), \quad (4.18)$$

from which we see that the reactor angle  $\theta_{13}$  is practically zero. The mass matrix  $\mathcal{M}'_\nu$  is brought on diagonal form by a rotation in the 1-2-plane through an angle  $\theta_{12}$  which obeys

$$\tan \theta_{12} \simeq 1 - \frac{\lambda}{2\sqrt{2}} \left( \frac{Y_\mu^\nu f_6}{Y_e^\nu f} \right) + \frac{\lambda^2}{16} \left( \frac{Y_\mu^\nu f_6}{Y_e^\nu f} \right)^2 + \mathcal{O}(\lambda^4). \quad (4.19)$$

Assuming  $Y_e^\nu, Y_\mu^\nu, f$ , and  $f_6$  to be positive, the neutrino mass eigenvalues are

$$\begin{aligned} m_{\nu_1} &= \frac{1}{2} \frac{Y_\mu^{\nu 2} \epsilon^2}{f M_x} \left( -\sqrt{2} \frac{Y_e^\nu}{Y_\mu^\nu} + \frac{1}{2} \frac{f_6}{f} \lambda \right) \lambda + \mathcal{O}(\lambda^3), \\ m_{\nu_2} &= \frac{1}{2} \frac{Y_\mu^{\nu 2} \epsilon^2}{f M_x} \left( \sqrt{2} \frac{Y_e^\nu}{Y_\mu^\nu} + \frac{1}{2} \frac{f_6}{f} \lambda \right) \lambda + \mathcal{O}(\lambda^3), \\ m_{\nu_3} &= -\frac{1}{2} \frac{Y_\mu^{\nu 2} \epsilon^2}{f M_x}, \end{aligned} \quad (4.20)$$

<sup>3</sup>We note that both Eqs. (4.1) and (4.12) reproduce similar features in the limit  $\lambda \rightarrow 0$ .

and exhibit a normal neutrino mass hierarchy  $m_1 < m_2 \ll m_3$ . Note, that the masses obey here  $m_2 - m_1 \ll (m_1 + m_2)/2$  which is in contrast to the conventional scenario of normal hierarchical neutrino masses, where  $m_1 \ll m_2$  [28]. From Eq. (4.20) we find the solar and atmospheric mass squared differences

$$\Delta m_{\odot}^2 \simeq \frac{\sqrt{2}}{2} Y_e^\nu Y_\mu^\nu \frac{f_6}{f} \left( \frac{Y_\mu^\nu \epsilon^2}{f M_x} \right)^2 \lambda + \mathcal{O}(\lambda^3), \quad (4.21)$$

$$\Delta m_{\text{atm}}^2 \simeq \frac{Y_\mu^{\nu 2}}{4} \left( \frac{Y_\mu^\nu \epsilon^2}{f M_x} \right)^2 \frac{1}{\lambda^2} - \frac{Y_e^{\nu 2}}{2} \left( \frac{Y_\mu^\nu \epsilon^2}{f M} \right)^2 + \mathcal{O}(\lambda), \quad (4.22)$$

which lead to the relation

$$\frac{\Delta m_{\odot}^2}{\Delta m_{\text{atm}}^2} \simeq 2\sqrt{2}\lambda^3 \left( \frac{Y_e^\nu f_6}{Y_\mu^\nu f} \right) + \mathcal{O}(\lambda^5). \quad (4.23)$$

Comparing Eq. (4.19) with Eq. (4.23) we note that there exists a parameter range where the solar angle  $\theta_{12}$  may be substantially varied while  $\Delta m_{\odot}^2/\Delta m_{\text{atm}}^2$  is kept constant or vice versa. For illustration, we choose  $\lambda = 0.22$ ,  $Y_e^\nu = f$ ,  $Y_\mu^\nu = f_6$ , and the ratio  $Y_\mu^\nu/Y_e^\nu = 2.5$ . In this case, we have a maximal atmospheric mixing angle  $\theta_{23} \simeq \pi/4$  and a reactor mixing angle close to zero, *i.e.*,  $\theta_{13} \simeq 0$ . Taking the best-fit value  $\Delta m_{\text{atm}}^2 = 2.5 \times 10^{-3} \text{ eV}^2$  [11], we obtain the solar parameters

$$\Delta m_{\odot}^2 \simeq 7.5 \times 10^{-5} \text{ eV}^2, \quad \theta_{12} \simeq 32^\circ, \quad (4.24)$$

which are close to the best-fit value within the 90% C.L. region of the MSW LMA-I solution [14]. The strength of  $\theta_{13}$  determines the splitting between the scales which correspond to  $\Delta m_{\text{atm}}^2$  and the resulting  $\mathcal{CP}$  violation, which is in this case, of course, practically zero due to vanishing  $\theta_{13}$ . The system predicts an effective neutrinoless double beta decay mass  $m_{ee} \simeq 10^{-3} \text{ eV}$ . Of course, the numerical results here can be altered by suitably varying the Yukawa couplings. In the above considerations, we have taken the Dirac matrix  $M_D$  to be practically diagonal and ignored the off-diagonal entries present in the general form of  $M_D$  in Eq. (4.16) which are of the order  $\simeq \lambda^2 \epsilon$ . Actually, in Eq. (4.17), these terms lead to corrections of the effective neutrino mass matrix which are of the order  $\simeq \lambda^2 m_3$ . As a consequence,  $\theta_{23}$ ,  $\theta_{13}$ , and  $\Delta m_{\text{atm}}^2$  receive only small corrections which are  $\lambda^2$ -suppressed. Moreover, we observe in Eq. (4.18) that the impact of the  $\lambda^2 m_3$ -contributions on Eqs. (4.19) and (4.21) may be absorbed into the Yukawa coupling  $f_6$  by an appropriate redefinition. Therefore, to leading order, the numerical estimates given above should not be significantly altered by fully taking the off-diagonal entries of  $M_D$  into account. We reiterate that the striking aspect is the underlying lattice structure which ensures large solar and atmospheric mixing angles  $\theta_{12}$  and  $\theta_{23}$  while keeping the reactor angle  $\theta_{13}$  small. Any modifications to the large mixing angles can be associated with the  $\mathcal{CP}$  symmetry of the scheme whose breaking (which is parameterized by  $\lambda$ ) can be either soft or hard.

	$\Phi_1$	$\Phi_2$	$\Phi_3$	$\Psi_e$	$\Psi_\mu$	$\Psi_\tau$
$SU(3)_1$	$\square$	1	$\bar{\square}$	$\square$	1	1
$SU(3)_2$	$\bar{\square}$	$\square$	1	1	$\bar{\square}$	1
$SU(3)_3$	1	$\bar{\square}$	$\square$	1	1	$\bar{\square}$

Table 4.2: Transformation properties of the link fields and SM leptons in the  $SU(3)^3$  model.

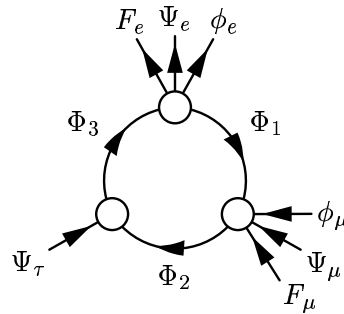


Figure 4.5: Moose diagram for the three-site model.

### 4.3 Three-site models

We briefly outline two variations of the model described in Sec. 4.2 which can equally well accommodate the neutrino data and are based on three lattice sites, where each site corresponds to one generation.

#### 4.3.1 A $SU(3)^3$ model

Let us consider the product gauge group  $\prod_{i=1}^3 SU(3)_i$  where the  $SU(3)_i$  ( $i = 1, 2, 3$ ) subgroups are connected by the link variables  $\Phi_i$  ( $i = 1, 2, 3$ ) which transform as bifundamental representations  $\Phi_i \subset (3_i, \bar{3}_{i+1})$  under the  $SU(3)_i$  symmetries. Here, the index  $i + 3$  is identified with  $i$ . The fields from the set  $\Psi_e$  transform under  $\mathbb{3}_1$ , while the fields from  $\Psi_\mu$  transform under  $\bar{\mathbb{3}}_2$ , and the fields from  $\Psi_\tau$  transform under  $\bar{\mathbb{3}}_3$ . The representations of the link fields and the SM leptons under the  $SU(3)^3$  product gauge group are shown in Table 4.2. Hence, like in the example of the two-site model, each generation is put on a different lattice site and the periodicity requirement is reflected by the closed lattice geometry.

We shall now be interested in a possible origin of the non-renormalizable operators which can softly break the  $\bar{L}$  symmetry at tree-level. To this end, we will consider the complete renormalizable theory including the heavy fundamental states which generate these higher-dimensional terms when they are integrated out in the low-energy limit. Without any such particles, gauge invariance requires both the charged lepton mass matrix as well as the Dirac neutrino mass matrix to be on diagonal form, *i.e.*, the Dirac matrices exactly conserve the individual lepton numbers. At the decon-



struction scale, the product gauge group is broken down to the diagonal subgroup  $SU(3)_{\text{diag}}$  while preserving the  $\bar{L}$  symmetry. Again, the right-handed Majorana mass matrix would give rise to a massless right-handed neutrino and is  $\mathcal{CP}$  conserving like the two-site model. A soft breaking of the  $\bar{L}$  symmetry in the right-handed Majorana sector may be achieved by putting on each of the sites representing  $SU(3)_1$  and  $SU(3)_2$  two extra SM singlet fields. For this purpose, we introduce two SM singlet scalar fields  $\phi_e$  and  $\phi_\mu$  as well as two heavy SM singlet Dirac fermions  $F_e = (F_{eL}, F_{eR})^T$  and  $F_\mu = (F_{\mu L}, F_{\mu R})^T$ , where  $F_{\alpha L}$  and  $F_{\alpha R}$  ( $\alpha = e, \mu$ ) denote the left- and the right-handed components of  $F_\alpha$ . The fields  $\phi_e$  and  $F_e$  both transform as  $3_1$  under  $SU(3)_1$  whereas  $\phi_\mu$  and  $F_\mu$  both transform as  $\bar{3}_2$  under  $SU(3)_2$  (see Fig. 4.5). At this stage, the extra particles are vector-like representations of the gauge symmetries and leave the model free from chiral anomalies. A soft breaking of the  $\bar{L}$  symmetry is realized by imposition of a  $Z_4$  symmetry such that

$$\begin{aligned} Z_4 : \quad \ell_\alpha &\longrightarrow -\ell_\alpha, & E_\alpha &\longrightarrow -E_\alpha, & N_\alpha &\longrightarrow -N_\alpha, \\ & \phi_\alpha &\longrightarrow -\phi_\alpha, & F_{\alpha L} &\longrightarrow iF_{\alpha L}, & \Phi_3 &\longrightarrow -\Phi_3, \end{aligned} \quad (4.25)$$

where  $\alpha$  runs only over the two flavors  $\alpha = e, \mu$ . Note that the  $Z_4$  symmetry acts differently on the left- and right-handed components of the fields  $F_e$  and  $F_\mu$ . The  $Z_4$  charges are therefore expected to become anomalous when the discrete symmetry is gauged. In orbifold constructions, however, different transformation properties of left- and right-handed components of higher-dimensional Dirac spinors may naturally appear [84]. The resulting renormalizable Yukawa interactions of the neutrinos can be written as

$$\begin{aligned} \mathcal{L}_Y^\nu = & \sum_{\alpha=e,\mu,\tau} Y_\alpha^\nu \bar{\ell}_\alpha \tilde{H} N_\alpha + f_1 \bar{N}_e^c \Phi_1^* N_\mu + f_2 \bar{N}_e^c \Phi_3 N_\tau + \sqrt{f_3} \bar{N}_\mu^c \phi_\mu F_{\mu R} \\ & + \sqrt{f_6} \bar{N}_e^c \phi_e F_{eR} + \bar{F}_{eR}^c M_e F_{eR} + \bar{F}_{\mu R}^c M_\mu F_{\mu R} + \text{h.c.}, \end{aligned} \quad (4.26)$$

where  $Y_\alpha^\nu$  ( $\alpha = e, \mu, \tau$ ) and  $f_i$  ( $i = 1, 2, 3, 6$ ) denote complex Yukawa couplings which we take to be of order unity. The terms  $\sim \bar{N}_e^c \phi_e F_{eR}$  and  $\sim \bar{N}_\mu^c \phi_\mu F_{\mu R}$  are gauge invariant since the decomposition

$$3_i \otimes 3_i \otimes 3_i = 10_i \oplus 8_i \oplus 8_i \oplus 1, \quad (4.27)$$

where  $i = 1, 2$ , contains a  $SU(3)_i$  singlet which allows such interactions. In Eq. (4.26), the  $SU(3)_1$  and  $SU(3)_2$  symmetries are broken by the bare Majorana masses  $M_e$  and  $M_\mu$  at some high mass scale. When the fields  $\phi_\alpha$  acquire the VEVs  $\langle \phi_\alpha \rangle = M_x$  ( $\alpha = e, \mu$ ), the heavy fermions  $F_{eR}$  and  $F_{\mu R}$  are integrated out, leading to the dimension-five terms

$$f_3 \frac{\langle \phi_\mu \rangle^2}{M_\mu} \bar{N}_\mu^c N_\mu \simeq \lambda f_3 M_x \bar{N}_\mu^c N_\mu, \quad f_6 \frac{\langle \phi_e \rangle^2}{M_e} \bar{N}_e^c N_e \simeq \lambda f_6 M_x \bar{N}_e^c N_e, \quad (4.28)$$

where we have set  $M_e \simeq M_\mu$  and introduced the small expansion parameter  $\lambda \simeq M_x/M_e \simeq M_x/M_\mu$ . The corresponding Froggatt-Nielsen type diagram is given in

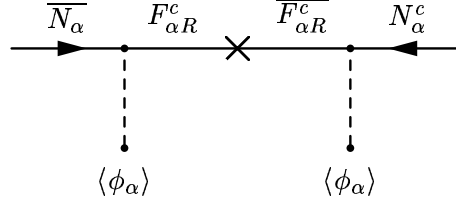


Figure 4.6: Dimension-five operator generating for  $\alpha = e, \mu$  the effective Majorana mass terms  $\sim \lambda M_x \overline{N_\alpha^c} N_\alpha$  at the high scale.

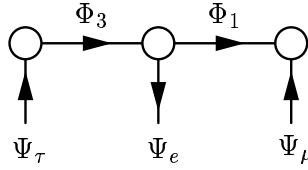


Figure 4.7: Moose diagram for the  $U(1)^3$  model.

Fig. 4.6. The Dirac neutrino mass matrix  $M_D$  is on strictly diagonal form and the invertible heavy right-handed neutrino mass matrix is given by

$$M_R = M_x \begin{pmatrix} \lambda f_6 & f_1 & f_2 \\ f_1 & \lambda f_3 & 0 \\ f_2 & 0 & 0 \end{pmatrix}. \quad (4.29)$$

Comparison with Eq. (4.16) shows that we obtain in this case relations for the neutrino mass and mixing angles which are similar to Eqs. (4.19) and (4.23). It is not surprising to find these relations because the spirit of breaking the underlying  $\overline{L}$  symmetry in either examples has been similar.

### 4.3.2 A $U(1)^3$ model

We now deviate from the above model in Eq. (4.26) and use only local  $U(1)$  symmetries by setting  $\Phi_2 \rightarrow 0$  and identifying  $SU(3)_i \rightarrow U(1)_i$  ( $i = 1, 2, 3$ ). Moreover, we will not explicitly introduce the fields  $\phi_\alpha$  and  $F_\alpha$  from Section 4.3.1. The fields in the set  $\Psi_e$  are all assigned a  $U(1)_1$  charge  $+1$  whereas the fields in  $\Psi_\mu$  carry the  $U(1)_2$  charge  $-1$  and the fields in  $\Psi_\tau$  carry the  $U(1)_3$  charge  $-1$ . The corresponding moose diagram is shown in Fig. 4.7. The  $U(1)^3$  charge structure of the left- and right-handed neutrino pairs is shown in Table 4.3 and the corresponding charges of the right-handed neutrino pairs is given in Table 4.4. Implicitly, we will assume that the fundamental scalar fields involved in the effective scalar operators of the Froggatt-Nielsen mechanism are site variables. Moreover we assume that these scalars carry only unit (and no multiple)  $U(1)$  charges, which is analogous to the requirement of having only fundamental or anti-fundamental representations of the matter fields in

		$N_e$	$N_\mu$	$N_\tau$
	$U(1)^3$	(1, 0, 0)	(0, -1, 0)	(0, 0, -1)
$\overline{\nu}_e$	(-1, 0, 0)	(0, 0, 0)	(-1, -1, 0)	(-1, 0, -1)
$\overline{\nu}_\mu$	(0, 1, 0)	(1, 1, 0)	(0, 0, 0)	(0, 1, -1)
$\overline{\nu}_\tau$	(0, 0, 1)	(1, 0, 1)	(0, -1, 1)	(0, 0, 0)

Table 4.3:  $U(1)^3$  charge structure of the left- and right-handed neutrino pairs. The same charge assignment holds for the charged lepton-antilepton pairs.

		$N_e$	$N_\mu$	$N_\tau$
	$U(1)^3$	(1, 0, 0)	(0, -1, 0)	(0, 0, -1)
$\overline{N}_e^c$	(1, 0, 0)	(2, 0, 0)	(1, -1, 0)	(1, 0, -1)
$\overline{N}_\mu^c$	(0, -1, 0)	(1, -1, 0)	(0, -2, 0)	(0, -1, -1)
$\overline{N}_\tau^c$	(0, 0, -1)	(1, 0, -1)	(0, -1, -1)	(0, 0, -2)

Table 4.4:  $U(1)^3$  charge structure of the right-handed neutrino pairs.

the  $SU(m)$  case. Hence, the Dirac and Majorana mass matrices exhibit after SSB the structures

$$M_D \simeq \epsilon \begin{pmatrix} 1 & \lambda^2 & \lambda^2 \\ \lambda^2 & 1 & \lambda^2 \\ \lambda^2 & \lambda^2 & 1 \end{pmatrix}, \quad M_R \simeq M_x \begin{pmatrix} \lambda & 1 & 1 \\ 1 & \lambda & \lambda \\ 1 & \lambda & \lambda \end{pmatrix}, \quad (4.30)$$

where only the order of magnitude of the matrix elements has been indicated. Note in Eq. (4.30), that the dimension-six mass terms in the (2, 3) and (3, 2) entries of  $M_D$  are suppressed by two powers of  $\lambda$  due to the absence of the field  $\Phi_2$ , which would otherwise carry the charge difference. Since the dimension-four and -five mass terms of the right-handed neutrinos are generated by both the scalar link- and site variables, the Majorana mass matrix below the deconstruction scale contains elements which are only  $\lambda$  suppressed as compared with the Dirac sector. In this model,  $\mathcal{CP}$  symmetry is broken and is generated from non-trivial mixings from both the Dirac and Majorana sector. The parameter  $\lambda$  is undetermined and is taken to be a soft term such that large neutrino mixings are essentially generated from the heavy right-handed sector while the Dirac sector remains practically unmixed. Again for this example, it is straightforward to accommodate the present neutrino data for an appropriate choice of  $\lambda$ .

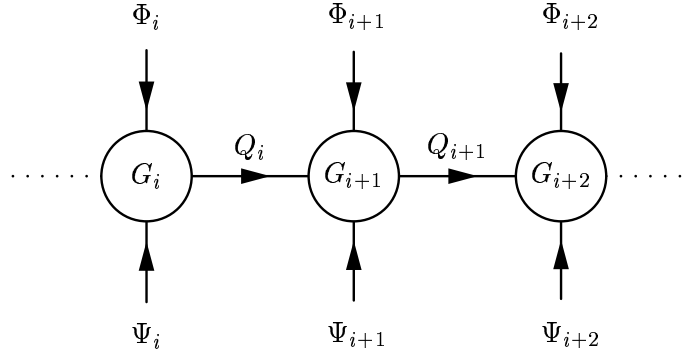


Figure 4.8: View at the sites  $i, i + 1$ , and  $i + 2$  of the moose diagram for a deconstructed large extra dimension compactified on  $\mathcal{S}^1$ .

## 4.4 Deconstructed large extra dimensions

In theories with continuous extra dimensions, the fundamental scale of quantum gravity may be lowered from the 4D Planck scale  $\simeq 10^{19}$  GeV down to the TeV scale, when the compactification radius  $R$  is large [3]. For a number of  $\delta$  large extra dimensions, for example, the spreading of the gravitational force in the bulk implies<sup>4</sup> that  $R \simeq 10^{-17+30/\delta}$  cm. If  $\delta = 2$ , we arrive at the phenomenologically relevant case of sub-mm extra dimensions. Clearly, in this scenario, one would naturally expect the cutoff scale to be of the order TeV. This, however, implies for the remodeled extra dimensions an inverse lattice spacing of similar order and therefore a large number of lattice sites.

Contrary to the usual picture, we will now analyze a possible deconstruction setup, where the inverse lattice spacing is in the sub-eV range [81]. This allows us to study the latticization of large extra dimensions for a small number of gauge groups. To be specific, we consider a periodic model for a deconstructed 5D  $U(1)$  gauge theory compactified on  $\mathcal{S}^1$ . The setup is defined by a  $U(1)^N = \prod_{i=1}^N U(1)_i$  product gauge group with  $N$  scalar link variables  $Q_i$  ( $i = 1, \dots, N$ ) where the link field  $Q_i$  carries the  $U(1)$ -charges  $(q, -q)$  under the neighboring groups  $U(1)_i \times U(1)_{i+1}$ . Periodicity of the lattice geometry is ensured by the identification  $i + N = i$ . On the  $i$ th lattice site, we put one Dirac fermion  $\Psi_i$  and one scalar  $\Phi_i$  which carry both the charge  $-q$  of the group  $U(1)_i$ . The corresponding moose diagram is shown in Fig. 4.8. We impose a discrete  $Z_2$ -parity

$$Z_2 \quad : \quad \Phi_i \longrightarrow -\Phi_i \quad (i = 1, 2, \dots, N), \quad (4.31)$$

which forbids at tree-level any renormalizable Yukawa interactions between the site variables  $\Psi_i$  and  $\Phi_j$  ( $i, j = 1, 2, \dots, N$ ). Then, the most general scalar potential is

<sup>4</sup>Here, compactification on a torus with equal radii is assumed.

given by

$$\begin{aligned}
V = & \sum_{i=1}^N \left[ m^2 \Phi_i^\dagger \Phi_i + M^2 Q_i^\dagger Q_i + \frac{1}{2} \lambda_1 (\Phi_i^\dagger \Phi_i)^2 + \frac{1}{2} \lambda_2 (Q_i^\dagger Q_i)^2 \right. \\
& + \lambda_3 (Q_i^\dagger Q_i) \left( \sum_{j=1}^N \Phi_j^\dagger \Phi_j \right) + \mu \Phi_{i-1} Q_i \Phi_i^\dagger + \mu^* \Phi_i Q_i^\dagger \Phi_{i-1}^\dagger \\
& + \lambda_4 (\Phi_i^\dagger \Phi_i) \left( \sum_{j \neq i} \Phi_j^\dagger \Phi_j \right) + \lambda_5 (Q_i^\dagger Q_i) \left( \sum_{j \neq i} Q_j^\dagger Q_j \right) \\
& \left. + \lambda_6 (Q_i Q_{i+1}) (\Phi_i \Phi_{i+2}^\dagger) + \lambda_6^* (Q_{i+1}^\dagger Q_i^\dagger) (\Phi_{i+2} \Phi_i^\dagger) \right], \tag{4.32}
\end{aligned}$$

where  $\lambda_1, \lambda_2, \dots, \lambda_5$  are dimensionless real parameters of order unity and  $\lambda_6$  is a complex-valued order unity coefficient. In Eq. (4.32), we can take the dimensionful quantities  $m$  and  $\mu$  to be of the order of the electroweak scale  $m, \mu \simeq 10^2$  GeV and make the mass  $M$  very large, *i.e.*,  $M \gg m, \mu$ . We will minimize the potential by going to the real basis

$$Q_i = q_i^a + i q_i^b \longrightarrow \begin{pmatrix} q_i^a \\ q_i^b \end{pmatrix}, \quad \Phi_i = \phi_i^a + i \phi_i^b \longrightarrow \begin{pmatrix} \phi_i^a \\ \phi_i^b \end{pmatrix}. \tag{4.33}$$

The term  $\mu \Phi_{i-1} Q_i \Phi_i^\dagger$  in Eq. (4.32) reads

$$\begin{aligned}
\mu \Phi_{i-1} Q_i \Phi_i^\dagger + & = \mu \left[ \phi_{i-1}^a q_i^a \phi_i^a - \phi_{i-1}^b q_i^b \phi_i^a + \phi_{i-1}^b q_i^a \phi_i^b + \phi_{i-1}^a q_i^b \phi_i^b \right. \\
& \left. + i (\phi_{i-1}^b q_i^a \phi_i^a + \phi_{i-1}^a q_i^b \phi_i^a - \phi_{i-1}^a q_i^a \phi_i^b + \phi_{i-1}^b q_i^b \phi_i^b) \right]. \tag{4.34}
\end{aligned}$$

Also, the term  $\lambda_6 (Q_i Q_{i+1}) (\Phi_i \Phi_{i+2}^\dagger)$  in Eq. (4.32) is given by

$$\begin{aligned}
\lambda_6 (Q_i Q_{i+1}) (\Phi_i \Phi_{i+2}^\dagger) = & \lambda_6 \left[ (q_i^a q_{i+1}^a - q_i^b q_{i+1}^b) (\phi_i^a \phi_{i+2}^a + \phi_i^b \phi_{i+2}^b) \right. \\
& - (q_i^b q_{i+1}^a + q_i^a q_{i+1}^b) (\phi_i^b \phi_{i+2}^a - \phi_i^a \phi_{i+2}^b) \\
& + i \lambda_6 \left[ (q_i^a q_{i+1}^a - q_i^b q_{i+1}^b) (\phi_i^b \phi_{i+2}^a - \phi_i^a \phi_{i+2}^b) \right. \\
& \left. + (q_i^b q_{i+1}^a + q_i^a q_{i+1}^b) (\phi_i^a \phi_{i+2}^a + \phi_i^b \phi_{i+2}^b) \right]. \tag{4.35}
\end{aligned}$$

Note that for a supersymmetric case, the term  $\lambda_6$  would have to vanish at the renormalizable level due to the holomorphy of the superpotential. Then, the phase of  $\mu$  could be absorbed into the Yukawa couplings of the fermions  $\Psi_i$ , thereby giving rise to a non-trivial warp factor. Since we restrict ourselves here to the simpler case of a flat background with zero warp factor, we take the parameters  $\mu$  and  $\lambda_6$  to be real.

Then, the scalar potential in Eq. (4.32) can be written as

$$\begin{aligned}
V = & \sum_{i=1}^N \left\{ m^2 [(\phi_i^a)^2 + (\phi_i^b)^2] + M^2 [(q_i^a)^2 + (q_i^b)^2] + \frac{1}{2} \lambda_1 [(\phi_i^a)^2 + (\phi_i^b)^2]^2 \right. \\
& \frac{1}{2} \lambda_2 [(q_i^a)^2 + (q_i^b)^2]^2 + \lambda_3 [(\phi_i^a)^2 + (\phi_i^b)^2] \left[ \sum_{j=1}^N (q_j^a)^2 + (q_j^b)^2 \right] \\
& + \lambda_4 [(\phi_i^a)^2 + (\phi_i^b)^2] \left[ \sum_{j \neq i} (\phi_j^a)^2 + (\phi_j^b)^2 \right] \\
& + \lambda_5 [(q_i^a)^2 + (q_i^b)^2] \left[ \sum_{j \neq i} (q_j^a)^2 + (q_j^b)^2 \right] \\
& + \mu [\phi_{i-1}^a q_i^a \phi_i^a - \phi_{i-1}^b q_i^b \phi_i^a + \phi_{i-1}^b q_i^a \phi_i^b + \phi_{i-1}^a q_i^b \phi_i^b] \\
& + \mu [\phi_i^a q_{i+1}^a \phi_{i+1}^a - \phi_i^b q_{i+1}^b \phi_{i+1}^a + \phi_i^b q_{i+1}^a \phi_{i+1}^b + \phi_i^a q_{i+1}^b \phi_{i+1}^b] \\
& + \frac{1}{2} \lambda_6 [(q_{i-2}^a q_{i-1}^a - q_{i-2}^b q_{i-1}^b)(\phi_{i-2}^a \phi_i^a + \phi_{i-2}^b \phi_i^b) \\
& - (q_{i-2}^b q_{i-1}^a + q_{i-2}^a q_{i-1}^b)(\phi_{i-2}^b \phi_i^a - \phi_{i-2}^a \phi_i^b)] \\
& + \frac{1}{2} \lambda_6 [(q_{i-1}^a q_i^a - q_{i-1}^b q_i^b)(\phi_{i-1}^a \phi_{i+1}^a + \phi_{i-1}^b \phi_{i+1}^b) \\
& - (q_{i-1}^b q_i^a + q_{i-1}^a q_i^b)(\phi_{i-1}^b \phi_{i+1}^a - \phi_{i-1}^a \phi_{i+1}^b)] \\
& + \frac{1}{2} \lambda_6 [(q_i^a q_{i+1}^a - q_i^b q_{i+1}^b)(\phi_i^a \phi_{i+2}^a + \phi_i^b \phi_{i+2}^b) \\
& - (q_i^b q_{i+1}^a + q_i^a q_{i+1}^b)(\phi_i^b \phi_{i+2}^a - \phi_i^a \phi_{i+2}^b)] \\
& + \frac{1}{2} \lambda_6 [(q_{i+1}^a q_{i+2}^a - q_{i+1}^b q_{i+2}^b)(\phi_{i+1}^a \phi_{i+3}^a + \phi_{i+1}^b \phi_{i+3}^b) \\
& \left. - (q_{i+1}^b q_{i+2}^a + q_{i+1}^a q_{i+2}^b)(\phi_{i+1}^b \phi_{i+3}^a - \phi_{i+1}^a \phi_{i+3}^b) \right] \Big\}, \tag{4.36}
\end{aligned}$$

where we have symmetrically reorganized the sum, such that all operators carrying the index “ $i$ ” are explicitly displayed<sup>5</sup>. We are interested in a minimum of  $V$  with the following vacuum structure

$$\langle Q_i \rangle = \begin{pmatrix} u \\ 0 \end{pmatrix}, \quad \langle \Phi_i \rangle = \begin{pmatrix} v \\ 0 \end{pmatrix}, \quad i = 1, 2, \dots, N, \tag{4.37}$$

*i.e.*, all link variables  $Q_i$  have a real universal VEV  $u$  and all site variables  $\Phi_i$  have a

---

<sup>5</sup>To avoid double-counting, the coefficients  $\mu$  and  $\lambda_6$  have been given pre-factors  $\frac{1}{2}$  and  $\frac{1}{4}$ , respectively.

real universal VEV  $v$ . From Eq. (4.36) we obtain

$$\begin{aligned}
\frac{\partial V}{\partial \phi_i^a} &= 2m^2 \phi_i^a + 2\lambda_1 [(\phi_i^a)^2 + (\phi_i^b)^2] \phi_i^a \\
&+ 2\lambda_3 \phi_i^a \left[ \sum_{j=1}^N (q_j^a)^2 + (q_j^b)^2 \right] + 2\lambda_4 \phi_i^a \left[ \sum_{j \neq i} (\phi_j^a)^2 + (\phi_j^b)^2 \right] \\
&+ \mu [\phi_{i-1}^a q_i^a - \phi_{i-1}^b q_i^b] + \mu [q_{i+1}^a \phi_{i+1}^a + q_{i+1}^b \phi_{i+1}^b] \\
&+ \frac{1}{2} \lambda_6 [(q_{i-2}^a q_{i-1}^a - q_{i-2}^b q_{i-1}^b) \phi_{i-2}^a - (q_{i-2}^b q_{i-1}^a + q_{i-2}^a q_{i-1}^b) \phi_{i-2}^b] \\
&+ \frac{1}{2} \lambda_6 [(q_i^a q_{i+1}^a - q_i^b q_{i+1}^b) \phi_{i+2}^a + (q_i^b q_{i+1}^a + q_i^a q_{i+1}^b) \phi_{i+2}^b], \tag{4.38}
\end{aligned}$$

$$\begin{aligned}
\frac{\partial V}{\partial \phi_i^b} &= 2m^2 \phi_i^b + 2\lambda_1 [(\phi_i^a)^2 + (\phi_i^b)^2] \phi_i^b \\
&+ 2\lambda_3 \phi_i^b \left[ \sum_{j=1}^N (q_j^a)^2 + (q_j^b)^2 \right] + 2\lambda_4 \phi_i^b \left[ \sum_{j \neq i} (\phi_j^a)^2 + (\phi_j^b)^2 \right] \\
&+ \mu [\phi_{i-1}^b q_i^a + \phi_{i-1}^a q_i^b] + \mu [-q_{i+1}^b \phi_{i+1}^a + q_{i+1}^a \phi_{i+1}^b] \\
&+ \frac{1}{2} \lambda_6 [(q_{i-2}^a q_{i-1}^a - q_{i-2}^b q_{i-1}^b) \phi_{i-2}^b + (q_{i-2}^b q_{i-1}^a + q_{i-2}^a q_{i-1}^b) \phi_{i-2}^a] \\
&+ \frac{1}{2} \lambda_6 [(q_i^a q_{i+1}^a - q_i^b q_{i+1}^b) \phi_{i+2}^b - (q_i^b q_{i+1}^a + q_i^a q_{i+1}^b) \phi_{i+2}^a], \tag{4.39}
\end{aligned}$$

which gives for the VEVs in Eq. (4.37) the minimization condition

$$m^2 + [\lambda_1 + (N-1)\lambda_4] v^2 + (N\lambda_3 + \frac{1}{2}\lambda_6) u^2 + \mu u = 0, \tag{4.40}$$

and  $\langle \partial V / \partial \phi_i^b \rangle = 0$  is automatic for these VEVs. The partial derivatives for the link fields are

$$\begin{aligned}
\frac{\partial V}{\partial q_i^a} &= 2M^2 q_i^a + 2\lambda_2 [(q_i^a)^2 + (q_i^b)^2] q_i^a + 2\lambda_3 q_i^a \left[ \sum_{j=1}^N (\phi_j^a)^2 + (\phi_j^b)^2 \right] \\
&+ \mu (\phi_{i-1}^a \phi_i^a + \phi_{i-1}^b \phi_i^b) + 2\lambda_5 q_i^a \left[ \sum_{j \neq i} (q_j^a)^2 + (q_j^b)^2 \right] \\
&+ \frac{1}{2} \lambda_6 [q_{i-1}^a (\phi_{i-1}^a \phi_{i+1}^a + \phi_{i-1}^b \phi_{i+1}^b) - q_{i-1}^b (\phi_{i-1}^b \phi_{i+1}^a - \phi_{i-1}^a \phi_{i+1}^b)] \\
&+ \frac{1}{2} \lambda_6 [q_{i+1}^a (\phi_i^a \phi_{i+2}^a + \phi_i^b \phi_{i+2}^b) - q_{i+1}^b (\phi_i^b \phi_{i+2}^a - \phi_i^a \phi_{i+2}^b)], \tag{4.41}
\end{aligned}$$

and

$$\begin{aligned}
\frac{\partial V}{\partial q_i^b} = & 2M^2 q_i^b + 2\lambda_2 [(q_i^a)^2 + (q_i^b)^2] q_i^b + 2\lambda_3 q_i^b \left[ \sum_{j=1}^N (\phi_j^a)^2 + (\phi_j^b)^2 \right] \\
& + \mu (-\phi_{i-1}^b \phi_i^a + \phi_{i-1}^a \phi_i^b) + 2\lambda_5 q_i^b \left[ \sum_{j \neq i} (q_j^a)^2 + (q_j^b)^2 \right] \\
& + \frac{1}{2} \lambda_6 [-q_{i-1}^b (\phi_{i-1}^a \phi_{i+1}^a + \phi_{i-1}^b \phi_{i+1}^b) - q_{i-1}^a (\phi_{i-1}^b \phi_{i+1}^a - \phi_{i-1}^a \phi_{i+1}^b)] \\
& + \frac{1}{2} \lambda_6 [-q_{i+1}^b (\phi_i^a \phi_{i+2}^a + \phi_i^b \phi_{i+2}^b) - q_{i+1}^a (\phi_i^b \phi_{i+2}^a - \phi_i^a \phi_{i+2}^b)], \quad (4.42)
\end{aligned}$$

yielding for the VEVs in Eq. (4.37) the minimization condition

$$u \left[ M^2 + (\lambda_2 + (N-1)\lambda_5) u^2 + (N\lambda_3 + \frac{1}{2}\lambda_6) v^2 \right] + \frac{1}{2} \mu v^2 = 0, \quad (4.43)$$

and  $\langle \partial V / \partial q_i^b \rangle = 0$  is again satisfied for these VEVs. For large  $M \gg v$  and moderate  $N$  we obtain from Eq. (4.43) a naturally small value for  $u$  since [81]

$$u = \frac{m^2 \mu}{2[\lambda_1 + (N-1)\lambda_4] M^2} + \mathcal{O}(M^{-4}), \quad (4.44)$$

*i.e.*, the VEVs of the link variables are suppressed via the non-canonical or type-II seesaw mechanism [22, 82], which is employed in left-right-symmetric models to generate small neutrino masses. By substituting Eq. (4.44) into Eq. (4.40), one finds for the VEVs of the scalar site variables

$$v^2 = \frac{-m^2}{\lambda_1 + (N-1)\lambda_4} + \mathcal{O}(M^{-2}). \quad (4.45)$$

For the choice  $M \simeq 10^8 \dots 10^9$  GeV, we therefore obtain  $v \simeq 10^2$  GeV and a seesaw suppressed value  $u \simeq 10^{-1} \dots 10^{-3}$  eV of the inverse lattice spacing. The relevant mass and mixing terms of the untwisted fermion modes read

$$\mathcal{L}_{\text{mass}} = M_f \sum_{n=1}^N \left[ \bar{\Psi}_{nL} \left( \frac{Q_{n+1}^\dagger}{u} \Psi_{(n+1)R} - \Psi_{nR} \right) - \bar{\Psi}_{nR} \left( \Psi_{nL} - \frac{Q_n}{u} \Psi_{(n-1)L} \right) \right], \quad (4.46)$$

where  $M_f = u \simeq 10^{-2}$  eV. In the infrared, the Lagrangian in Eq. (4.46) gives identical KK towers for the left- and right-handed components and KK masses in the sub-eV range. If the bulk fermion is identified with a right-handed (SM singlet) neutrino, the KK masses are in the right range to allow for higher-dimensional neutrino oscillations [84].



## Chapter 5

# Summary and Conclusions

In this thesis, we have studied possibilities to obtain naturally the MSW LMA solution of the solar neutrino problem in models. Due to the connection of neutrino masses with GUT scale physics, it is particularly challenging to explore possible concepts which could predict the MSW LMA solution from first principles. In this respect, we have presented several models which highlight different phenomenological and model-building aspects.

Our first model, is based on an enlarged scalar sector and a collection of horizontal symmetries of the discrete and continuous type. Here, the leptons of the 2nd and 3rd generations are put into irreps of a discrete non-Abelian horizontal symmetry, which is defined in terms of the generators of the dihedral group  $\mathcal{D}_4$ . As a result, a vacuum alignment mechanism produces for the charged leptons and the neutrinos the mass matrix textures

$$\begin{pmatrix} \epsilon^3 & \epsilon^2 & \epsilon^4 \\ \epsilon^3 & \epsilon & \epsilon^2 \\ \epsilon^3 & \epsilon^2 & 1 \end{pmatrix} \quad \text{and} \quad \begin{pmatrix} \epsilon^2 & 1 & 1 \\ 1 & \epsilon^4 & \epsilon^4 \\ 1 & \epsilon^4 & \epsilon^4 \end{pmatrix},$$

respectively, where the small number  $\epsilon \simeq 10^{-1}$  parameterizes the horizontal symmetry breaking. In the neutrino mass matrix, the entries “1” are (to leading order) exactly degenerate due to the non-Abelian symmetry and the vacuum alignment mechanism, thereby implying that the atmospheric mixing angle  $\theta_{23}$  is close to maximal. The model predicts the hierarchical charged lepton mass spectrum, an inverse hierarchical neutrino mass spectrum, a large (but not necessarily close to maximal) solar mixing angle  $\theta_{12}$ , and a small reactor mixing angle  $\theta_{13}$ . Setting the Dirac  $\mathcal{CP}$ -violation phase  $\delta$  to zero, we have the relation  $\theta_{12} = \pi/4 - \theta_{13} + \mathcal{O}(\epsilon^2)$ , between the solar and the reactor mixing angle. In this case, the typical values for the mixing angles are

$$\theta_{12} \simeq 41^\circ, \quad \theta_{13} \simeq 4^\circ, \quad \text{and} \quad \theta_{23} \simeq 44^\circ,$$

where all dimensionless Yukawa couplings have been set equal to unity. A mild tuning of the order unity coefficients can give the values

$$\theta_{12} \simeq 37^\circ, \quad \theta_{13} \simeq 8^\circ, \quad \text{and} \quad \theta_{23} \simeq 44^\circ,$$

but the solar mixing angle is bounded from below by  $37^\circ \lesssim \theta_{12}$  and cannot get close to the best-fit value  $\theta_{12} \simeq 32^\circ$ . Hence, although the model generically gives a significant deviation from maximal solar mixing, this scheme still prefers a solar mixing angle, which seems to be somewhat too large.

The MSW LMA solution is obtained more comfortably in our second model for normal hierarchical neutrino masses. Here, we make use of a similar discrete non-Abelian flavor symmetry and vacuum alignment mechanism like in the inverse hierarchical model. Therefore, we also obtain an exactly maximal  $\nu_\mu$ - $\nu_\tau$ -mixing and the strict hierarchy  $m_\mu \ll m_\tau$  between the muon and the tau mass. In this model, however, the charges are elegantly organized in terms of deconstructed  $SU(m)$  gauge symmetries. The non-Abelian discrete symmetry is identified as a split extension of the Klein group  $Z_2 \times Z_2$  where the lift of every fermion and scalar representation is equivalent with  $\mathcal{D}_4$ . The charged lepton masses arise from Wilson-line type operators which correspond to  $SU(m)$  gauge theories compactified on the circle  $\mathcal{S}^1$ . Hence, the model gives the realistic charged lepton mass ratios  $m_e/m_\tau \simeq \lambda^6$  and  $m_\mu/m_\tau \simeq \lambda^2$ , where  $\lambda \simeq 0.22$  is the Wolfenstein parameter. As for the charged lepton mass matrix is diagonal here, the leptonic mixing angles stem exclusively from the neutrino sector. Enforced by the horizontal symmetries, the vacuum structure leads to a mass matrix squared of the left-handed neutrinos, which reads exactly

$$m_\nu^2 \begin{pmatrix} \rho^2 \epsilon^2 & \rho \epsilon^2 & -\rho \epsilon^2 \\ \rho \epsilon^2 & 1 + \epsilon^2 & 1 - \epsilon^2 \\ -\rho \epsilon^2 & 1 - \epsilon^2 & 1 + \epsilon^2 \end{pmatrix}, \quad \epsilon \simeq 1/\sqrt{N-1},$$

where  $\rho$  is an order unity parameter and  $N$  is the number of lattice sites of a dynamically generated  $\mathcal{S}^1/Z_2$  orbifold which is experienced by a right-handed Dirac neutrino. Actually, all  $\mathcal{CP}$  violation phases can be rotated into the right-handed sectors and hence we obtain the leptonic mixing angles

$$\theta_{12} = \arctan \left[ (2\sqrt{2})^{-1} \left( \rho^2 - 2 + \sqrt{(2-\rho)^2 + 8} \right) \right], \quad \theta_{13} = 0, \quad \theta_{23} = \pi/4.$$

In other words, the symmetries give exact predictions for the atmospheric and the reactor mixing angles while providing an order-of-magnitude-understanding of the solar mixing angle  $\theta_{12}$ , which is typically large but not necessarily close to maximal. To be specific, setting the real order unity parameter  $\rho$  to its most natural value  $\rho = 1$ , the model yields the solar mixing angle  $\theta_{12} = \arctan 1/\sqrt{2} \simeq 35^\circ$ . Note that this result is independent of  $N$ . Since the neutrinos exhibit a normal mass hierarchy through their mixing with the right-handed neutrino propagating in the latticized  $\mathcal{S}^1/Z_2$  orbifold, the ratio  $\Delta m_\odot^2/\Delta m_{\text{atm}}^2 \simeq 3/2(N-1)$  is suppressed by the discrete analog of the continuum theory volume factor. If the orbifold is characterized by a number of  $57 \pm 17$  lattice sites, the model yields without tuning of parameters the MSW LMA solution (LMA-I) of the solar neutrino problem within the 90% C.L. region.

A less predictive but more minimalistic approach to the MSW LMA solution is offered by a class of models which provide a dynamical origin of the seesaw mechanism in terms of deconstruction. In particular, we have demonstrated for a basic two-site model, that deconstruction can reproduce in an anomaly-free setup the dimension-five seesaw operator and maximal mixing angles when the inverse lattice spacing is identified with the seesaw scale. In realistic three- and four-site models we have given an explicit mechanism of how to break the individual lepton numbers down to the diagonal subgroup  $\bar{L} = L_e - L_\mu - L_\tau$  in the right-handed Majorana sector. The inclusion of non-renormalizable Wilson-line type operators corresponds to a soft breaking of the  $\bar{L}$  symmetry in the right-handed sector and generates the Dirac and Majorana neutrino mass matrix textures

$$M_D = \langle H \rangle \begin{pmatrix} 1 & \lambda^2 & \lambda^2 \\ \lambda^2 & 1 & \lambda^2 \\ \lambda^2 & \lambda^2 & 1 \end{pmatrix} \quad \text{and} \quad M_R = M_x \begin{pmatrix} \lambda & 1 & 1 \\ 1 & \lambda & \lambda \\ 1 & \lambda & \lambda \end{pmatrix},$$

where  $\lambda \simeq 0.22$  and  $M_x \simeq 10^{15}$  GeV is the GUT scale. By this, the bimaximal mixing characterizing the  $\bar{L}$  symmetry is transformed into the bilarge mixing as required by the MSW LMA solution, along with the appropriate solar and atmospheric mass squared differences.

When deconstruction is used as a calculational tool for higher-dimensional gauge theories, one usually assumes the number of replicated gauge groups to be large. A small number of gauge groups, however, may be more preferable when deconstruction is considered as a model building tool in four dimensions. Both views on deconstruction can be combined in a novel technique which we have applied to the relevant case of deconstructed large extra dimensions. Here, a replicated type-II seesaw mechanism has been used to generate lattice spacings in the sub-eV range. This allows to study the phenomenology of deconstructed sub-mm extra dimensions with a small number of  $\lesssim 10$  lattice sites. In this context, one may think, *e.g.*, of applications to higher-dimensional neutrino oscillations or Casimir energies in extra dimensions.

In total, we have seen that realistic and predictive models of lepton masses seem to require new and unconventional approaches to give naturally the MSW LMA solution from underlying symmetry principles. Exact predictions for mixing parameters are particularly challenging in the neutrino sector, where two mixing angles are large. Moreover, since neutrinos can be viewed as a window on GUT scale physics, the techniques which help to understand the MSW LMA solution may be of deeper significance for more fundamental theories. In this respect, the application of deconstruction to realistic neutrino mass models is especially interesting, since it could combine rigorous 4D GUT physics with the benefits of extra dimensions, which are expected to set the arena for a unification of all forces including gravity.

# Appendix A

## The Wilson-Dirac Action

In this appendix, we will first consider the usual 4D lattice formulation of a Dirac fermion before applying the construction to the transverse lattice description of a 5D fermion in the bulk.

### A.1 Four-dimensional lattice

In continuous Minkowski space-time the action for a massive four-component Dirac spinor  $\Psi(x)$  is given by

$$S = \int dx^4 \bar{\Psi}(x) (i\gamma^\mu \partial_\mu + m) \Psi(x). \quad (\text{A.1})$$

For our purposes it will prove convenient to work in the chiral (or Weyl) representation where the gamma matrices take the form

$$\gamma^0 = \begin{pmatrix} 0 & \mathbb{1} \\ \mathbb{1} & 0 \end{pmatrix}, \quad \vec{\gamma} = \begin{pmatrix} 0 & \vec{\sigma} \\ -\vec{\sigma} & 0 \end{pmatrix}, \quad \gamma_5 = i\gamma^0\gamma^1\gamma^2\gamma^3 = \begin{pmatrix} -\mathbb{1} & 0 \\ 0 & \mathbb{1} \end{pmatrix}, \quad (\text{A.2})$$

where  $\sigma^i$  ( $i = 1, 2, 3$ ) are the Pauli matrices. Then, the left- and right-handed chiral components of  $\Psi$  are given by  $\Psi_L = \frac{1}{2}(1 - \gamma_5)$  and  $\Psi_R = \frac{1}{2}(1 + \gamma_5)$ , respectively. The fermion field  $\Psi(x)$  is put on a 4D hypercubic lattice<sup>1</sup> by assigning a four-component Dirac spinor to each lattice point

$$x_\mu = n_\mu a_\mu, \quad n_\mu = 0, 1, \dots, N - 1 \quad (\mu = 0, 1, 2, 3), \quad (\text{A.3})$$

where  $a_\mu$  is the lattice spacing in direction  $\mu$ . In other words, we associate with each lattice site  $x \equiv (x_\mu)$  an independent four-component spinor variable  $\Psi(x)$ . For simplicity, we consider here the case of universal spatial lattice spacing  $a \equiv a_k$  ( $k = 1, 2, 3$ ) and allow only the lattice spacing in time direction to be different from  $a$ . Defining  $n \equiv (n_\mu) = (n_0, n_1, n_2, n_3)$ , it is then seen from Eq. (A.3) that  $x^0 = n_0 a_0$

---

<sup>1</sup>For a pedagogical introduction to quantum fields on a lattice see, *e.g.*, Ref. [86].

and  $\vec{x} = \vec{n}a$ , in which case one has the identification  $\Psi_n \equiv \Psi(x)$ . Now, we replace the derivatives of the continuum theory by the nearest neighbor forward and backward difference operators [87]

$$\partial_\mu \Psi(x) = \frac{1}{a_\mu} [\Psi(x + a\hat{\mu}) - \Psi(x)], \quad (\text{A.4a})$$

$$\partial_\mu^* \Psi(x) = \frac{1}{a_\mu} [\Psi(x) - \Psi(x - a\hat{\mu})], \quad (\text{A.4b})$$

where  $\hat{\mu}$  denotes the unit vector in direction  $\mu$ . With this definition, we obtain from Eq. (A.1) a naively discretized version of the Dirac action

$$\begin{aligned} S &= a_0 a^3 \sum_{n,\mu} \frac{1}{2} \bar{\Psi}(x) i\gamma^\mu (\partial_\mu^* + \partial_\mu) \Psi(x) + a_0 a^3 m \sum_n \bar{\Psi}(x) \Psi(x) \\ &= a_0 a^3 \sum_{n,\mu} \frac{1}{2a_\mu} \bar{\Psi}(x) i\gamma^\mu [\Psi(x + a_\mu \hat{\mu}) - \Psi(x - a_\mu \hat{\mu})] \\ &\quad + a_0 a^3 m \sum_n \bar{\Psi}(x) \Psi(x), \end{aligned} \quad (\text{A.5})$$

which we can also write more explicitly as

$$\begin{aligned} S &= a^3 \sum_n \left[ \frac{1}{2} \bar{\Psi}_n i\gamma^0 (\Psi_{n+\hat{0}} - \Psi_{n-\hat{0}}) \right. \\ &\quad \left. \sum_{k=1}^3 \frac{a_0}{2a} \bar{\Psi}_n i\gamma^k (\Psi_{n+\hat{k}} - \Psi_{n-\hat{k}}) + a_0 m \bar{\Psi}_n \Psi_n \right]. \end{aligned} \quad (\text{A.6})$$

We are now in a position to perform a Wick rotation

$$a_0 = |a_0| \exp(-i\varphi), \quad \varphi : 0 \longrightarrow \frac{\pi}{2}, \quad a_0 \longrightarrow -ia_4, \quad (\text{A.7})$$

where we have introduced  $a_4 \equiv |a_0|$ . This yields the Euclidean version of the action via  $iS \longrightarrow S_{\mathcal{I}}$  and we obtain (suppressing  $\mathcal{I}$ )

$$S = a^3 a_4 \sum_n \left[ \sum_{\mu=1}^4 \frac{1}{2a_\mu} \bar{\Psi}_n i\gamma_\mu (\Psi_{n+\hat{\mu}} - \Psi_{n-\hat{\mu}}) + m \bar{\Psi}_n \Psi_n \right], \quad (\text{A.8})$$

where we have defined  $n_4 \equiv n_0$ ,  $\hat{4} \equiv \hat{0}$ , and  $\gamma_4 = i\gamma^0$ . Unfortunately, the lattice version of the Dirac action in Eq. (A.8) describes  $2^4 = 16$  independent copies of the continuum fermion. This lattice artefact is called *fermion doubling* problem. The presence of the unwanted fermion doublers can be understood in terms of the triangle anomaly: for  $m = 0$  the UV divergence of the known  $\gamma_5$  anomaly is regulated on the lattice, which is achieved by the generation of pairs of fermions with opposite chirality [88]. There

exist several methods for ameliorating the doubling problem in QCD-like theories. We will consider here the widely used technique of Wilson [70], where the action is augmented by a momentum-dependent “mass term” which vanishes in the continuum limit  $a \rightarrow 0$ . This gives the fermion doublers a mass of the order of the UV cutoff and decouples them from continuum physics [86]. To this end, we substitute in Eq. (A.8) the fermion mass term via

$$\begin{aligned} m \sum_n \bar{\Psi}_n \Psi_n &\longrightarrow m \sum_n \bar{\Psi}_n \Psi_n - \frac{ar}{2} \sum_{n,\mu} \bar{\Psi}_n \partial_\mu^* \partial_\mu \Psi_n \\ &= m \sum_n \bar{\Psi}_n \Psi_n - \frac{ar}{2} \sum_{n,\mu} \frac{1}{a^2} \bar{\Psi}_n [(\Psi_{n+\hat{\mu}} - \Psi_n) - (\Psi_n - \Psi_{n-\hat{\mu}})] \\ &= \left(m + \frac{4r}{a}\right) \sum_n \bar{\Psi}_n \Psi_n - \frac{r}{2a} \sum_{n,\mu} \bar{\Psi}_n (\Psi_{n+\hat{\mu}} + \Psi_{n-\hat{\mu}}), \end{aligned} \quad (\text{A.9})$$

where  $r$  is an arbitrary parameter. Putting Eqs. (A.8) and (A.9) together, we obtain the Wilson-Dirac action

$$S = -a^3 a_4 \sum_n \left[ \sum_{\mu=1}^4 \bar{\Psi}_n \frac{r - i\gamma_\mu}{2} \Psi_{n+\hat{\mu}} + \bar{\Psi}_n \frac{r + i\gamma_\mu}{2} \Psi_{n-\hat{\mu}} - \left(m + \frac{4r}{a}\right) \bar{\Psi}_n \Psi_n \right]. \quad (\text{A.10})$$

In Eq. (A.10), Wilson’s choice  $r = 1$  [89] is of particular relevance, for, the operators  $\frac{1}{2}(1 \pm i\gamma_\mu)$  become orthogonal rank two projectors

$$\left(\frac{1}{2}(1 \pm i\gamma_\mu)\right)^2 = \frac{1}{2}(1 \pm i\gamma_\mu), \quad \text{Tr} \left(\frac{1}{2}(1 \pm i\gamma_\mu)\right) = 2, \quad (\text{A.11})$$

implying that part of the spinor field no longer propagates and one doubler per dimension is removed [90]. This treatment is also called Wilson’s projection operator technique. Let us now introduce gauge interactions on the lattice by assuming invariance under gauge transformations  $\Lambda(x)$ . The gauge covariant differentiation on the lattice requires the presence of a link variable  $\Phi(x, \mu)$  with values in the gauge group which transforms according to

$$\Phi(x, \mu) \rightarrow \Lambda(x)\Phi(x, \mu)\Lambda(x + a\hat{\mu})^{-1}, \quad (\text{A.12})$$

where we have, for clarity, assumed a uniform lattice spacing  $a_\mu \rightarrow a$ . Then, the gauge covariant difference operators are given by

$$\nabla_\mu \Psi(x) = \frac{1}{a} [\Phi(x, \mu)\Psi(x + a\hat{\mu}) - \Psi(x)], \quad (\text{A.13a})$$

$$\nabla_\mu^* \Psi(x) = \frac{1}{a} [\Psi(x) - \Phi(x - a\hat{\mu}, \mu)^{-1}\Psi(x - a\hat{\mu})]. \quad (\text{A.13b})$$

The description in terms of the gauge potentials  $A_\mu^a(x)$  of the continuum theory is exhibited by the parameterization

$$\Phi(x, \mu) = \exp(-iaA_\mu^a(x)T^a) = 1 - iaA_\mu^a(x)T^a + \dots, \quad (\text{A.14})$$

which also shows that the operators in Eqs. (A.13) indeed reduce to the covariant derivative  $D_\mu$  of the continuum theory in the limit  $a \rightarrow 0$ . The gauge invariant lattice fermion action  $S_F$  is found by replacing in Eq. (A.10) the derivatives by the covariant derivatives

$$S_F = \frac{a^4}{2} \sum_{x,\mu} \bar{\Psi}(x) [i\gamma_\mu (\nabla_\mu^* + \nabla_\mu) + 2m - a\nabla_\mu^* \nabla_\mu] \Psi(x), \quad (\text{A.15})$$

where we have chosen  $r = 1$ . Although Wilson's projection operator technique proves to be convenient for calculation, it has the drawback that in the limit  $m \rightarrow 0$  the chiral symmetry of the theory is explicitly broken by the addition of the large mass term  $\propto r/a$  to the action. However, a solution to this problem may be provided by methods involving renormalization-group "block-spin" transformations for fermions [91].

## A.2 Transverse lattice description of a 5D fermion

Consider a 5D Dirac field  $\Psi(x^\mu, x^5)$ , where  $x^5$  denotes the fifth dimension<sup>2</sup>. In the Weyl basis, one can decompose  $\Psi(x^\mu, x^5)$  as<sup>3</sup>

$$\Psi(x^\mu, x^5) = \begin{pmatrix} \Psi_L(x^\mu, x^5) \\ \Psi_R(x^\mu, x^5) \end{pmatrix}. \quad (\text{A.16})$$

If  $\Psi$  transforms according to the fundamental representation of a bulk  $SU(m)$  gauge symmetry, the Lagrangian is given by<sup>4</sup>

$$\mathcal{L} = \bar{\Psi} (i\gamma^\mu D_\mu - \gamma_5 D_5) \Psi - \frac{1}{4} \text{Tr} (F^{MN} F_{MN}), \quad (\text{A.17})$$

where the covariant derivative is  $D_M = \partial_M + ig_5 \hat{A}_M^a T^a$  and the gamma matrices have been defined in Eq. (A.2). In Ref. [35], the fermion Lagrangian for the aliphatic model of deconstructed extra dimensions has been motivated by the transverse lattice technique [68,69] applied to the 5th dimension. We shall now explicitly re-derive this result by applying the treatment of the 4D lattice theory in App. A.1 to a latticized 5th dimension with lattice spacing  $a \equiv a_5$ . For this purpose, let us discretize the bulk coordinate  $x^5$  in terms of

$$x^5 = na, \quad n = 0, 1, 2, \dots, \quad \frac{1}{\sqrt{a}} \Psi_n \equiv \Psi(x^5), \quad \frac{\Phi_n}{v} \equiv \Phi(x^5, 5), \quad (\text{A.18})$$

where the link variable  $\Phi_n$  becomes a non-linear  $\sigma$ -model field in the deconstructed theory and the factor  $1/v$  has been introduced for correct normalization. Note in

<sup>2</sup>We will denote here bulk coordinates by capital letters  $M, N = 0, 1, 2, 3, 5$ .

<sup>3</sup>For a discussion of Dirac neutrinos in the bulk see, *e.g.*, Refs. [83–85].

<sup>4</sup>We follow here the notation of Ref. [35].

Eq. (A.18) that the dimensionalities match, since  $\Psi(x^5)$  is a 5D spinor with  $[m]^2$  and  $\Psi_n$  is a 4D spinor with  $[m]^{3/2}$ . In analogy with App. A.1, we identify for a vanishing bare mass  $m = 0$  the 5D Dirac-Wilson operator of the transverse lattice with

$$D_W = \frac{1}{2} [-\gamma_5(\nabla_5^* + \nabla_5) - a\nabla_5^*\nabla_5], \quad (\text{A.19})$$

where  $\nabla_5$  and  $\nabla_5^*$  denote the covariant forward and backward derivatives, respectively. After integrating out the 5th dimension, we obtain from Eq. (A.19) the effective 4D Lagrangian  $\mathcal{L}_{\text{mass}}$  which generates the masses for the KK modes

$$\mathcal{L}_{\text{mass}} = \frac{1}{2a} \sum_n \bar{\Psi}_n [-\gamma_5(\nabla_5^* + \nabla_5) - a\nabla_5^*\nabla_5] \Psi_n. \quad (\text{A.20})$$

We assume here that the link-Higgs fields  $\Phi_n$  transform according to the bi-fundamental representation  $\Phi_n \subset (\bar{m}_{n-1}, m_n)$  of some product gauge symmetry  $\prod_{n=0}^N SU(m)_n$  and take universal VEVs  $\langle \Phi_n \rangle \equiv v$  at the deconstruction scale. The fermions  $\Psi_n$  transform according to the fundamental representation  $m_n$  of the corresponding gauge group  $SU(m)_n$ . Then,  $\nabla_5$  and  $\nabla_5^*$  can be written as

$$\nabla_5 \Psi_n = \frac{1}{a} \left[ \frac{\Phi_{n+1}^\dagger}{v} \Psi_{n+1} - \Psi_n \right], \quad \nabla_5^* \Psi_n = \frac{1}{a} \left[ \Psi_n - \frac{\Phi_n}{v} \Psi_{n-1} \right]. \quad (\text{A.21})$$

In Eq. (A.20), we therefore find for the first terms

$$\begin{aligned} \bar{\Psi}_n \gamma_5 (\nabla_5^* + \nabla_5) \Psi_n &= \bar{\Psi}_n^\dagger \gamma_0 \gamma_5 (\nabla_5^* + \nabla_5) \Psi_n \\ &= \frac{1}{a} (\bar{\Psi}_{nL} - \bar{\Psi}_{nR}) \left( \frac{\Phi_{n+1}^\dagger}{v} \Psi_{n+1} - \frac{\Phi_n}{v} \Psi_{n-1} \right) \\ &= \frac{1}{a} \left[ \bar{\Psi}_{nL} \left( \frac{\Phi_{n+1}^\dagger}{v} \Psi_{(n+1)R} - \frac{\Phi_n}{v} \Psi_{(n-1)R} \right) \right. \\ &\quad \left. - \bar{\Psi}_{nR} \left( \frac{\Phi_{n+1}^\dagger}{v} \Psi_{(n+1)L} - \frac{\Phi_n}{v} \Psi_{(n-1)L} \right) \right]. \end{aligned} \quad (\text{A.22})$$

Furthermore, in Eq. (A.20) it holds

$$\begin{aligned} \nabla_5^* \nabla_5 \Psi_n &= \frac{1}{a^2} \left[ \frac{\Phi_{n+1}^\dagger}{v} \Psi_{n+1} - \Psi_n - \frac{\Phi_n}{v} \left( \frac{\Phi_n^\dagger}{v} \Psi_n - \Psi_{n-1} \right) \right] \\ &= \frac{1}{a^2} \left[ \left( \frac{\Phi_{n+1}^\dagger}{v} \Psi_{n+1} - \Psi_n \right) - \left( \Psi_n - \frac{\Phi_n}{v} \Psi_{n-1} \right) \right], \end{aligned} \quad (\text{A.23})$$



where we have used that in the non-linear  $\sigma$ -model approximation  $\Phi_n/v$  can be represented as a unitary matrix. From Eq. (A.23) it follows that

$$\begin{aligned} \bar{\Psi}_n \nabla_5^* \nabla_5 \Psi_n &= \frac{1}{a^2} \left[ \bar{\Psi}_n \left( \frac{\Phi_{n+1}^\dagger}{v} \Psi_{n+1} - \Psi_n \right) - \bar{\Psi}_n \left( \Psi_n - \frac{\Phi_n}{v} \Psi_{n-1} \right) \right] \\ &= \frac{1}{a^2} \left[ \bar{\Psi}_{nL} \left( \frac{\Phi_{n+1}^\dagger}{v} \Psi_{(n+1)R} - 2\Psi_{nR} + \frac{\Phi_n}{v} \Psi_{(n-1)R} \right) \right. \\ &\quad \left. - \bar{\Psi}_{nR} \left( -\frac{\Phi_{n+1}^\dagger}{v} \Psi_{(n+1)L} + 2\Psi_{nL} - \frac{\Phi_n}{v} \Psi_{(n-1)L} \right) \right]. \end{aligned} \quad (\text{A.24})$$

Inserting Eqs. (A.22) and (A.24) into Eq. (A.20) one obtains

$$\mathcal{L}_{\text{mass}} = -\frac{1}{a} \sum_n \left[ \bar{\Psi}_{nL} \left( \frac{\Phi_{n+1}^\dagger}{v} \Psi_{(n+1)R} - \Psi_{nR} \right) - \bar{\Psi}_{nR} \left( \Psi_{nL} - \frac{\Phi_n}{v} \Psi_{(n-1)L} \right) \right]. \quad (\text{A.25})$$

Upon substituting  $-1/a \rightarrow M_f$ , we identify Eq. (A.25) with the mass and mixing terms of the aliphatic model for a fermion in a deconstructed 5D gauge theory [35].

# Appendix B

## The Dihedral Group $\mathcal{D}_4$

The dihedral groups  $\mathcal{D}_n$ , where  $n = 2, 3, \dots$ , are the point-symmetry groups with an  $n$ -fold axis (this is also called the *principal axis*) and a system of 2-fold axes at right angle to it. The group  $\mathcal{D}_n$  is therefore the symmetry group of a regular  $n$ -gon. These groups contain  $2n$  elements and for  $n > 2$  they are non-Abelian ( $\mathcal{D}_2$  is isomorphic with the Klein group  $Z_2 \times Z_2$ ). In Fig. B.1 the horizontal plane is shown for the case  $n = 4$ , where  $a, a', b$ , and  $b'$  denote the four two-fold axes and the 4-fold axis is perpendicular to the paper. We denote by  $C_n$  the operation of rotation through  $2\pi/n$  about the principal axis. The  $k$ -fold application of this transformation will be written as  $C_n^k$  and the identity transformation  $C_n^n$  as  $E$ . The rotations through  $\pi$  about the axes  $a, a', b$ , and  $b'$  will be referred to as  $C_a, C_{a'}, C_b$ , and  $C_{b'}$ , respectively. Then, the dihedral group  $\mathcal{D}_4$  has eight elements in following five classes:

$$E; \quad C_4, C_4^3; \quad C_4^2; \quad C_a, C_b; \quad C_{a'}, C_{b'}. \quad (\text{B.1})$$

Adopting the notation of Ref. [92] we will refer to the five classes which are associated with the sequence in Eq. (B.1) as  $E, C_4(2), C_4^2, C_2(2)$ , and  $C_2(2)$ . Calling the 4 irreducible singlet representations  $\mathbf{1}_A, \mathbf{1}_B, \mathbf{1}_C$ , and  $\mathbf{1}_D$  respectively, the decomposition

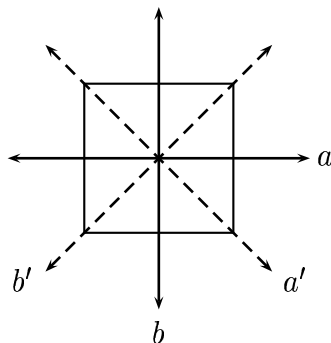


Figure B.1: Horizontal plane with the system of two-fold axes for  $\mathcal{D}_4$ .

$\mathcal{D}_4$	$E$	$C_4^2$	$C_4(2)$	$C_2(2)$	$C_{2'}(2)$
$\mathbf{1}_A$	1	1	1	1	1
$\mathbf{1}_B$	1	1	1	-1	-1
$\mathbf{1}_C$	1	1	-1	1	-1
$\mathbf{1}_D$	1	1	-1	-1	1
$\mathbf{2}$	2	-2	0	0	0

Table B.1: Character table for the group  $\mathcal{D}_4$ .

$\mathcal{D}_4$	$\mathbf{1}_A$	$\mathbf{1}_B$	$\mathbf{1}_C$	$\mathbf{1}_D$	$\mathbf{2}$
$\mathbf{1}_A$	$\mathbf{1}_A$	$\mathbf{1}_B$	$\mathbf{1}_C$	$\mathbf{1}_D$	$\mathbf{2}$
$\mathbf{1}_B$		$\mathbf{1}_A$	$\mathbf{1}_D$	$\mathbf{1}_C$	$\mathbf{2}$
$\mathbf{1}_C$			$\mathbf{1}_A$	$\mathbf{1}_B$	$\mathbf{2}$
$\mathbf{1}_D$				$\mathbf{1}_A$	$\mathbf{2}$

Table B.2: Multiplication table for the group  $\mathcal{D}_4$ .

of the product of the two-dimensional irrep  $\mathbf{2}$  reads

$$\mathbf{2} \times \mathbf{2} = \mathbf{1}_A + \mathbf{1}_B + \mathbf{1}_C + \mathbf{1}_D. \quad (\text{B.2})$$

The character table for the group  $\mathcal{D}_4$  is given in table B.1. Denoting  $\mathbf{2}$  as  $(a, b)$  we have for the singlet representations

$$\mathbf{1}_A = a_1 a_2 + b_1 b_2, \quad (\text{B.3a})$$

$$\mathbf{1}_B = a_1 b_2 - a_2 b_1, \quad (\text{B.3b})$$

$$\mathbf{1}_C = a_1 a_2 - b_1 b_2, \quad (\text{B.3c})$$

$$\mathbf{1}_D = a_1 b_2 + a_2 b_1. \quad (\text{B.3d})$$

From the character table of  $\mathcal{D}_4$  one determines the decomposition of the product of any two representations as shown in table B.2. In the vector representation of  $\mathcal{D}_4$ , the  $2 \times 2$  representation matrices corresponding to the different classes can be written

$(\mathcal{D}_4, T_1)$	$(C_4, d_1)$	$(C_4^3, d_2)$	$(C_4^2, d_3)$	$(C_a, d_4)$	$(C_b, d_5)$	$(C_{a'}, d_6)$	$(C_{b'}, d_7)$
$(C_4, d_1)$	$(C_4^2, d_3)$	$(E, e)$	$(C_4^3, d_2)$	$(C_{a'}, d_6)$	$(C_{b'}, d_7)$	$(C_b, d_5)$	$(C_a, d_4)$
$(C_4^3, d_2)$	$(E, e)$	$(C_4^2, d_3)$	$(C_4, d_1)$	$(C_{b'}, d_7)$	$(C_{a'}, d_6)$	$(C_a, d_4)$	$(C_b, d_5)$
$(C_4^2, d_3)$	$(C_4^3, d_2)$	$(C_4, d_1)$	$(E, e)$	$(C_b, d_5)$	$(C_a, d_4)$	$(C_{b'}, d_7)$	$(C_{a'}, d_6)$
$(C_a, d_4)$	$(C_{b'}, d_7)$	$(C_{a'}, d_6)$	$(C_b, d_5)$	$(E, e)$	$(C_4^2, d_3)$	$(C_4^3, d_2)$	$(C_4, d_1)$
$(C_b, d_5)$	$(C_{a'}, d_6)$	$(C_{b'}, d_7)$	$(C_a, d_4)$	$(C_4^2, d_3)$	$(E, e)$	$(C_4, d_1)$	$(C_4^3, d_2)$
$(C_{a'}, d_6)$	$(C_a, d_4)$	$(C_b, d_5)$	$(C_{b'}, d_7)$	$(C_4, d_1)$	$(C_4^3, d_2)$	$(E, e)$	$(C_4^2, d_3)$
$(C_{b'}, d_7)$	$(C_b, d_5)$	$(C_a, d_4)$	$(C_{a'}, d_6)$	$(C_4^3, d_2)$	$(C_4, d_1)$	$(C_4^2, d_3)$	$(E, e)$

Table B.3: Group table of the dihedral group  $\mathcal{D}_4$ . The brackets indicate the homomorphism  $\mathcal{D}_4 \simeq T_1$  between  $\mathcal{D}_4$  and the right transversal  $T_1 = \{e, d_1, \dots, d_7\}$  for  $\mathcal{K}_1$  (see Sec. 3.3.3).

as

$$\begin{aligned}
E & : D(E) = \begin{pmatrix} 1 & 0 \\ 0 & 1 \end{pmatrix}, \\
C_4(2) & : D(C_4) = \begin{pmatrix} 0 & 1 \\ -1 & 0 \end{pmatrix}, \quad D(C_4^3) = \begin{pmatrix} 0 & -1 \\ 1 & 0 \end{pmatrix}, \\
C_4^2 & : D(C_4^2) = \begin{pmatrix} -1 & 0 \\ 0 & -1 \end{pmatrix}, \\
C_2(2) & : D(C_a) = \begin{pmatrix} 1 & 0 \\ 0 & -1 \end{pmatrix}, \quad D(C_b) = \begin{pmatrix} -1 & 0 \\ 0 & 1 \end{pmatrix}, \\
C_{2'}(2) & : D(C_{a'}) = \begin{pmatrix} 0 & -1 \\ -1 & 0 \end{pmatrix}, \quad D(C_{b'}) = \begin{pmatrix} 0 & 1 \\ 1 & 0 \end{pmatrix}. \tag{B.4}
\end{aligned}$$

Before concluding this section, let us construct the dihedral groups from semi-direct products. For this purpose, let  $N \simeq Z_n$  for any  $n \in \mathbb{N}$ , let  $H \simeq Z_2$ , and let the map  $\varphi : H \rightarrow \text{Aut}(N)$  send  $h \in H$  to the automorphism in  $\text{Aut}(N)$  sending each element of  $N$  to its inverse. Then, the external semi-direct product  $N \rtimes_{\varphi} H$  of  $N$  by  $H$  with respect to  $\varphi$  is the dihedral group  $\mathcal{D}_n$ . One can also define the *infinite dihedral group*  $\mathcal{D}_{\infty} = N \rtimes_{\varphi} H$ , where  $N \simeq Z$  and the group  $H$  and the map  $\varphi$  are as above.

## Appendix C

# Minimization of the Tree-Level Potential

We will rewrite the potential  $V_A(\Phi, \Omega)$  in Eqs. (2.15) and (3.36) in terms of the parameterization in Eqs. (2.13) and (3.35) as follows

$$V_A = d_1 v_1^4 c_\alpha^2 s_\alpha^2 + d_2 v_2^4 c_\beta^2 s_\beta^2 + d_3 v_1^2 v_2^2 (c_\alpha^2 - s_\alpha^2)(c_\beta^2 - s_\beta^2), \quad (\text{C.1})$$

where  $s_\alpha \equiv \sin(\alpha)$  and  $c_\alpha \equiv \cos(\alpha)$  (correspondingly for  $\beta$ ). Hence, it is

$$\frac{\partial V_A}{\partial \alpha} = 2d_1 v_1^4 (c_\alpha^3 s_\alpha - c_\alpha s_\alpha^3) - 4d_3 v_1^2 v_2^2 c_\alpha s_\alpha (c_\beta^2 - s_\beta^2),$$

$$\frac{\partial V_A}{\partial \beta} = 2d_2 v_2^4 (c_\beta^3 s_\beta - c_\beta s_\beta^3) - 4d_3 v_1^2 v_2^2 c_\beta s_\beta (c_\alpha^2 - s_\alpha^2).$$

As a result, at  $(\alpha, \beta) = (\frac{\pi}{4}, \frac{\pi}{4})$  it is  $(\partial_\alpha, \partial_\beta)V_A = (0, 0)$ , *i.e.*,  $(\alpha, \beta) = (\frac{\pi}{4}, \frac{\pi}{4})$  is an extremum of the potential  $V_A$ . For the second derivatives it follows

$$\frac{\partial^2 V_A}{\partial \alpha^2} = 2d_1 v_1^4 (s_\alpha^4 + c_\alpha^4 - 6c_\alpha^2 s_\alpha^2) - 4d_3 v_1^2 v_2^2 (c_\alpha^2 - s_\alpha^2)(c_\beta^2 - s_\beta^2),$$

$$\frac{\partial^2 V_A}{\partial \beta^2} = 2d_2 v_2^4 (s_\beta^4 + c_\beta^4 - 6c_\beta^2 s_\beta^2) - 4d_3 v_1^2 v_2^2 (c_\beta^2 - s_\beta^2)(c_\alpha^2 - s_\alpha^2),$$

$$\frac{\partial^2 V_A}{\partial \alpha \partial \beta} = 16d_3 v_1^2 v_2^2 c_\alpha s_\alpha c_\beta s_\beta.$$

At  $(\alpha, \beta) = (\frac{\pi}{4}, \frac{\pi}{4})$  we therefore obtain for the matrix of second derivatives of the potential

$$\begin{pmatrix} \frac{\partial^2 V_A}{\partial \alpha^2} & \frac{\partial^2 V_A}{\partial \alpha \partial \beta} \\ \frac{\partial^2 V_A}{\partial \alpha \partial \beta} & \frac{\partial^2 V_A}{\partial \beta^2} \end{pmatrix} = \begin{pmatrix} -2d_1 v_1^4 & 4d_3 v_1^2 v_2^2 \\ 4d_3 v_1^2 v_2^2 & -2d_2 v_2^4 \end{pmatrix}, \quad (\text{C.2})$$

where, due to the choice  $d_1, d_2 < 0$ , the diagonal elements are positive. Hence, if the parameters obey the conditions

$$d_1, d_2 < 0 \quad \text{and} \quad d_1 d_2 > 4d_3^2, \quad (\text{C.3})$$

the matrix in Eq. (C.2) is positive definite, *i.e.*, the scalar excitations which oscillate in the  $(\alpha, \beta)$ -subspace about  $(\alpha, \beta) = (\frac{\pi}{4}, \frac{\pi}{4})$  have positive masses and  $(\alpha, \beta) = (\frac{\pi}{4}, \frac{\pi}{4})$  is a minimum of the scalar potential  $V_A$ . Let us now rewrite the part of the multi-scalar potential  $V_B(\Phi, \Omega)$  in Eqs. (2.15) and (3.36) using the parameterization in Eqs. (2.13) and (3.35) as follows

$$\begin{aligned} V_B = & 2d_4v_1^4c_\alpha^2s_\alpha^2\cos(2\varphi) + 2d_5v_2^4c_\beta^2s_\beta^2\cos(2\psi) \\ & + 4d_6v_1^2v_2^2c_\alpha s_\alpha c_\beta s_\beta \cos(\varphi) \cos(\psi) \\ & - 4d_7v_1^2v_2^2c_\alpha s_\alpha c_\beta s_\beta \sin(\varphi) \sin(\psi), \end{aligned} \quad (\text{C.4})$$

where we have used the notation of Eq. (C.1). Hence, one concludes

$$\begin{aligned} \frac{\partial V_B}{\partial \alpha} &= 4d_4v_1^4(c_\alpha^3s_\alpha - c_\alpha s_\alpha^3) \cos(2\varphi) + 4d_6v_1^2v_2^2(c_\alpha^2 - s_\alpha^2)c_\beta s_\beta \cos(\varphi) \cos(\psi) \\ &\quad - 4d_7v_1^2v_2^2(c_\alpha^2 - s_\alpha^2)c_\beta s_\beta \sin(\varphi) \sin(\psi), \\ \frac{\partial V_B}{\partial \beta} &= 4d_5v_2^4(c_\beta^3s_\beta - c_\beta s_\beta^3) \cos(2\psi) + 4d_6v_1^2v_2^2(c_\beta^2 - s_\beta^2)c_\alpha s_\alpha \cos(\varphi) \cos(\psi) \\ &\quad - 4d_7v_1^2v_2^2(c_\beta^2 - s_\beta^2)c_\alpha s_\alpha \sin(\varphi) \sin(\psi), \end{aligned}$$

and

$$\begin{aligned} \frac{\partial V_B}{\partial \varphi} &= -4d_4v_1^4c_\alpha^2s_\alpha^2\sin(2\varphi) - 4d_6v_1^2v_2^2c_\alpha s_\alpha c_\beta s_\beta \sin(\varphi) \cos(\psi) \\ &\quad - 4d_7v_1^2v_2^2c_\alpha s_\alpha c_\beta s_\beta \cos(\varphi) \sin(\psi), \\ \frac{\partial V_B}{\partial \psi} &= -4d_5v_2^4c_\beta^2s_\beta^2\sin(2\psi) - 4d_6v_1^2v_2^2c_\alpha s_\alpha c_\beta s_\beta \cos(\varphi) \sin(\psi) \\ &\quad - 4d_7v_1^2v_2^2c_\alpha s_\alpha c_\beta s_\beta \sin(\varphi) \cos(\psi). \end{aligned}$$

As a result, at the points  $(\alpha, \beta) = (\frac{\pi}{4}, \frac{\pi}{4})$ , where  $\varphi, \psi \in \{0, \pi\}$ , it is

$$(\partial_\alpha, \partial_\beta, \partial_\varphi, \partial_\psi)V_B = (0, 0, 0, 0),$$

*i.e.*, these points are extrema of  $V_B$ . Furthermore, one finds at  $(\alpha, \beta) = (\frac{\pi}{4}, \frac{\pi}{4})$  vanishing mixed second derivatives

$$\frac{\partial^2 V_B}{\partial \varphi \partial \alpha} = \frac{\partial^2 V_B}{\partial \psi \partial \alpha} = \frac{\partial^2 V_B}{\partial \varphi \partial \beta} = \frac{\partial^2 V_B}{\partial \psi \partial \beta} = 0,$$

implying that the matrix of the second derivatives of  $V_B$  with respect to the parameters  $\alpha, \beta, \varphi, \psi$  breaks up into a block-diagonal form with submatrices which respectively correspond to the subspaces  $(\alpha, \beta)$  and  $(\varphi, \psi)$ . The second derivatives of  $V_B$

with respect to  $\alpha$  and  $\beta$  are

$$\begin{aligned}\frac{\partial^2 V_B}{\partial \alpha^2} &= 4d_4 v_1^4 (s_\alpha^4 + c_\alpha^4 - 6c_\alpha^2 s_\alpha^2) \cos(2\varphi) - 16d_6 v_1^2 v_2^2 c_\alpha s_\alpha c_\beta s_\beta \cos(\varphi) \cos(\psi) \\ &\quad + 16d_7 v_1^2 v_2^2 c_\alpha s_\alpha c_\beta s_\beta \sin(\varphi) \sin(\psi), \\ \frac{\partial^2 V_B}{\partial \beta^2} &= 4d_5 v_2^4 (s_\beta^4 + c_\beta^4 - 6c_\beta^2 s_\beta^2) \cos(2\psi) - 16d_6 v_1^2 v_2^2 c_\alpha s_\alpha c_\beta s_\beta \cos(\varphi) \cos(\psi) \\ &\quad + 16d_7 v_1^2 v_2^2 c_\alpha s_\alpha c_\beta s_\beta \sin(\varphi) \sin(\psi), \\ \frac{\partial^2 V_B}{\partial \alpha \partial \beta} &= 4d_6 v_1^2 v_2^2 (c_\alpha^2 - s_\alpha^2)(c_\beta^2 - s_\beta^2) \cos(\varphi) \cos(\psi) \\ &\quad - 4d_7 v_1^2 v_2^2 (c_\alpha^2 - s_\alpha^2)(c_\beta^2 - s_\beta^2) \sin(\varphi) \sin(\psi).\end{aligned}$$

Therefore, at the points  $(\alpha, \beta) = (\frac{\pi}{4}, \frac{\pi}{4})$ , where  $\varphi, \psi \in \{0, \pi\}$ , the matrix of the second order derivatives is

$$\left( \frac{\partial^2 V_B}{\partial \alpha \partial \beta} \right) = 4 \begin{pmatrix} -d_4 v_1^4 - \sigma d_6 v_1^2 v_2^2 & 0 \\ 0 & -d_5 v_2^4 - \sigma d_6 v_1^2 v_2^2 \end{pmatrix}, \quad (\text{C.5})$$

where  $\sigma \equiv \cos(\varphi) \cos(\psi) = \pm 1$  can take either sign for  $\varphi, \psi \in \{0, \pi\}$ . However, from Eq. (C.4) it is seen that the product  $d_6 \sigma$  must be negative in the lowest energy state, *i.e.*, the sign of  $d_6$  determines whether  $\varphi = \psi + k \cdot 2\pi$  or  $\varphi = \psi + k \cdot \pi$  for some integer  $k$ . The matrix of second order derivatives can therefore be rewritten as

$$\left( \frac{\partial^2 V_B}{\partial \alpha \partial \beta} \right) = 4 \begin{pmatrix} -d_4 v_1^4 + |d_6| v_1^2 v_2^2 & 0 \\ 0 & -d_5 v_2^4 + |d_6| v_1^2 v_2^2 \end{pmatrix}, \quad (\text{C.6})$$

where  $d_4, d_5 < 0$ , *i.e.*, the matrix is positive definite. The second derivatives of  $V_B$  with respect to  $\varphi$  and  $\psi$  are

$$\begin{aligned}\frac{\partial^2 V_B}{\partial \varphi^2} &= -8d_4 v_1^4 c_\alpha^2 s_\alpha^2 \cos(2\varphi) \\ &\quad - 4d_6 v_1^2 v_2^2 c_\alpha s_\alpha c_\beta s_\beta \cos(\varphi) \cos(\psi) + 4d_7 v_1^2 v_2^2 c_\alpha s_\alpha c_\beta s_\beta \sin(\varphi) \sin(\psi), \\ \frac{\partial^2 V_B}{\partial \psi^2} &= -8d_5 v_2^4 c_\beta^2 s_\beta^2 \cos(2\psi) \\ &\quad - 4d_6 v_1^2 v_2^2 c_\alpha s_\alpha c_\beta s_\beta \cos(\varphi) \cos(\psi) + 4d_7 v_1^2 v_2^2 c_\alpha s_\alpha c_\beta s_\beta \sin(\varphi) \sin(\psi), \\ \frac{\partial^2 V_B}{\partial \psi \partial \varphi} &= 4d_6 v_1^2 v_2^2 c_\alpha s_\alpha c_\beta s_\beta \sin(\varphi) \sin(\psi) - 4d_7 v_1^2 v_2^2 c_\alpha s_\alpha c_\beta s_\beta \cos(\varphi) \cos(\psi).\end{aligned}$$

At the points  $(\alpha, \beta) = (\frac{\pi}{4}, \frac{\pi}{4})$ , where  $\varphi, \psi \in \{0, \pi\}$ , the matrix of the second derivatives of  $V_B$  with respect to  $\varphi$  and  $\psi$  reads

$$\left( \frac{\partial^2 V_B}{\partial \varphi \partial \psi} \right) = \begin{pmatrix} -2d_4 v_1^4 + |d_6| v_1^2 v_2^2 & \pm d_7 v_1^2 v_2^2 \\ \pm d_7 v_1^2 v_2^2 & -2d_5 v_2^4 + |\sigma| d_6 v_1^2 v_2^2 \end{pmatrix}, \quad (\text{C.7})$$

where  $d_4, d_5 < 0$ , *i.e.*, the diagonal elements are positive. In Eq. (C.7), we have already used that the potential is minimized when  $d_6\sigma$  is negative. Taking everything into account, if the coefficients in the multi-scalar potential satisfy besides Eq. (C.3) also the conditions

$$d_4, d_5 < 0 \quad \text{and} \quad (-2d_4v_1^4 + |d_6|v_1^2v_2^2)(-2d_5v_2^4 + |d_6|v_1^2v_2^2) > d_7^2v_1^4v_2^4, \quad (\text{C.8})$$

then the matrix in Eq. (C.7) is positive definite, *i.e.*, all modes oscillating in the  $(\alpha, \beta, \varphi, \psi)$ -subspace about the points  $(\alpha, \beta) = (\frac{\pi}{4}, \frac{\pi}{4})$ , where  $\varphi, \psi \in \{0, \pi\}$ , have positive masses and hence these points are indeed local minima of both the potentials  $V_A$  and  $V_B$ . In the special case  $\Phi = \Omega$ , one can, without loss of generality, choose in  $V_A(\Phi, \Phi)$  and  $V_B(\Phi, \Phi)$  the parameters  $d_2 = d_3 = 0$  and  $d_5 = d_6 = d_7 = 0$ , *i.e.*, only  $d_1$  and  $d_4$  are in general nonzero. If, for this choice of potentials, the conditions

$$d_1 < 0 \quad \text{and} \quad d_4 < 0, \quad (\text{C.9})$$

are satisfied, the points  $(\alpha, \varphi) \in \{(\frac{\pi}{4}, 0), (\frac{\pi}{4}, \pi)\}$  minimize  $V_\Delta(\Phi, \Phi)$ .

Let us now extend the above discussion to a number of  $N$  scalar  $\mathcal{G}$ -doublets, each of which is parameterized in a self-explanatory notation by the angles  $(\alpha_i, \varphi_i)$ , where  $i = 1, \dots, N$ . We denote by  $V_\Delta(i, j)$  the most general scalar interaction which involves only the scalars parameterized by  $(\alpha_i, \varphi_i)$  and  $(\alpha_j, \varphi_j)$  and breaks the associated  $SU(2)_{\text{acc}}$  symmetries. Clearly,  $V_\Delta(i, j)$  has a structure similar to  $V_\Delta(\Phi, \Omega)$  and we can also decompose in analogy with  $V_\Delta(\Phi, \Omega) = V_A(\Phi, \Omega) + V_B(\Phi, \Omega)$  the operator  $V_\Delta(i, j)$  as  $V_\Delta(i, j) = V_A(i, j) + V_B(i, j)$ . Moreover, we assume that the symmetry content of our model (*e.g.*, the gauge symmetries corresponding to the Wilson loops) allow us to write the total renormalizable  $SU(2)_{\text{acc}}$  symmetry breaking part of the scalar potential  $V_\Delta$  as a sum of the operators  $V_\Delta(i, j)$ , *i.e.*, we have<sup>1</sup>

$$V_\Delta = \frac{1}{2} \sum_{i,j=1}^N V_\Delta(i, j), \quad V_A = \frac{1}{2} \sum_{i,j=1}^N V_A(i, j), \quad V_B = \frac{1}{2} \sum_{i,j=1}^N V_B(i, j),$$

where we can set  $V_A(i, j) = V_A(j, i)$  and  $V_B(i, j) = V_B(j, i)$ . We define the real and symmetric  $N \times N$  matrices of second derivatives

$$M_A(N) \equiv \frac{\partial^2 V_A}{\partial \alpha_i \partial \alpha_j} \quad \text{and} \quad M_B(N) \equiv \frac{\partial^2 V_B}{\partial \varphi_i \partial \varphi_j} \quad (i, j = 1, \dots, N), \quad (\text{C.10})$$

each of which is a function of the  $2N$  parameters  $(\alpha_i, \varphi_i)$ . Now, consider an extremum  $(\alpha_i^{\text{ex}}, \varphi_i^{\text{ex}})$  ( $i = 1, \dots, N$ ) of  $V_\Delta$ . We suppose that at the extremum the  $(N-1) \times (N-1)$ -dimensional submatrices  $M_A(N-1)$  and  $M_B(N-1)$  of  $M_A(N)$  and  $M_B(N)$  are positive definite. Moreover, let us assume that the  $2 \times 2$  matrices

$$\begin{pmatrix} \frac{\partial^2 V_A(i, N)}{\partial \alpha_i \partial \alpha_i} & \frac{\partial^2 V_A(i, N)}{\partial \alpha_i \partial \alpha_N} \\ \frac{\partial^2 V_A(i, N)}{\partial \alpha_N \partial \alpha_i} & \frac{\partial^2 V_A(i, N)}{\partial \alpha_N \partial \alpha_N} \end{pmatrix} \quad \text{and} \quad \begin{pmatrix} \frac{\partial^2 V_B(i, N)}{\partial \varphi_i \partial \varphi_i} & \frac{\partial^2 V_B(i, N)}{\partial \varphi_i \partial \varphi_N} \\ \frac{\partial^2 V_B(i, N)}{\partial \varphi_N \partial \varphi_i} & \frac{\partial^2 V_B(i, N)}{\partial \varphi_N \partial \varphi_N} \end{pmatrix}, \quad (\text{C.11})$$

<sup>1</sup>The factor  $\frac{1}{2}$  has been introduced to avoid double-counting.



where  $i = 1, \dots, N - 1$ , are all positive definite. Then,  $M_A(N)$ , for example, can be written as (correspondingly for  $M_B(N)$ )

$$M_A(N) = \left( \begin{array}{c|c} M_A(N-1) & \begin{matrix} 0 \\ \vdots \\ 0 \end{matrix} \\ \hline \begin{matrix} 0 & \dots & 0 \end{matrix} & 0 \end{array} \right) + \begin{pmatrix} m_{11} & 0 & 0 & \dots & m_{1N} \\ 0 & m_{22} & 0 & \dots & m_{2N} \\ 0 & 0 & m_{33} & \dots & m_{3N} \\ \vdots & \vdots & \vdots & \ddots & \vdots \\ m_{N1} & m_{N2} & m_{N3} & \dots & m_{NN} \end{pmatrix}. \quad (\text{C.12})$$

Consider now an arbitrary  $N$ -component column-vector  $\vec{x} \equiv (x_i)$ . For the product  $\vec{x}^T M_A(N) \vec{x}$ , the first matrix in Eq. (C.12) yields a positive number, since  $M_A(N-1)$  is by assumption positive definite. Hence, it follows

$$\vec{x}^T M_A(N) \vec{x} > \sum_{i=1}^{N-1} \left( m_{ii} x_i^2 + 2m_{iN} x_i x_N + \frac{\partial^2 V_A(i, N)}{\partial \alpha_N \partial \alpha_N} x_N^2 \right), \quad (\text{C.13})$$

where we have used that  $m_{iN} = m_{Ni}$ . Note in Eq. (C.13), that

$$m_{NN} = \sum_{i=1}^{N-1} \frac{\partial^2 V_A(i, N)}{\partial \alpha_N \partial \alpha_N}. \quad (\text{C.14})$$

Then, by positive definiteness of the  $2 \times 2$  matrices in Eq. (C.11), we see that each bracket in Eq. (C.13) is positive-valued. Therefore,  $\vec{x}^T M_A(N) \vec{x}$  is positive for any  $\vec{x}$ , implying that  $M_A(N)$  is actually positive definite. In total, this shows that for  $M_A(N)$  and  $M_B(N)$  to be positive definite at  $(\alpha_i^{\text{ex}}, \varphi_i^{\text{ex}})$  ( $i = 1, \dots, N$ ), it is sufficient to assume that all  $2 \times 2$  matrices

$$\begin{pmatrix} \frac{\partial^2 V_A(i, j)}{\partial \alpha_i \partial \alpha_i} & \frac{\partial^2 V_A(i, j)}{\partial \alpha_i \partial \alpha_j} \\ \frac{\partial^2 V_A(i, j)}{\partial \alpha_j \partial \alpha_i} & \frac{\partial^2 V_A(i, j)}{\partial \alpha_j \partial \alpha_j} \end{pmatrix} \quad \text{and} \quad \begin{pmatrix} \frac{\partial^2 V_B(i, j)}{\partial \varphi_i \partial \varphi_i} & \frac{\partial^2 V_B(i, j)}{\partial \varphi_i \partial \varphi_j} \\ \frac{\partial^2 V_B(i, j)}{\partial \varphi_j \partial \varphi_i} & \frac{\partial^2 V_B(i, j)}{\partial \varphi_j \partial \varphi_j} \end{pmatrix}, \quad (\text{C.15})$$

for  $i, j = 1, \dots, N$ , are positive definite. In other words, to find the minimum of the total  $SU(2)_{\text{acc}}$  symmetry breaking part  $V_\Delta$ , it is sufficient to minimize each of the potentials  $V_\Delta(i, j)$  individually.



# Acknowledgments

First of all, I would like to thank Prof. Manfred Lindner for the scientific education and the freedom he gave me in following my interests. I owe a lot to his admirable flexibility and abilities in all kinds of fields. Next, I thank Tommy Ohlsson for his friendship, his help over the years and his invitations to Stockholm. Furthermore, I thank Florian Bauer for the scientific collaboration, his help in technical problems, the exchange of ideas and the nice atmosphere in our office. In addition, I thank K.R.S. Balaji for the various stimulating discussions, his enthusiasm in developing projects and for proof-reading. Also, I would like to thank Martin Freund for his willing to help. Generally, I thank the group for their kindness and cooperation. Finally, I thank my mother for making my studies and this work possible.

Garching, June 2003

Gerhart Seidl

# Bibliography

- [1] T. Kaluza, *Sitzungsber. Preuss. Akad. Wiss. Berlin K1* (1921) 966; O. Klein, *Z. Phys.* 37 (1926) 895.
- [2] J. Scherk and J.H. Schwarz, *Phys. Lett. B* 82 (1979) 60; *Nucl. Phys. B* 153 (1979) 61; E. Witten, *Nucl. Phys. B* 258 (1985); P. Candelas, G. T. Horowitz, A. Strominger, and E. Witten, *Nucl. Phys. B* 258 (1985) 46; L. Dixon, J. Harvey, C. Vafa, and E. Witten, *Nucl. Phys. B* 261 (1985) 651.
- [3] N. Arkani-Hamed, S. Dimopoulos, and G. Dvali, *Phys. Lett. B* 429 (1998) 263; I. Antoniadis, N. Arkani-Hamed, S. Dimopoulos, and G. Dvali, *Phys. Lett. B* 436 (1998) 257; N. Arkani-Hamed, S. Dimopoulos, and G. Dvali, *Phys. Rev D* 59 (1999) 086004.
- [4] N. S. Manton, *Nucl. Phys. B* 158 (1979), 141; D. B. Fairlie, *J. Phys. G* 5 (1997) L55; *Phys. Lett. B* 82 (1979) 97; G. Chapline and R. Slansky, *Nucl. Phys. B* 209 (1982) 461; Y. Hosotani, *Phys. Lett. B* 126 (1983) 309, *Phys. Lett. B* 129 (1983) 193; L. J. Hall, H. Murayama, and Y. Nomura, *Nucl. Phys. B* 645 (2002) 85; R. Dermisek, S. Raby, and S. Nandi, *Nucl. Phys. B* 641 (2002), 327.
- [5] C. Wetterich, *Nucl. Phys. B* 260 (1985) 402; A. Strominger, *Phys. Rev. Lett.* 55 (1985) 2547; A. Strominger and E. Witten, *Commun. Math. Phys.* 101 (1985) 341; J. Bijnens and C. Wetterich, *Phys. Lett. B* 199 (1987) 525.
- [6] N. Cabibbo, *Phys. Rev. Lett.* 10 (1963) 531; M. Kobayashi, T. Maskawa, *Prog. Theor. Phys.* 49 (1973) 652.
- [7] Z. Maki, M. Nakagawa, and S. Sakata, *Prog. Theor. Phys.* 28 (1962) 870.
- [8] R. Barbieri, L. J. Hall, and A. Romanino, *Phys. Lett. B* 401 (1997) 47; R. Barbieri, P. Creminelli, and A. Romanino, *Nucl. Phys. B* 559 (1999) 17; P. H. Frampton and Adrija Rašin, *Phys. Lett. B* 478 (2000) 424; Z. Berezhiani and A. Rossi, *J. High Energy Phys.* 9903 (1999) 002; T. Blažek, S. Raby, and K. Tobe, *Phys. Rev. D* 62 (2000) 055001; A. Aranda, C. D. Carone, and R. F. Lebed, *Phys. Lett. B* 474 (2000) 170; A. Aranda, C. D. Carone, and R. F. Lebed, *Phys. Rev. D* 62 (2000) 016009.

- [9] Super-Kamiokande Collaboration, S. Fukuda, et al., Phys. Rev. Lett. 86 (2001) 5651; Super-Kamiokande Collaboration, S. Fukuda, et al., Phys. Lett. B 539 (2002) 179.
- [10] SNO Collaboration, Q. R. Ahmad, et al., Phys. Rev. Lett. 87 (2001) 071301; SNO Collaboration, Q. R. Ahmad, et al., Phys. Rev. Lett. 89 (2002) 011302.
- [11] Super-Kamiokande Collaboration, Y. Fukuda, et al., Phys. Rev. Lett. 81 (1998) 1562; Super-Kamiokande Collaboration, S. Fukuda, et al., Phys. Rev. Lett. 85 (2000) 3999; Super-Kamiokande Collaboration, T. Toshito, et al., [hep-ex/0105023](#).
- [12] KamLAND Collaboration, K. Eguchi, et al., Phys. Rev. Lett. 90 (2003) 021802.
- [13] S. P. Mikheyev and A. Y. Smirnov, Yad. Fiz. 42 (1985) 1441; S. P. Mikheyev and A. Y. Smirnov, Nuovo Cimento C 9 (1986) 17; L. Wolfenstein, Phys. Rev. D 17 (1978) 2369.
- [14] V. Barger and D. Marfatia, Phys. Lett. B 555 (2003) 144; G. L. Fogli, E. Lisi, D. Montanino, A. Palazzo, and A. M. Rotunno, Phys. Rev. D 67 (2003) 073002; M. Maltoni, T. Schwetz, and J. W. F. Valle, Phys. Rev. D 67 (2003) 093003; J. N. Bahcall, M. C. Gonzalez-Garcia, and C. Peña-Garay, J. High Energy Phys. 0302 (2003) 009; P. C. de Holanda and A. Y. Smirnov, JCAP 0302 (2003) 001.
- [15] CHOOZ Collaboration, M. Apollonio, et al., Phys. Lett. B 420 (1998) 397; CHOOZ Collaboration, M. Apollonio, et al., Phys. Lett. B 466 (1999) 415.
- [16] C. L. Bennett, et al., [astro-ph/0302207](#).
- [17] Ø. Elgarøy, et al., Phys. Rev. Lett. 89 (2002) 061301.
- [18] D. N. Spergel, et al., [astro-ph/0302209](#).
- [19] E. Witten, Nucl. Phys. Proc. Suppl. 91 (2000) 3.
- [20] T. Yanagida, in *Proceedings of the Workshop on the Unified Theory and Baryon Number in the Universe*, edited by O. Sawada and A. Sugamoto (KEK, Tsukuba, 1979), p. 79.
- [21] M. Gell-Mann, P. Ramond and R. Slansky, *Complex Spinors and Unified Theories*, in *Supergravity*, Proceedings of the Workshop on Supergravity, Stony Brook, New York, 1979, edited by P. van Nieuwenhuizen and D.Z. Freedman (North-Holland, Amsterdam, 1979), p. 315.
- [22] R. N. Mohapatra and G. Senjanović, Phys. Rev. Lett. 44 (1980) 912.

- [23] J. K. Elwood, N. Irges, and P. Ramond, *Phys. Rev. Lett* 81 (1998) 5064; N. Irges, S. Lavignac, and P. Ramond, *Phys. Rev. D* 58 (1998) 035003; F. S. Ling and P. Ramond, *Phys. Lett. B* 543 (2002) 29; Q. Shafi and Z. Tavartkiladze, *Phys. Lett. B* 459 (1999) 563; Q. Shafi and Z. Tavartkiladze, *Phys. Lett. B* 482 (2000) 145; J. Sato and T. Yanagida, *Nucl. Phys. Proc. Suppl.* 77 (1999) 293; G. Altarelli, F. Feruglio, and I. Masina, *J. High Energy Phys.* 0011 (2000) 040; N. Maekawa, *Prog. Theor. Phys.* 106 (2001) 401.
- [24] Y. Grossman, Y. Nir, and Y. Shadmi, *J. High Energy Phys.* 9810 (1998) 007; M. S. Berger and K. Seyon, *Phys. Rev. D* 64 (2001) 053006; G. C. Branco and J. I. Silva-Marcos, *Phys. Lett. B* 526 (2002) 104.
- [25] R. N. Mohapatra and S. Nussinov, *Phys. Rev. D* 60 (1999) 013002.
- [26] C. Wetterich, *Phys. Lett. B* 451 (1999) 397.
- [27] S. F. King and G. G. Ross, *Phys. Lett. B* 520 (2001) 243.
- [28] W. Grimus and L. Lavoura, *J. High Energy Phys.* 07 (2001) 045; W. Grimus and L. Lavoura, *Eur. Phys. J. C* 28 (2003) 123.
- [29] R. N. Mohapatra, A. Pérez-Lorenzana, and C. A. de Sousa Pires, *Phys. Lett. B* 474 (2000) 355.
- [30] K. S. Babu, E. Ma, and J. W. F. Valle, *Phys. Lett. B* 552 (2003) 207.
- [31] S. F. King, [hep-ph/0208266](https://arxiv.org/abs/hep-ph/0208266).
- [32] I. Dorsner and S.M. Barr, *Nucl. Phys. B* 617 (2001) 493.
- [33] N. Seiberg, *Nucl. Phys. Proc. Suppl.* 67 (1998) 158; R. Gopakumar, S. Minwalla, N. Seiberg, and A. Strominger, *J. High. Energy Phys.* 08 (2000) 008.
- [34] N. Arkani-Hamed, A. G. Cohen, and H. Georgi, *Phys. Rev. Lett.* 86 (2001) 4757.
- [35] C. T. Hill, S. Pokorski, and J. Wang, *Phys. Rev. D* 64 (2001) 105005.
- [36] N. Arkani-Hamed, A. G. Cohen, and H. Georgi, *Phys. Lett. B* 513 (2001) 232.
- [37] H. C. Cheng, C. T. Hill, and J. Wang, *Phys. Rev. D* 64 (2001) 095003.
- [38] C. Csaki, G. D. Kribs, and J. Terning, *Phys. Rev. D* 65 (2002) 015004; H. C. Cheng, K. T. Matchev, and J. Wang, *Phys. Lett. B* 521 (2001) 308.
- [39] P. H. Chankowski, A. Falkowski, and S. Pokorski, *J. High Energy Phys.* 0208 (2002) 003; A. Falkowski, C. Grojean, and S. Pokorski, *Phys. Lett. B* 535 (2002) 258; L. Randall, Y. Shadmi, and N. Weiner *J. High Energy Phys.* 0301 (2003) 055.

- [40] A. Falkowski and H. D. Kim, *J. High Energy Phys.* 0208 (2002) 052.
- [41] T. R. Taylor and G. Veneziano, *Phys. Lett. B* 212 (1988) 147; K. R. Dienes, E. Dudas, and T. Gherghetta, *Nucl. Phys. B* 537 (1999) 47.
- [42] N. Arkani-Hamed, A. G. Cohen, and H. Georgi, *J. High Energy Phys.* 0207 (2002) 020; N. Arkani-Hamed, A. G. Cohen, and H. Georgi, [hep-th/0108089](#); P. Brax, A. Falkowski, Z. Lalak, and S. Pokorski, *Phys. Lett. B* 538 (2002) 426; N. Arkani-Hamed, A. G. Cohen, E. Katz, A. E. Nelson, T. Gregoire, and J. G. Wacker, *J. High Energy Phys.* 0207 (2002) 034; T. Gregoire and J. G. Wacker, *J. High Energy Phys.* 0208 (2002) 019.
- [43] C. Csaki, J. Erlich, C. Grojean, and G. D. Kribs, *Phys. Rev. D* 65 (2002) 015003; H. C. Cheng, D. E. Kaplan, M. Schmalz, and W. Skiba, *Phys. Lett. B* 515 (2001) 395.
- [44] W. Skiba and D. Smith, *Phys. Rev. D* 65 (2002) 095002; C. T. Hill and A. K. Leibovich, *Phys. Rev. D* 66 (2002) 075010; N. Arkani-Hamed, H. C. Cheng, P. Creminelli, and L. Randall, [hep-th/0301218](#).
- [45] H. Abe, T. Kobayashi, N. Maru, and K. Yoshioka, *Phys. Rev. D* 67 (2003) 045019.
- [46] E. Witten, [hep-ph/021018](#).
- [47] P. H. Frampton and S. L. Glashow, *Phys. Lett. B* 461 (1999) 95; A. S. Joshipura and S. D. Rindani, *Phys. Lett. B* 464 (1999) 239; L. Lavoura, *Phys. Rev. D* 62 (2000) 093011; Y. Nir, *J. High. Energy Phys.* 0006 (2000) 39; L. Lavoura and W. Grimus, *J. High. Energy Phys.* 0009 (2000) 007; T. Kitabayashi and M. Yasue, *Phys. Lett. B* 508 (2001) 85.
- [48] R. Kuchimanchi and R.N. Mohapatra, *Phys. Rev. D* 66 (2002) 051301.
- [49] S. F. King, *Nucl. Phys. B* 562 (1999) 57; S. F. King, *J. High Energy Phys.* 0209 (2002) 11.
- [50] Y. Nir and Y. Shadmi, *J. High. Energy Phys.* 9905 (1999) 023; Y. Nomura and T Sugimoto, *Phys. Rev. D* 61 (2000) 093003; C. H. Albright and S. M. Barr, *Phys. Rev. D* 64 (2001) 073010; K. S. Babu and S. M. Barr, *Phys. Lett. B* 525 (2002) 289.
- [51] C. D. Froggatt and H. B. Nielsen, *Nucl. Phys. B* 147 (1979) 277.
- [52] F. Wilczek and A. Zee, *Phys. Rev. Lett.* 42 (1979) 421; S. Weinberg, *Phys. Rev. Lett.* 43 (1979) 1566.
- [53] K.S. Babu and C.N. Leung, *Nucl. Phys. B* 619 (2001) 667.

- [54] C.D. Froggatt, H.B. Nielsen and Y. Takanishi, Nucl. Phys. B 631 (2002) 285; H.B. Nielsen and Y. Takanishi, Phys. Lett. B 543 (2002) 249.
- [55] M. Leurer, Y. Nir and N. Seiberg, Nucl. Phys. B 398 (1993) 319.
- [56] M. B. Green and J. H. Schwarz, Phys. Lett. B. 149 (1984).
- [57] E. Witten, Phys. Lett. B 105 (1981), 267; M. Leurer, Y. Nir, and N. Seiberg, Nucl. Phys. B 420 (1994) 468.
- [58] Particle Data Group, D.E. Groom et al., Eur. Phys. J. C 15 (2000) 1, <http://pdg.lbl.gov/>.
- [59] T. Ohlsson and G. Seidl, Phys. Lett. B 537 (2002) 95.
- [60] T. Ohlsson and G. Seidl, Nucl. Phys. B 643 (2002) 247.
- [61] T. Ohlsson and H. Snellman, J. Math. Phys. 41 (2000) 2768, 42 (2001) 2345(E); T. Ohlsson, Phys. Scripta T93 (2001) 18.
- [62] V. Barger et al., Phys. Lett. B 437 (1998) 107.
- [63] G. Seidl, [hep-ph/0301044](http://arxiv.org/abs/hep-ph/0301044).
- [64] H. Georgi, Nucl. Phys. B 266 (1986), 274.
- [65] M. R. Douglas and G. Moore, [hep-th/9603167](http://arxiv.org/abs/hep-th/9603167).
- [66] N. Arkani-Hamed, A. G. Cohen, and H. Georgi, J. High. Energy Phys. 0207 (2002) 020.
- [67] L. Randall and R. Sundrum, Phys. Rev. Lett. 83 (1999) 4690.
- [68] W. A. Bardeen and R. B. Pearson, Phys. Rev. D 14 (1976), 547.
- [69] W. A. Bardeen, R. B. Pearson, and E. Rabinovici, Phys. Rev. D 21 (1980) 1037.
- [70] K. G. Wilson, Phys. Rev. D 10 (1974) 2445.
- [71] H. C. Cheng, C. T. Hill, S. Pokorski, and J. Wang, Phys. Rev. D 64 (2001) 065007.
- [72] T. Gherghetta and A. Pomarol, Nucl. Phys. B 586 (2000) 141; S. J. Huber and Q. Shafi, Phys. Lett. B 498 (2001) 256.
- [73] S. T. Petcov, Phys. Lett. B 110 (1982) 245; C. N. Leung and S. T. Petcov, Phys. Lett. B 125 (1983) 461; R. Barbieri, L. J. Hall, D. Smith, A. Strumia, and N. Weiner, J. High Energy Phys. 9812 (1998) 017.



- 
- [74] Q. Shafi and Z. Tavartkiladze, Phys. Rev. D 67 (2003) 075007.
- [75] H. Kurzweil and B. Stellmacher, *Theorie der Endlichen Gruppen* (Springer, Berlin Heidelberg, 1998).
- [76] L. Wolfenstein, Phys. Rev. Lett. 51 (1983) 1945.
- [77] R. Rosenfeld and J. L. Rosner, Phys. Lett. B 516 (2001), 408.
- [78] Z.-z. Xing, Phys. Lett. B 545 (2002) 352.
- [79] K. R. S. Balaji, M. Lindner, and G. Seidl, hep-ph/0303245.
- [80] T. Gregoire and J. G. Wacker, hep-ph/0207164.
- [81] F. Bauer, M. Lindner, and G. Seidl, *in preparation*.
- [82] E. Ma and U. Sarkar, Phys. Rev. Lett. 80 (1998) 5716.
- [83] N. Arkani-Hamed, S. Dimopoulos, G. Dvali, and J. March-Russel, Phys. Rev. D 65 (2002) 024032.
- [84] K. R. Dienes, E. Dudas, and T. Gherghetta, Nucl. Phys. B 557 (1999) 25.
- [85] A. Pilaftsis, Phys. Rev. D 60 (1999) 105023.
- [86] J. Smit, *Introduction to Quantum Fields on a Lattice* (Cambridge University Press, Cambridge, 2002).
- [87] M. Lüscher, hep-th/0102028
- [88] Y. Tomozawa, Ann. Phys. 131 (1981) 95.
- [89] K. G. Wilson, in *New Phenomena in Subnuclear Physics*, ed. A. Zichichi (Plenum, New York, 1977).
- [90] M. Creutz, *Quarks, Gluons and Lattices* (Cambridge University Press, Cambridge, 1983).
- [91] P. H. Ginsparg and K. G. Wilson, Phys. Rev. D 25 (1982) 2649.
- [92] M. Hamermesh, *Group Theory and Its Application to Physical Problems* (Dover, New York, 1989).